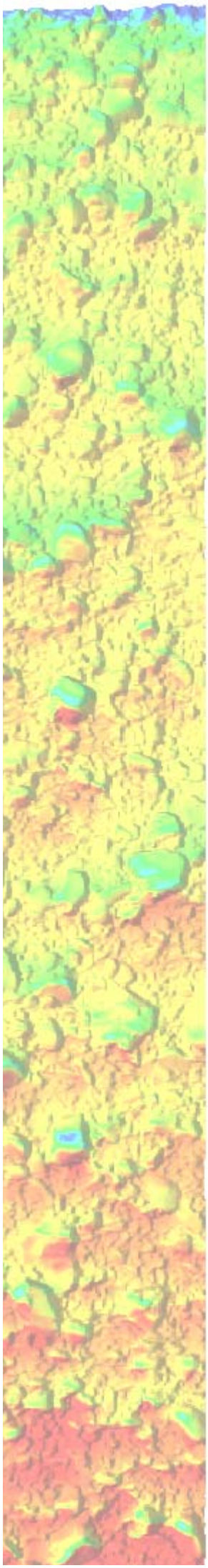

Numerical Modelling and Hydraulics

Nils Reidar B. Olsen

Department of Hydraulic and Environmental Engineering
The Norwegian University of Science and Technology

5th edition, January 2017.

ISBN 82-7598-074-7

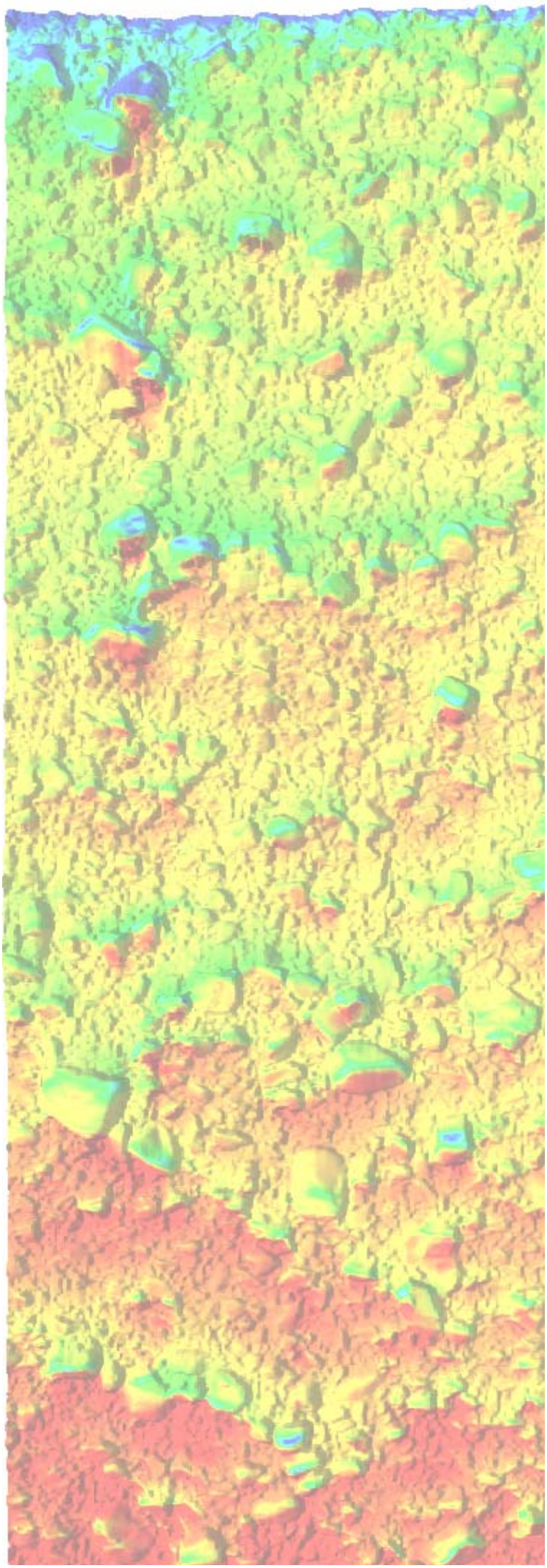

Foreword

The class “Numerical Modelling and Hydraulics” is a new name for the old course “Hydroinformatics”, which was offered for the first time in the spring 2001 at the Norwegian University of Science and Technology. It is an undergraduate course for the 3rd/4th year students. The prerequisite was a basic course in hydraulics/hydromechanics/fluid mechanics, that includes the derivation of the basic equations, for example the continuity equation and the momentum equation.

When I started my employment at the Norwegian University of Science and Technology, I was asked to teach the course and make a plan for its content. The basis was the discontinued course “River Hydraulics”, which also included topics on limnology. I was asked to include topics on water quality and also on numerical modelling. When adding topics to a course, it is also necessary to remove something. I have removed some of the basic hydraulics on the momentum equation, as this is taught in other courses the students had previously. I have also removed parts of the special topics of river hydraulics such as compound sections and bridge and culvert analysis. The compound sections hydraulics I believe can not be used in practical engineering anyway, as the geometry is too simplified compared with a natural river. The bridge analysis is based on simplifications of 1D flow models for a 3D situation. In the future, I believe a fully 3D model will be used instead, and this topic will be obsolete. Some of the topics on marine engineering have been removed, as a new course “Marine Physical Environment” at Department of Structural Engineering at NTNU is covering these subjects. This course also contains some ice hydraulics and related cold climate engineering, topics which has not been included in the present text.

The resulting course included classical hydraulics, sediment transport, numerics and water quality. It was difficult to find one textbook covering all topics. The books were also very expensive, so it was difficult to ask the students to buy several books. Instead I wrote the present notes. I want to thank the Department for giving me time for this, and hope the book will be of interest for the students.

I also want to thank all the people helping me with material, advice and corrections to the book. Dr. Knut Alfredsen has provided advice and material on the numerical solution of the Saint-Venant’s equation and on the habitat modelling. Prof. Torkild Carstens has given advice on jets, plumes and water abstraction. Prof. Liv Fiksdal provided advice about water biology and Mr. Yngve Robertsen has given advice on the flood wave formulas. I also want to thank my students taking the course in the spring 2001, finding to a large number of errors and making suggestions for improvements. For an earlier version, Prof. Hubert Chanson provided useful corrections.

The new name reflects the focus of numerical models and hydraulics. The word “Hydroinformatics” is very broad and covers a large number of topics not included in the present book. In addition to numerical models, also some topics of Hydraulics are covered, for example flood waves, sediment transport, stratified flow and physical model tests.

In memory of Prof. Dagfinn K. Lysne

Table of content

Appendix

1. Introduction

1.1 Motivation

In today's society, environmental issues are an important concern in planning projects related to water resources. Discharges of pollutants into rivers and lakes are not allowed, unless special permission is given by the appropriate authority. In an application for discharge into a receiving water body, an assessment of potential damages must be included. A numerical model is useful in the computation of the effects of the pollution.

Over the last years, flooding of rivers and dam safety have been major issues in Norway. The new regulations for planning, construction and operation of dams has increased demands for dam safety. All Norwegian dams will have to be evaluated with regards to failure, and the downstream effects have to be assessed. In this connection, flood zone mapping of most major rivers have to be undertaken, and this will create considerable work for hydraulic engineers in years to come.

The last twenty years have also seen the evolution of computers into a very applicable tool for solving hydraulic engineering problems. Many of the present-day numerical algorithms were invented in the early 1970's. At that time, the computers were still too slow to be used for most practical flow problems. But in the last few years the emergence of fast and inexpensive personal computers have changed this. All the numerical methods taught in this course are applied in programs running on a PC.

The most modern numerical models often have sophisticated user interfaces, showing impressive colour graphics. People can easily be led to an understanding that the computer solves all the problems with minimum knowledge of the user. Although present day computer programs can compute almost all problems, the accuracy of the result is still uncertain. An inexperienced user may produce convincing and impressive colour figures, but the accuracy of the result may still not be good enough to have a value in practical engineering. It is therefore important that the user of the computer programs has sufficient knowledge of both the numerical methods and their limitation and also the physical processes being modelled. The present book therefore gives several chapters on processes as basic hydraulics, limnology, sediment transport, water quality etc. The knowledge should be used to provide reasonable input for the numerical models, and assessing their results. Many empirical formulas are given, providing further possibilities for checking the result of the numerical method for simpler cases.

The numerical methods also have limitations with regards to other issues, for example modelling of steep gradients, discontinuities, processes at different scales etc. The numerical models itself may be prone to special problems, for example instabilities. Often, a computer program may not include all processes occurring in the water body. The user needs to be aware of the details of the numerical methods, its capabilities and limitations to assess the accuracy of the results.

1.2 Classification of computer programs

There exist a large number of computer programs for modelling fluvial hydraulics and limnology problems. The programs have varying degree of sophistication and reliability. The science of numerical modelling is progressing rapidly, making some programs obsolete while new programs are emerging.

The computer programs can be classified according to:

- what is computed
- how many dimensions are used
- particulars of the numerical methods

Many computer programs are tailor-made for one specific application. Examples are:

- Water surface profiles (HEC2)
- Flood waves (DAMBRK)
- Water quality in rivers (QUAL2E)
- Sediment transport and bed changes (HEC6)
- Habitat modelling (PHABSIM)

This is particularly the case for one-dimensional models, developed several years ago, when the computational power was much less than today. There are also more modern one-dimensional programs, using more sophisticated user interfaces and also including modules for computing several different problems. Examples are:

- HEC-RAS
- MIKE11
- ISIS

In recent years, a number of multi-dimensional computer programs have been developed. These also often include modules for computing several different processes, for example water quality, sediment transport and water surface profiles.

Multi-dimensional programs may be:

- two-dimensional depth-averaged
- three-dimensional with a hydrostatic pressure assumption
- fully three-dimensional

There also exist width-averaged two-dimensional models, but these are mostly used for research purposes.

The three-dimensional models solve the Navier-Stokes equations in two or three dimensions. Sometimes the equations are only solved in the horizontal directions, and the continuity equation is used to obtain the vertical velocity. This is called a solution with a hydrostatic pressure assumption. The fully 3D models solve the Navier-Stokes equations also in the vertical direction. This gives better accuracy when the vertical acceleration is significant.

The various algorithms used by these types of programs are described in the following chapters, together with the physics involved.

2. River hydraulics

The classical river hydraulics described in this chapter forms the basis for the numerical modelling of flood waves and river pollutant dispersion. In this chapter, a hydrostatic pressure is assumed in the vertical direction, and also that the water flow is one-dimensional.

2.1 Uniform flow

The definition of uniform flow can be visualized by looking at water flow in a very long flume, where the water depth and velocities are constant at any point over the length of the flume. In a natural river this never occurs, but the concept is useful for developing hydraulic engineering formulas. Fig. 2.1.1 shows a section of a wide channel, with forces on the water. *I* is the slope of the water surface and *h* is the water depth.

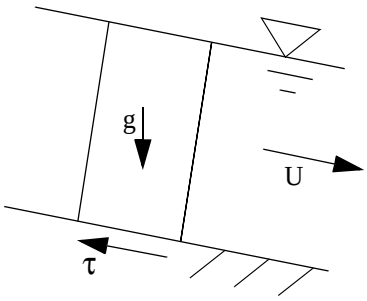

Fig. 2.1.1 Forces on a water volume in uniform flow

The forces on the water volume in the direction parallel to the river bed/ surface will be:

Bed shear: $F_b = \tau \Delta x$

Gravity: $F_g = \rho g_x V = \rho g I \Delta x h$

The direction of the flow is called *x*, *h* is the water depth, *I* is the slope of the water surface, g_x is the component of the gravity in the x-direction and τ is the shear stress on the bed. Setting the two forces equal to each other gives the formula for the bed shear stress:

$$\tau = \rho g h I \qquad (2.1.1)$$

The density of water is denoted ρ, and *g* is the acceleration of gravity. A method to compute *I* is presented in the next chapter.

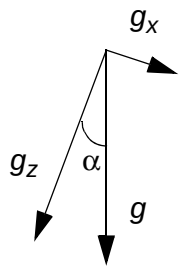

$g_x = g\sin\alpha = g\tan\alpha = gI$ for small angles

The vertical velocity profile in a river with uniform flow can be described by boundary layer theory. Early experiments were carried out by Nikuradse (1933) using uniform spheres, and later Schlichting (1936) using particles of varying shapes. The experiments produced the following formula for the vertical velocity profile for uniform flow (Schlichting, 1979):

$$\frac{U}{u_*} = \frac{1}{\kappa}\ln\left(\frac{30y}{k_s}\right) \qquad (2.1.2)$$

U is the velocity, and it is a function of the distance, *y*, from the bed. The parameter κ is an empirical constant, equal to 0.4. The formula only applies for rough surfaces, and k_s is a roughness coefficient. It is equivalent to the particle diameter of the spheres glued to the wall to model roughness elements. The variable u_* is the shear velocity, given by:

$$u_* = \sqrt{\frac{\tau}{\rho}} \qquad (2.1.3)$$

Eq. 2.1.2 is also called the logarithmic profile for the water velocity. Schlicting's formulas were based on data from experiments done in air, but since non-dimensional parameters were used, the results worked very well also for water flow. Schlichting found the wall laws applies for

all boundary layers, also for non-uniform flow, as long as only the velocities very close to the wall are considered.

To use the formula, the next question is which roughness to choose. There exist a number of different relations between the effective roughness and the grain size distribution on the river bed. Van Rijn (1982) found the following formula, based on 120 flume data sets:

$$k_s = 3d_{90} \tag{2.1.4}$$

The variable d_{90} denotes the grain size sieve where 90 % of the material is finer. Van Rijn reported that there were large uncertainties in this formula, and that the number 3 was an average value where the data set suggested a variation range between 1 and 10. Other researchers have used different formulas. Hey (1979) suggested the following formula based on data from a natural river with coarse material, and laboratory experiments with cubical/spherical elements:

$$k_s = 3.5d_{84} \tag{2.1.6}$$

Kamphuis (1974) made a new formula based on his flume experiments:

$$k_s = 2d_{90} \tag{2.1.7}$$

The value 2 varied between 1.5 and 2.5 in the experiments. Kamphuis used a zero reference level of $0.7d_{90}$, which will affect the results.

Schlichting (1979) carried out laboratory experiments with spheres and cones. Using 45 degree cones placed right beside each other, the k_s value was equal to the cone height.

In other words, it is difficult to obtain an exact estimate of the k_s value.

2.2 Friction formulas

A number of researchers have developed formulas for the average velocity in a channel with uniform flow, given the water depth, water slope and a friction factor. The formulas are empirical, and the friction factors often depend on the water depth. The most common formulas are:

Manning's formula:

Manning's formula:

$$U = \frac{1}{n} r_h^{\frac{2}{3}} I^{\frac{1}{2}} \tag{2.2.1}$$

The hydraulic radius, r_h, is given by:

$$r_h = \frac{A}{P} \tag{2.2.2}$$

where A is the cross-sectional area of the river and P is the wetted perimeter.

Often the Strickler's M value is used instead of Manning's coefficient, n.

The relation is:

Some Manning's coefficients:

Glass models:
0.009-0.01
Cement models:
0.011-0.013
Concrete lined channels:
0.012-0.017
Earth lined channels:
0.018-0.04
Rock lined channels:
0.025-0.045
Earth lined rivers:
0.02-0.05
Mountain rivers with stones:
0.04-0.07
Rivers with weed:
0.05-0.15

$$M = \frac{1}{n} \tag{2.2.3}$$

giving:

$$U = M\, r_h^{\frac{2}{3}} I^{\frac{1}{2}} \tag{2.2.4}$$

Given the grain size distribution on the bed, the Manning's friction factor can be estimated by the following empirical formula (Meyer-Peter and Müller, 1948):

$$M = \frac{26}{(d_{90})^{\frac{1}{6}}} \tag{2.2.5}$$

Given the water velocity and the friction factor, the formulas can be used to predict the water depth. Together with the continuity equation (2.2.6) the formulas can also be used to estimate the water surface slope or the friction loss for non-uniform flow. Thereby the water elevations can be found. A further description is given in Chapter 3.

Continuity equation:

$$q = Uh \tag{2.2.6}$$

The water discharge pr. unit width of the river is often denoted *q*.

2.3 Singular losses

Using the Energy Equation/Bernoulli's Equation for the water flow in a river, it is possible to compute the energy loss and the water surface location. The friction loss is given by the roughness of the river bed. There are also other energy losses, called singular losses. These are identified with particular constructions in the rivers, for example a bridge pier, or a river bend. The head losses are associated with eddies generated around the loss point, usually in connection with flow expansion. A recirculation zone forms, dissipating energy. The head loss, h_f, can be computed as:

$$h_f = k\frac{U^2}{2g} \tag{2.3.1}$$

where *k* is a head loss coefficient related to the geometry of the river/ obstruction.

In natural rivers, it is often difficult to identify singular losses and assign a value to each loss. Instead, a different Manning's friction factor is often used, where the effective friction factor is used, as a combination of the singular losses and the friction loss. The friction factor is then found by calibration.

It is possible to use Eq. 2.3.1 for river contractions, for example in connection with bridges and bridge piers. However, the head loss coefficient is difficult to find without using measurements in the field/lab.

2.4 Critical flow

Looking at one-dimensional water flow in a channel, there are two types of energy: Kinematic energy due to the water velocity, and pressure due to the water depth, *y*, and weight of the water. The sum of these energies is called the specific energy height of the section, *E* [meters]:

$$E = E_P + E_U = y + \frac{U^2}{2g} \tag{2.4.1}$$

The specific energy may change along the length of the river, depending on the water discharge, roughness, bed slope etc. If the water is given a specific energy, Eq. 2.4.1 can be used to find the water depth:

$$y = E - \frac{U^2}{2g} \tag{2.4.2}$$

Introducing the continuity equation (2.2.6), the equation can be written:

$$y = E - \frac{q^2}{2gy^2} \tag{2.4.3}$$

or

$$y^3 - Ey^2 + \frac{q^2}{2g} = 0 \tag{2.4.4}$$

This third-order equation has three possible solutions. Only two are physically possible. If we solve for the specific energy, we get:

$$E = y + \frac{q^2}{2gy^2} \tag{2.4.5}$$

The minimum specific energy to transport a given volume of water is obtained by derivation of Eq. 2.4.5, and setting the result to zero:

$$\frac{dE}{dy} = 1 - \frac{q^2}{gy^3} = 0 \tag{2.4.6}$$

$$y_c = \sqrt[3]{\frac{q^2}{g}} \tag{2.4.7}$$

The Froude number:

$$Fr = \frac{U}{\sqrt{gy}}$$

Using the continuity equation, the equation above can also be written:

$$\frac{U_c}{\sqrt{gy_c}} = 1 \tag{2.4.8}$$

The term on the left side of the equation is also called the Froude number. For a minimum amount of specific energy, the Froude number is unity, as given in Eq. 2.4.8. If the Froude number is below unity, the flow is subcritical. The flow is supercritical if the value is higher than unity

Supercritical flow is very seldom encountered in natural rivers. It exists in water falls or rapids. If supercritical flow occur in a river with stones on the bed, usually a hydraulic jump is formed. Normally, the flow in a river

is subcritical.

The Froude number is important for the numerical solution of equations for water depth in a river. If critical flow occur, instabilities often emerge in the numerical algorithms.

Irregular cross-sections

The derivation above is valid for channels with rectangular cross-sections. For a channel with irregular cross-section, the water velocity is replaced by Q/A. The specific energy for the section becomes:

$$E = y + \frac{Q^2}{2gA^2} \qquad (2.4.9)$$

The minimum specific energy for the section is obtained by derivation with respect to y and setting this to zero, similar to what was done for the rectangular channel:

$$\frac{dE}{dy} = 1 - \frac{Q^2}{gA^3}\frac{dA}{dy} = 0 \qquad (2.4.10)$$

For small changes in the water level, the incremental cross-sectional area, *dA* is given by

$$dA = Bdy \qquad (2.4.11)$$

The top width of the cross-section is denoted *B*. Inserted into Eq. 2.4.10, this gives:

$$\frac{Q^2 B}{gA^3} = 1 \qquad (2.4.12)$$

The square root of the left side of the equation is the Froude number for a cross-section with a general complex geometry:

$$Fr = \sqrt{\frac{Q^2 B}{gA^3}} = \frac{U}{\sqrt{g\frac{A}{B}}} \qquad (2.4.13)$$

The hydraulic jump

The hydraulic jump is a transformation of the water flow from supercritical to subcritical flow. Visually, it looks like a standing wave in the channel. The water level is higher downstream than upstream.

It is possible to derive a relationship between the water level upstream, h_1, and downstream, h_2, of the jump.

The momentum equation gives the force on an obstacle as:

$$F = \rho Q(U_2 - U_1) + \rho g(A_2\overline{y_2} - A_1\overline{y_1}) \qquad (2.4.14)$$

The parameters $\overline{y}$ is the effective height of the hydrostatic pressure.

For a rectangular channel where *F*=0 and $\overline{y}$= 1/2 *y*:

$$0 = \rho Q(U_2 - U_1) + \frac{1}{2}\rho g(A_2 y_2 - A_1 y_1) \quad (2.4.15)$$

Divide by the width and the density:

$$0 = q(U_2 - U_1) + \frac{1}{2}g(y_2^2 - y_1^2) = q^2\left(\frac{1}{y_2} - \frac{1}{y_1}\right) + \frac{1}{2}g(y_2^2 - y_1^2) \quad (2.4.16)$$

Solve with respect to q^2:

$$q^2 = -\frac{\frac{1}{2}g(y_2^2 - y_1^2)}{\left(\frac{1}{y_2} - \frac{1}{y_1}\right)} = \frac{\frac{1}{2}g(y_2^2 - y_1^2)}{\left(\frac{1}{y_1} - \frac{1}{y_2}\right)} \quad (2.4.17)$$

Use the definition of the Froude number:

$$Fr_2^{\,2} = \frac{U_2^2}{g y_2} = \frac{q^2}{g y_2^3} \quad (2.4.18)$$

Solves the equation with respect to q^2, and eliminates q^2 with the equation above:

$$Fr_2^{\,2} g y_2^3 = \frac{\frac{1}{2}g(y_2^2 - y_1^2)}{\left(\frac{1}{y_1} - \frac{1}{y_2}\right)} = \frac{\frac{1}{2}g(y_2 - y_1)(y_2 + y_1)y_1 y_2}{(y_2 - y_1)} = \frac{1}{2}g(y_2 + y_1)y_1 y_2 \quad (2.4.19)$$

$$Fr_2^{\,2} = \frac{1}{2}(y_2 + y_1)\frac{y_1 y_2}{y_2^3} = \frac{1}{2}(y_2 + y_1)\frac{y_1}{y_2^2} = \frac{1}{2}\frac{y_1}{y_2}\left(\frac{y_1}{y_2} + 1\right) \quad (2.4.20)$$

Solves with respect to y_1/y_2:

$$\left(\frac{y_1}{y_2}\right)^2 + \frac{y_1}{y_2} - 2Fr_2^{\,2} = 0 \quad (2.4.21)$$

Solves the second order equation:

$$\frac{y_1}{y_2} = \frac{1}{2}(\sqrt{1 + 8Fr_2^{\,2}} - 1) \quad (2.4.22)$$

Given the water level and the Froude number downstream of the jump, the water level upstream of the jump can be computed. It can be shown that a formula where the indexes 1 and 2 are changed is also valid.

2.5 Steady non-uniform flow

It is possible to compute the water surface of a steady non-uniform flow by analytical formulas, as long as the cross-sectional shape is rectangular. The formulas are derived in the following. However, if the cross-section does not have rectangular shape, the water surface location have to be computed numerically. This is described in Chapter 3.

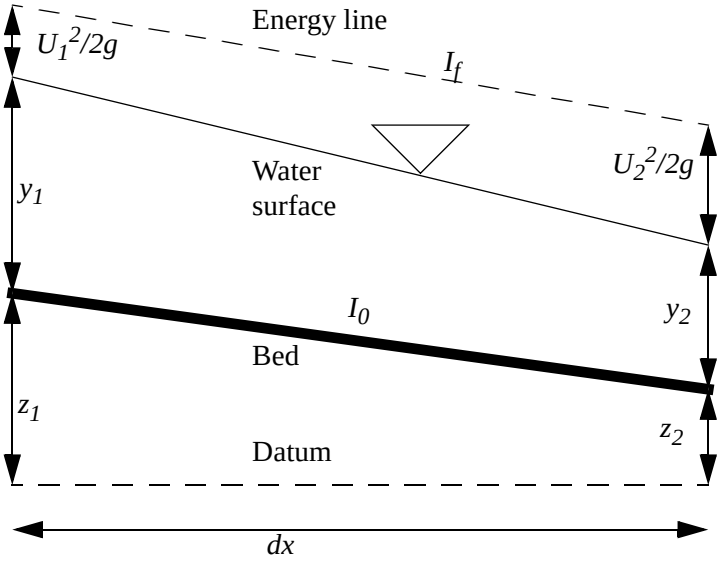

Figure 2.5.1 A longitudinal profile of a channel is shown, between the two cross-sections 1 and 2. The distance between the sections is *dx*. The water depths are denoted *y* and the bed level elevation is denoted *z*. The bed slope is denoted I_0, and the slope of the energy line is denoted I_f. Note the energy line is located a distance above the water level, equal to the velocity height, $U^2/2g$.

The derivation of the formula for the water depth is based on Fig. 2.5.1. The total height of the energy line is denoted *H*, so that:

$$H = z + y + \frac{U^2}{2g} \tag{2.5.1}$$

The energy slope, I_f, can be computed from for example Manning's formula. For our case, the slope can be written as:

$$I_f = \frac{H_2 - H_1}{dx} = \frac{d}{dx}\left(z + y + \frac{U^2}{2g}\right) = I_0 + \frac{d}{dx}\left(y + \frac{U^2}{2g}\right) \tag{2.5.2}$$

The term in the brackets most right in the equation is the specific energy, *E*, of the flow. The term can be rewritten:

$$\frac{d}{dx}\left(y + \frac{U^2}{2g}\right) = \frac{dE}{dx} = \frac{dE}{dy}\frac{dy}{dx} = \frac{dy}{dx}\left(\frac{dy}{dy} + \frac{1}{2g}\frac{dU^2}{dy}\right) \tag{2.5.3}$$

The continuity equation gives:

$$U^2 = \frac{Q^2}{A^2} \tag{2.5.4}$$

Derivation with respect to y gives:

$$\frac{dU^2}{dy} = \frac{d}{dy}\left(\frac{Q^2}{A^2}\right) = Q^2\frac{d}{dA}(A^{-2})\frac{dA}{dy} = -2Q^2A^{-3}\frac{dA}{dy} \quad (2.5.5)$$

The final formula needed is for a general cross-sectional shape:

$$\frac{dA}{dy} = B \quad (2.5.6)$$

This is inserted into Eq. 2.5.5, and the result of this in Eq. 2.5.3, giving:

$$\frac{d}{dx}\left(y + \frac{U^2}{2g}\right) = \frac{dy}{dx}\left(1 + \frac{1}{2g}(-2Q^2A^{-3}B)\right) = \frac{dy}{dx}(1 - Fr^2) \quad (2.5.7)$$

Inserted into Eq. 2.5.2, the result is:

$$I_f = I_0 + \frac{dy}{dx}(1 - Fr^2) \quad (2.5.8)$$

which can be rearranged to:

$$\frac{dy}{dx} = \frac{I_f - I_0}{1 - Fr^2} \quad (2.5.9)$$

In a wide, rectangular channel, the Froude number can be written:

$$Fr = \frac{U}{\sqrt{gy}} = \frac{Q}{By\sqrt{gy}} \quad (2.5.10)$$

Similarly, the friction slope, I_f, can be expressed as a function of constants and *y,* using Mannings Equation:

$$I_f = \frac{U^2}{M^2y^{\frac{4}{3}}} = \frac{Q^2}{M^2B^2y^{\frac{10}{3}}} \quad (2.5.11)$$

The water depth is here denoted *y*. It is used instead of the hydraulic radius, meaning the formula is only valid for wide, rectangular channels.

Eq. 2.5.10 and Eq. 2.5.11 can be inserted into Eq. 2.5.9, resulting in a formula for the change in the water depth only being a function of constants and *y*. This can then be integrated analytically to compute functions for changes in water depths in wide channels with constant width.

For more complex cases it is possible to use a spreadsheet to compute the water surface. Such cases can be channels with varying widths or non-rectangular cross-sections. An example of such a spreadsheet is given in the figure below. Note, for sub-critical flow we start with the downstream cross-section, which is no. 1 in the table.

Cross-section no.	Depth, *y*	U	Froude number, *Fr*	Energy slope, I_f	Δy
1	(given)	Continuity	Definition	Eq. 2.5.11	Eq. 2.5.9
2	$y_1+\Delta y_1$		Eq. 2.5.10		
3					
4					
1	1.0	1.0	0.322	0.000429	-0.04213
2	0.957				

The method of invoking more iterations is dependent on the particular spreadsheet program. For Lotus 123, use *F9* on the keyboard repeatedly. For MS Excel, use the menu *Tools, Options, Calculations*, and cross off *Iterations*, and give a number in the edit-field, for example 50.

Also note that the water depths are calculated in the cross-sections. The other parameters in the table are computed as an average value between cross-sections. This means the water velocity in the table is a function of two water depths. Iterations are therefore necessary.

The numbers in the spreadsheet is an example with a water discharge of 1 m^3/s in a 1 m wide channel, a Manning-Strickler value of 50 a slope of 0.001 and a dx of 50 meters.

Classification of surface profiles

Bakhmeteff (1932) proposed a classification system for water surface profiles, which is included in almost all textbooks on water surface profiles. The system is useful for understanding water surface profiles, but the classifications itself is rarely used in engineering practice. The profiles are classified according to the bed slope, the critical slope and the water depth, as given in Table 2.5.1. The water depth is denoted *y*, the slope is denoted *I*, and *E* is the specific energy of the water. Subscripts *0* denotes the bed and *c* denotes critical slope/depth. The figures at the right of the table show longitudinal profiles of the surface profiles. The lines for the critical depth and normal depth are also given. The normal depths are found by using for example Manning's equation, given the roughness, bed slope and water discharge. The critical depth is found from Eq. 2.4.7.

The system classifies each surface profile with a letter and a number. The letter is only a function of the slope of the river at the given discharge. The letters given in the table on the right are used.

:

Letter	Stands for	Bed slope
M	Mild	Subcritical
S	Steep	Supercritical
C	Critical	Critical
H	Horizontal	Horizontal
A	Adverse	Adverse

The number is an index for the actual Froude number in the channel. Subcritical flow is denoted 1 while super-

critical flow is denoted 3. The index 2 can mean either supercritical or subcritical, depending on the letter. This is given in more detail in Table 2.5.1.

Table 2.5.1. Classification of water surface profiles

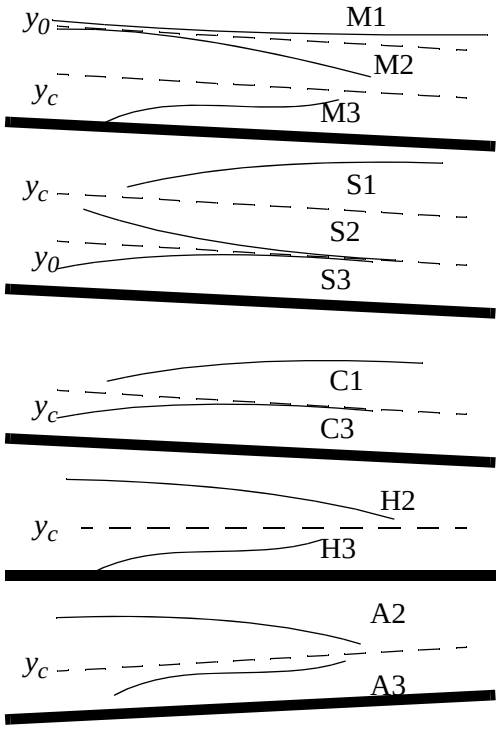

Channel slope	Profile type	Depth range	Fr	dy/dx	dE/dx
Mild $I_0<I_c$ $y_0>y_c$	M1	$y>y_0>y_c$	<1	>0	>0
	M2	$y_0>y>y_c$	<1	<0	<0
	M3	$y_0>y_c>y$	>1	>0	<0
Steep $I_0>I_c$ $y_0<y_c$	S1	$y>y_c>y_0$	<1	>0	>0
	S2	$y_c>y>y_0$	>1	<0	>0
	S3	$y_c>y_0>y$	>1	>0	<0
Critical $I_0=I_c$ $y_0=y_c$	C1	$y>y_c$	<1	>0	>0
	C3	$y<y_c$	>1	>0	<0
Horizontal $I_0=0$	H2	$y>y_c$	<1	<0	<0
	H3	$y<y_c$	>1	>0	<0
Adverse $I_0<0$	A2	$y>y_c$	<1	<0	<0
	A3	$y<y_c$	>1	>0	<0

Examples of water surface profiles: When a mild-sloping river flows into a reservoir, we have an M1 curve. The water profile just upstream a spillway can be M2, H2 or A2. Profiles just before a hydraulic jump can be M3, H3 or A3. The S1 profile can be found after a hydraulic jump in a steep channel.

2.6 Waves in rivers

It is possible to derive formulas for waves travelling up or down a channel with constant width and slope. Rough estimation of such waves can thereby be made, and the formulas can also be used to evaluate the results from numerical models. Two types of waves can be described:

- kinematic waves
- dynamic waves

Both types are derived and discussed in the following.

Dynamic wave

An equation for the dynamic wave is derived by looking at the longitudinal profile of the wave given in Fig. 2.6.1:

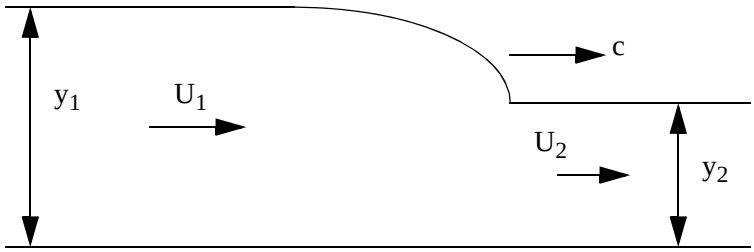

Fig 2.6.1 Definition sketch of a wave travelling down a river. The upstream depth and velocity are denoted h_1 and U_1, respectively and the downstream depth and velocity are denoted h_2 and U_2 respectively. The velocity of the wave is denoted c.

A steady situation is obtained if the reference system moves along the channel with velocity c. The water velocities upstream and downstream of the wave becomes $U_1 - c$ and $U_2 - c$, respectively. The momentum equation gives:

$$(U_1 - c)^2 y_1 + \frac{1}{2} g y_1^2 = (U_2 - c)^2 y_2 + \frac{1}{2} g y_2^2 \qquad (2.6.1)$$

Together with the continuity equation:

$$(U_1 - c) y_1 = (U_2 - c) y_2 \qquad (2.6.2)$$

Solving the continuity equation with respect to U_2:

$$U_2 = (U_1 - c)\frac{y_1}{y_2} + c \qquad (2.6.3)$$

Inserting this into the momentum equation, eliminating U_2:

$$(U_1 - c)^2 y_1 + \frac{1}{2} g (y_1^2 - y_2^2) = \left((U_1 - c)\frac{y_1}{y_2} + c - c\right)^2 y_2 \qquad (2.6.4)$$

Eliminating the c's on the right hand side, and moving the term to the left side:

$$(U_1 - c)^2 \left[y_1 - \left(\frac{y_1}{y_2}\right)^2 y_2 \right] + \frac{1}{2}(g(y_1^2 - y_2^2)) = 0 \qquad (2.6.5)$$

Simplifying the first term and changing the second term:

$$(U_1 - c)^2 \left(y_1 - \frac{y_1^2}{y_2} \right) + \frac{1}{2}(g(y_1 - y_2)(y_1 + y_2)) = 0 \qquad (2.6.6)$$

Further simplifying the first term and changing the sign of the second term:

$$(U_1 - c)^2 \frac{y_1}{y_2}(y_2 - y_1) - \frac{1}{2}(g(y_2 - y_1)(y_1 + y_2)) = 0 \qquad (2.6.7)$$

Dividing by the second part of the first term:

$$(U_1 - c)^2 = \frac{1}{2}\frac{y_2}{y_1} g(y_1 + y_2) \quad (2.6.8)$$

Taking the square root of each side, multiplying with -1 and moving U_1 to the other side:

$$c = U_1 \pm \sqrt{\frac{g}{2}\frac{y_2}{y_1}(y_2 + y_1)} \quad (2.6.9)$$

If the wave is small, y_2 and y_1 are approximately equal. The equation then becomes:

$$c = U \pm \sqrt{gy} \quad (2.6.10)$$

If Eq. 2.6.10 is combined with the definition of the Froude number, the following formula is obtained:

$$c = U \pm \frac{|U|}{|Fr|}$$

If $Fr < 1$, c can be both positive and negative. In subcritical flow, a wave can then travel both upstream and downstream a channel.

If $Fr > 1$ then c will always be positive. For supercritical flow, the wave can only travel downstream.

Kinematic wave

The formula for a kinematic wave with speed c, is derived from the continuity equation, looking at a similar situation as in Fig. 2.6.1. This gives:

$$c = \frac{dQ}{dA} \quad (2.6.11)$$

The differential of Q can be derived from Mannings Equation (Eq. 2.2.1) for a wide, rectangular channel, differentiated with respect to the water depth:

$$\frac{dQ}{dy} = \frac{d}{dy}(AU) = \frac{d}{dy}\left(By\frac{1}{n}I^{\frac{1}{2}}y^{\frac{2}{3}}\right) = \frac{d}{dy}\left(B\frac{1}{n}I^{\frac{1}{2}}y^{\frac{5}{3}}\right) = \frac{BI^{\frac{1}{2}}}{n}\frac{5}{3}y^{\frac{2}{3}} \quad (2.6.12)$$

or rewritten:

$$dQ = \frac{5}{3}\frac{BI^{\frac{1}{2}}}{n}y^{\frac{2}{3}}dy \quad (2.6.13)$$

The formula for the area of the cross-section is then differentiated with respect to y:

$$dA = Bdy \quad (2.6.14)$$

Inserting dA and dQ from the two equations above into Eq. 2.6.11 gives:

$$c = \frac{5}{3}\frac{1}{n}I^{\frac{1}{2}}y^{\frac{2}{3}} = \frac{5}{3}U \quad (2.6.15)$$

which is the formula for the kinematic wave.

Wave shape

Eq. 2.6.10 shows that the wave speed will increase with larger depth.

This is also given from Mannings Equation (2.2.1), as the increased water velocity will lead to increased depth. The shape of a wave will thereby change as it moves downstream the channel. Assuming the front and the end of the wave have smaller depths, and the maximum depth is at the center of the wave, two phenomena will take place:

1. The wave front will become steeper
2. The wave tail will become less steep

This can be seen in Fig. 2.6.2:

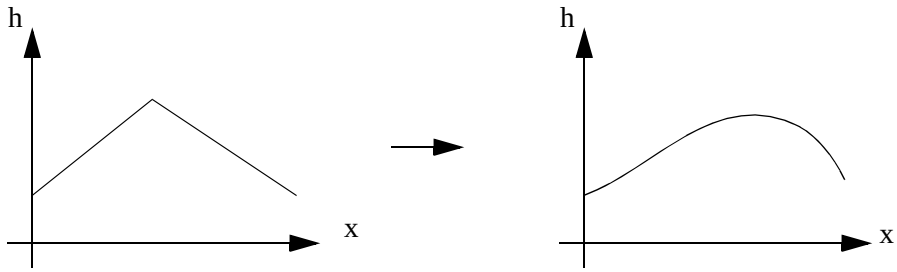

Figure 2.6.2. Change of wave shape over time. The initial wave is shown on the left. The water is flowing from the left to the right. The right figure shows the shape of the wave after some time. The front is steeper and the tail is less steep.

2.7 The Saint-Venant equations

A general flood wave for a one-dimensional situation is described by the Saint-Venant equations. Then the water velocity and water depth can vary both in time and along the one spatial dimension. The Saint-Venant equations is also called the full dynamic equation for computation of 1D flood waves.

The equation is derived by looking at a section of a channel as given in Fig. 2.7.1. The channel has a slope *I*, water depth *y*, width *B*, water discharge *Q* and velocity *U*.

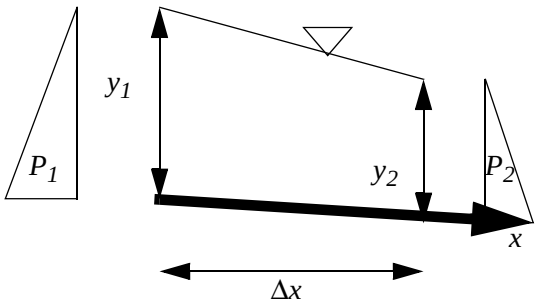

Figure 2.7.1 A longitudinal profile of a channel, between two sections 1 and 2. The distance between the sections is Δx. The water depth is denoted *y*. The bed slope is denoted I_0.

A continuity equation for this situation is first derived. Looking at the water discharge going out and in of the volume in the time period Δt, we obtain:

$$\Delta V = \left[Q - \left(Q + \frac{dQ}{dx}\Delta x \right) \right] \Delta t = -\frac{dQ}{dx}\Delta x \Delta t \qquad (2.7.1)$$

This amount of water must be equal to the volume change caused by ris-

ing/falling of the water level: $\frac{dy}{dt}$:

$$\Delta V = \frac{dy}{dt} B \Delta x \Delta t \tag{2.7.2}$$

Noting that B also may change as the water level rise/fall, one can instead write the equation as:

$$\Delta V = \frac{dA}{dt} \Delta x \Delta t \tag{2.7.3}$$

Where *A* is equal to the cross-sectional area of the flow. Note, in a rectangular channel, *B* is constant, and Eq. 2.7.2 is obtained.

Combining Eq. 2.7.1 and 2.7.3, the following equation is obtained:

Continuity equation:

$$\frac{dA}{dt} + \frac{dQ}{dx} = 0 \tag{2.7.4}$$

This is the continuity equation often used in connection with solving the Saint-Venant equation. The Saint-Venants equation itself is derived from Newton's second law:

$$\sum F = m\vec{a} \tag{2.7.5}$$

For the section in Fig. 2.7.1, The acceleration term on the right hand becomes:

$$m\vec{a} = \rho y B \Delta x \frac{dU}{dt} \tag{2.7.6}$$

Then the external forces on the volume are given. There are four forces:

1. Gravity component:

$$F_g = \rho g y B \Delta x I_0 \tag{2.7.7}$$

This is the same component as used for the derivation of the formula for the bed shear stress for uniform flow.

2. Bed shear stress:

$$F_b = -\tau B \Delta x \tag{2.7.8}$$

The term is negative, as the force is in the negative x-direction. Often, a friction slope is introduced:

$$I_f = \frac{\tau}{\rho g y} \tag{2.7.9}$$

The friction slope is computed from an empirical friction formula, for example the Manning's equation. The term then becomes:

$$F_b = -\rho g y I_f B \Delta x \tag{2.7.10}$$

3. Pressure gradient:

The pressure gradient is due to the different water level on each side of the element. The hydrostatic pressure force on a water cross-section in a rectangular channel is given as:

$$F = \frac{1}{2}\rho g B y^2 \tag{2.7.11}$$

For the control volume in Fig. 2.7.1, there are two forces, one on each side of the volume. The total force from the pressure gradient must therefore be the sum of these two hydrostatic forces.

$$F_p = \frac{1}{2}\rho g B {y_1}^2 - \frac{1}{2}\rho g B {y_2}^2 \tag{2.7.12}$$

The depth can be written as a function of the surface slope:

$$F_p = \frac{\rho g B}{2}\left[y^2 - \left(y + \frac{dy}{dx}\Delta x\right)^2\right] \tag{2.7.13}$$

$$F_p = \frac{\rho g B}{2}\left[y^2 - y^2 - \left(2\frac{dy}{dx} y \Delta x\right) - \left(\frac{dy}{dx}\Delta x\right)^2\right] \tag{2.7.14}$$

The last term contains a small number squared, so this is much smaller than the second last term. The last term is therefore neglected. This gives:

$$F_p = -\rho g\left(\frac{dy}{dx}\Delta x\right)(By) \tag{2.7.15}$$

The term is negative, because a positive depth-gradient will cause a pressure force in the negative x-direction.

4. Momentum term:

The momentum equation for the control volume is:

$$F_m = \rho Q(U_1 - U_2) = \rho U B y\left(U - \left(U + \frac{dU}{dx}\Delta x\right)\right) \tag{2.7.16}$$

$$F_m = -\rho U B y \frac{dU}{dx}\Delta x \tag{2.7.17}$$

The negative sign is because a positive velocity gradient will cause more momentum to leave the volume than what enters. This causes a force in the negative x-direction.

Setting the sum of all the four forces equal to the acceleration term, one obtains:

$$F_g + F_b + F_p + F_m = m\grave{a} \tag{2.7.18}$$

or:

$$\rho g y B \Delta x I_0 - \rho g y I_f B \Delta x - \rho g \frac{dy}{dx} \Delta x (By) - \rho U B \Delta x y \frac{dU}{dx} = \rho y B \Delta x \frac{dU}{dt} \quad (2.7.19)$$

Saint-Venant equation:

This can be simplified to:

$$g(I_0 - I_f) - g\frac{dy}{dx} = U\frac{dU}{dx} + \frac{dU}{dt} \quad (2.7.20)$$

The Saint-Venant equations must be solved by a numerical method. This is described in Chapter 3.

2.8 Measurements of water discharge in a natural river

There are several methods to measure the water discharge in a river. The most common method is to use a current meter and measure directly at various points in a cross-section of a river. This can be done at several water discharges, and a rating curve can be obtained, where the water discharge as a function of the water elevation is given. Using daily observations of the water levels, the curve can give a time series of the water discharge. This is used to predict floods and average water discharge in the river for use in hydropower plants or water supply.

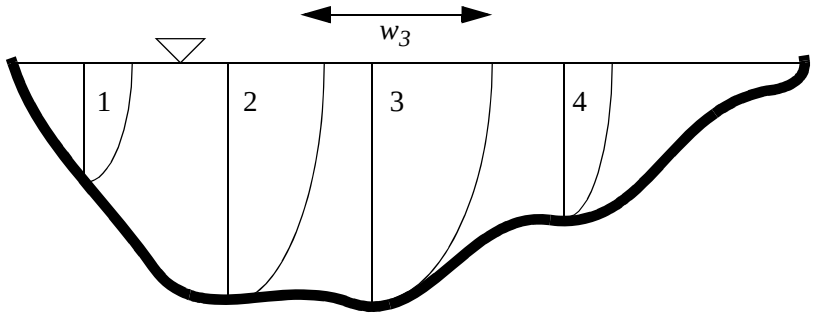

Figure 2.8.1 Cross-section with four measured velocity profiles. The average velocity in each profile is computed and multiplied with the depth and the width, *w,* of each sector. This is then summed up over all the profiles to get the water discharge.

Direct measurements of discharges in rivers today is usually done by an ADCP instrument. The ADCP is an abbreviation for Acoustic Doppler Current Profiler. The ADCP works by sending out an acoustic signal from the instrument into the water. Small particles in the water reflect the signal back to a receiver on the instrument. The signal will be a function of the speed of the particle relative to the instrument. By measuring at a large number of points in the cross-section, the discharge can be computed.

The ADCP is usually fitted on a boat which is dragged across the water surface in the cross-section. The beam of the instrument points vertically downwards, and measures several points in the vertical profile. An echo-sounding device is usually also included in the instrument, measuring the water depth. Modern ADCPs also have a bottom tracking device, measuring the distance the instrument has traversed. A GPS can also be fitted with the instrument, enabling correlation between measurements and for example a digital terrain model.

Figure 2.8.2 Picture of boat with ADCP for laboratory use.

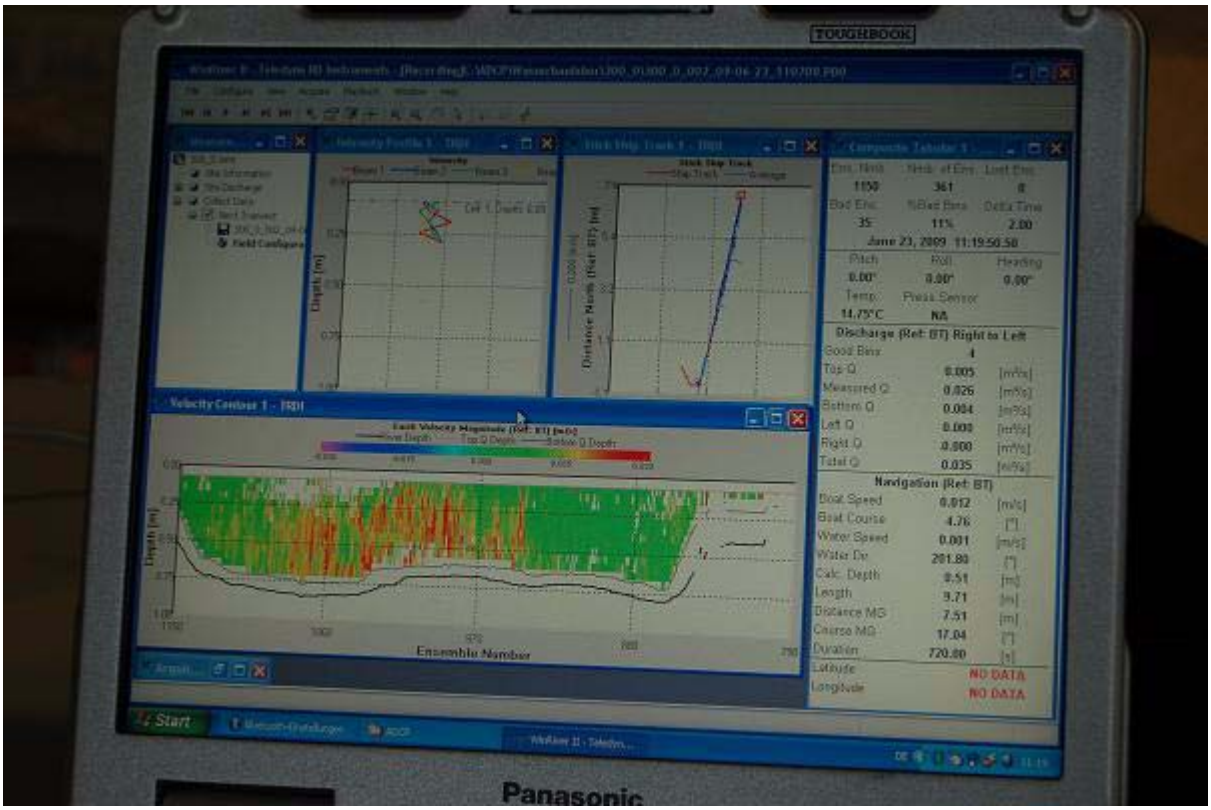

Figure 2.8.3 Example of results from the ADCP measurements

Another method is to use a tracer, for example radioactive material or a chemical that is easily measured for small concentrations in water. A known quantity, *m*, of the tracer is dumped in the river. Further downstream, where the tracer is completely mixed in the water, the concentration, *c*, is measured over time. The amount of tracer can be computed as:

$$m = \int cQdt \tag{2.8.1}$$

Assuming steady flow, the water discharge, *Q*, is constant. The quantity of tracer and the integral of the concentration measurement is known, so the discharge can be computed as:

$$Q = \frac{m}{\int cdt} \tag{2.8.2}$$

The method is expensive, as tracer is lost for each measurement. Also, the tracer may not be environmentally friendly. Therefore, the method is only used very seldom, and in situations where it is difficult to do point-velocity measurements. This can for example be during floods.

2.9 Problems

Problem 1. Uniform flow

A natural river with depth of 2 meters, has an average water velocity of 3 m/s. What is the maximum and minimum energy gradient? Is the flow supercritical or subcritical? Is this possible to see directly in the field?

Problem 2. Compound channel

A channel with the following cross-sectional geometry is considered:

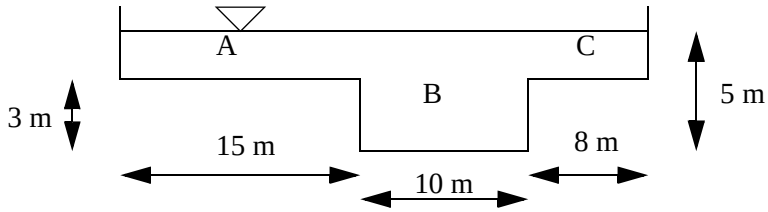

The channel can be divided in three sections, A, B and C. Section B is the main channel, and sections A and C are the overbanks. The slope of the channel is 1:500.

Compute the water discharge in the channel, given a Manning-Strickler coefficient of 60 for the whole channel.

Then, compute the water discharge in the channel given a Manning-Strickler coefficient of 60 for the main channel and 40 for the overbanks.

Problem 3. Steady non-uniform flow

Compute the water surface profile, using a spreadsheet, behind a low run-of-the river dam. The width of the river is 30 meters, the water discharge is 50 m^3/s, the dam height is 10 meters and the rivers slope is 1:400.

What happens if the slope is 1:100? Compute the water surface profile for this situation too.

Problem 4: Location of a hydraulic jump.

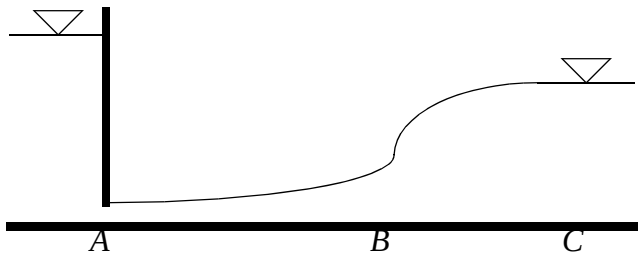

The figure shows a sketch of a longitudinal profile of the bed and water surface profile. Water is let out of a bottom outlet downstream a dam, at point *A*. At point *B*, a hydraulic jump occur. The water levels at point *A* and *C* are given, together with the water discharge. The question is to find the distance between *A* and *B*.

Data:

Water level (gate opening) at *A*: y_A=0.4 meters
Water level at *C*: y_C=3 meters
Discharge: Q=6 m^2/s.
Manning-Strickler coefficient: 50.

Problem 5. Discharge measurement using tracer

2 kg of tracer is dumped in a stream. Several km downstream, the following concentration is measured:

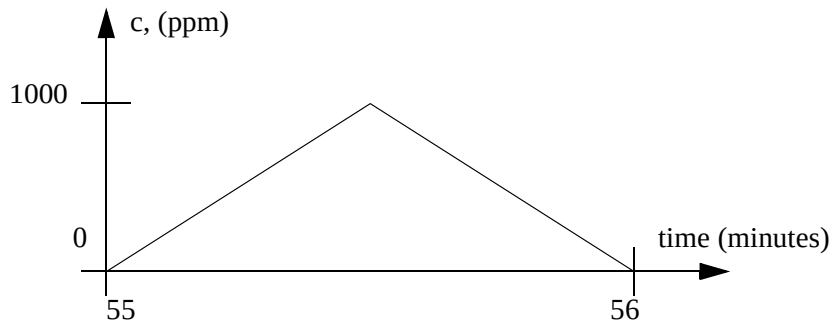

Compute the water discharge in the stream.

3. Numerical modelling of river flow in 1D

The 1D numerical model is the most commonly used tool in Hydraulic Engineering for evaluating effects of flood waves in rivers. Dispersion of pollutants in rivers is also mostly done using 1D models.

3.1 Steady flow

The steady flow computation uses the continuity equation and an equation for the friction loss to compute the velocity and location of the water surface. Manning's formula (Eq. 2.2.1) is most commonly used.

The computation starts with measuring the geometry of a number of cross-sections in the river. The distance and elevation of a number of points in the cross-sections are recorded. The distances between the cross-sections are also measured.

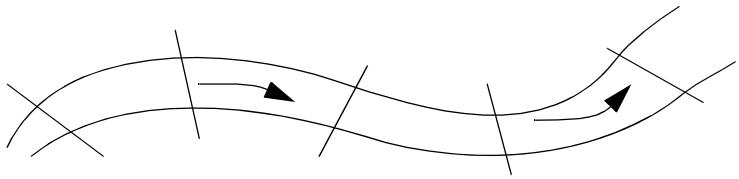

Figure 3.1.1. Sketch of a river with cross-sections.

For each section, a curve is made with the wetted area as a function of the water level. This curve is used in the following computations.

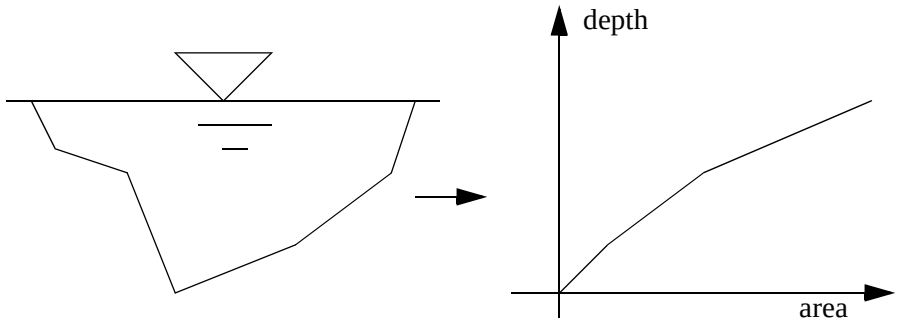

Figure 3.1.2. Generation of the curve for the cross-sectional area as a function of the water depth. The curve is used as geometry input for the numerical models.

The computation of the water elevation usually starts with a given value downstream, as this is the controlling value for subcritical flow. Then the water elevation of the upstream cross-section is to be found. The procedure outlined in Chapter 2.5 can be used, applying Eq. 2.5.9. Alternatively, a variation of the method is given in the following.

The energy loss between the cross-sections can be found by solving Manning's equation with respect to the friction slope:

$$I_f = \frac{U^2}{M^2 R^{\frac{4}{3}}} \qquad (3.1.1)$$

One problem is how to determine the friction coefficient, *M*. Usually, a calibration procedure has to be done, where the results are compared with measured water levels, and the *M* values adjusted to fit the data. Some data programs include automatic calibration procedures using this concept.

The hydraulic radius, *R*, is found from a similar curve as given in Fig. 3.1.2. Looking at Fig. 3.1.3, the water surface elevation difference, Δz, between the cross-sections can then be found using the Energy equation, giving:

$$z_1 - z_2 = \Delta z = I_f \Delta x + \left(\frac{U_2^2}{2g} - \frac{U_1^2}{2g} \right) \quad (3.1.2)$$

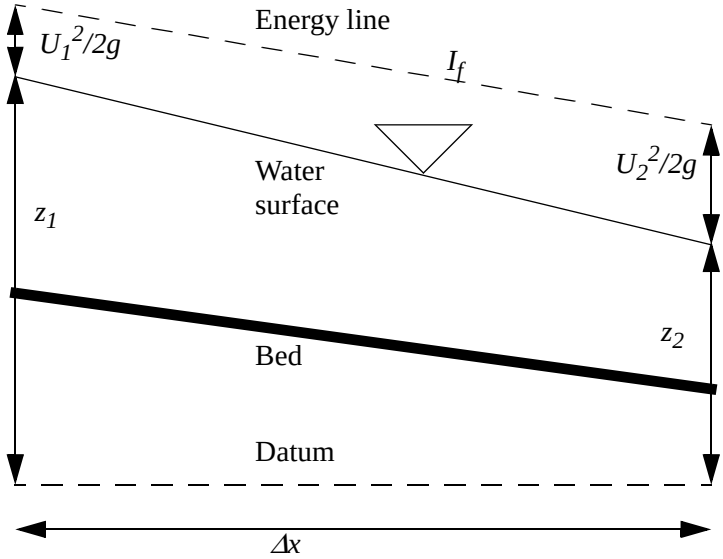

Figure 3.1.3 A longitudinal profile of a channel is shown, between two cross-sections 1 and 2. The distance between the sections is *dx*. The elevation of the water is denoted *z*. The slope of the energy line is denoted I_f.

The distance, Δx, between the cross-sections is given by the user. The water velocities at the two cross-sections 1 (upstream) and 2 (downstream) is computed from the water continuity equation:

$$U = \frac{Q}{A} \quad (3.1.3)$$

where the water discharge, *Q*, is a constant

The procedure is then to guess a value of Δz, giving the water level for both cross-sections. Then *A* and *R* are taken from the curves for the two cross-sections, and the average values used in Eq. 3.1.1. The velocities in Eq. 3.1.2 are computed from Eq. 3.1.3. Eq. 3.1.2 then gives a new estimate of Δz. After a few iterations, the values of Δz should be the same as the previous iteration, and the procedure has converged. The solution method is usually not sensitive to the initially guessed value, so for example Δz=0.0 could be used.

Control sections

Eq. 3.1.6 gives the changes in the water surface between two cross-sections. The question is then which cross-section should be used to start the computations.

For supercritical flow, the water surface is mainly determined by the upstream flow. Remember, the kinematic wave theory showed that a wave could not propagate upstream in supercritical flow. For subcritical flow, the flow is usually determined by the downstream water level. This means that the computations should start upstream and move downstream in supercritical flow. For subcritical flow, the computations should start downstream and move upstream.

Before starting the computations, the controlling sections should be determined. A typical example is a critical flow section, where the flow

goes from subcritical to supercritical. The computations can then start in this section and move upstream in the subcritical flow. It can also move downstream in the supercritical flow.

Another control for the water levels are reservoirs and lakes. Then the water surface is given. Usually, the flow is subcritical upstream of the lake. Then the computation starts in the lake and moves upstream.

One of the main problems is when the flow turns from supercritical to subcritical. A hydraulic jump will then form, and special algorithms based on the momentum equation have to be used. Often, these algorithms are not very stable, and it may be problematic to get a solution.

3.2 Unsteady flow

The one-dimensional water flow is governed by the Saint-Venant equations: water continuity:

$$\frac{\partial A}{\partial t} + \frac{\partial Q}{\partial x} = 0 \qquad (3.2.1)$$

and conservation of momentum:

$$\frac{\partial U}{\partial t} + U\frac{\partial U}{\partial x} + g\frac{\partial y}{\partial x} - g(I_b - I_f) = 0 \qquad (3.2.2)$$

The 1D models can be classified according to how many terms are used in Eq. 3.2.2. Solving the full Saint-Venant equations are described in Chapter 3.4. One simplification is to neglect the two first terms. This is called the equations for the diffusive wave:

$$g\frac{\partial y}{\partial x} - g(I_b - I_f) = 0 \qquad (3.2.3)$$

If the first three terms in Eq. 3.2.2 is neglected, the kinematic wave equation emerges:

$$g(I_b - I_f) = 0 \qquad (3.2.4)$$

Additionally, the continuity equation (3.2.1) is solved.

The solution of the kinematic wave equation is described in Chapter 3.3. The Muskingum method, or Hydrological routing, only uses the continuity equation. This method is described in Chapter 3.5.

3.3 Unsteady flow - kinematic wave

The simplest method to compute unsteady flow in a river is by the kinematic wave equation. There are several solution methods for this equation. Two methods are described here:

- Solution by differentials
- Analytical solution

Solution by differential is the standard form of solving wave equations. However, the kinematic wave is so simple that it is also possible to use

an analytical solution.

Analytical solution

The solution method is based on Eq. 2.6.9, the formula for the wave velocity, *c*:

$$c = KU \tag{3.3.1}$$

In Chapter 2 this equation was derived for a wide, rectangular channel, giving *K*=5/3. For a natural channel, *K,* may vary between 1.3 and 1.6.

The algorithm is based on tracking points in the hydrograph of the wave. For each point, the water depth and water velocity is computed, based on Manning's formula and the continuity equation. Then Eq. 3.3.1 is used to compute the wave speed. The time to travel a given distance to a downstream cross-section is then computed for each point in the hydrograph. An example is given in Table 3.3.1, taken from a spreadsheet. The spreadsheet is computed from left to right.

Table 3.3.1 Analytical computation of kinematic wave

Time for X=0 given as input data (min)	Discharge Given as input data (m^3/s)	Velocity from Manning's formula (m/s)	Depth, from continuity equation (m)	Wave speed, c, From Eq. 3.3.1 (m/s)	Time for X=5000 meters (min)	Time for X=10000 meters (min)
0	100	2.30	0.58	3.83	21.8	43.5
10	200	3.03	0.883	5.05	26.5	43.0
20	300	3.56	1.126	5.94	34.0	48.1
30	400	4.00	1.330	6.66	42.5	55.0
40	300	3.56	1.12	5.94	54.0	68.1
50	200	3.03	0.88	5.05	66.5	83.0
60	100	2.30	0.58	3.83	81.8	103.5

The table is computed for a wide channel with width of 500 meters, a slope of 1/200 and a Manning-Stricklers value of 60. Mannings equation and the continuity equations are two equations that are used to compute the two parameters *U* and *y*.

Using the continuity equation to eliminate *y* in Mannings equation gives:

$$U = M^{\frac{3}{5}} Q^{\frac{2}{5}} I^{\frac{3}{10}} B^{\frac{-3}{10}}$$

The result is in the two columns to the right in the spreadsheet, 5000 and 10 000 meters downstream. The time, *T*, in these columns are computed by the following equation:

$$T = T_0 + \frac{X}{c} \tag{3.3.2}$$

The use of the Mannings formula in the table is derived using the continuity equation to eliminate the water depth:

$$U = MI^{\frac{1}{2}}\left(\frac{Q}{UB}\right)^{\frac{2}{3}} \quad \text{or} \quad U = \left(\frac{MI^{\frac{1}{2}}Q^{\frac{2}{3}}}{B^{\frac{2}{3}}}\right)^{\frac{3}{5}} \tag{3.3.3}$$

Solution by differentials

There exist more involved methods to compute the kinematic wave. The continuity equation and a formula for the normal depth in a reach is then used. Note that Eq. 3.2.4 for the kinematic wave gives that the energy slope is equal to the bed slope. This means the flow is uniform, and a friction formula can be used, for example Manning's formula. If the velocity in this formula is replaced by Q/A, and the definition of the hydraulic radius is used, the following derivation can be made:

$$I_0 = I_f = \left(\frac{U}{Mr^{\frac{2}{3}}}\right)^2 = \left(\frac{QP^{\frac{2}{3}}}{AA^{\frac{2}{3}}M}\right)^2 \tag{3.3.4}$$

Solved with respect to A:

$$A = \left(\frac{P^{\frac{2}{5}}}{I_0^{\frac{3}{10}}M^{\frac{3}{5}}}\right)Q^{\frac{3}{5}} \tag{3.3.5}$$

The equation can be differentiated with respect to time, assuming that P, I_0 and M are constants:

$$\frac{dA}{dt} = \frac{3}{5}\left(\frac{P^{\frac{2}{5}}}{I_0^{\frac{3}{10}}M^{\frac{3}{5}}}\right)Q^{-\frac{2}{5}}\frac{dQ}{dt} \tag{3.3.6}$$

The continuity equation can be used:

$$\frac{\partial Q}{\partial x} + \frac{\partial A}{\partial t} = 0 \tag{3.3.7}$$

Combining Eq. 3.3.6 and Eq. 3.3.7 enables the elimination of A and gives an equation where only Q is unknown:

$$\frac{\partial Q}{\partial x} + \frac{3}{5}\left(\frac{P^{\frac{2}{5}}}{I_0^{\frac{3}{10}}M^{\frac{3}{5}}}\right)Q^{-\frac{2}{5}}\frac{\partial Q}{\partial t} = 0 \tag{3.3.8}$$

Assuming the term in the bracket is constant, the equation can be solved using first-order differences for time and second-order differences for

space. A notation of two subscripts is used, where the first subscript, i, denotes the space direction and the second, j, the time:

$$\frac{\partial Q}{\partial x} \approx \frac{Q_{i+1,j} - Q_{i-1,j}}{2\Delta x} \qquad (3.3.9)$$

$$\frac{\partial Q}{\partial t} \approx \frac{Q_{i,j+1} - Q_{i,j}}{\Delta t} \qquad (3.3.10)$$

Using these two equations we can transform Eq. 3.3.8 to:

$$\frac{Q_{i+1,j} - Q_{i-1,j}}{2\Delta x} + \frac{3}{5}\left(\frac{P^{\frac{2}{5}}}{I_0^{\frac{3}{10}} M^{\frac{3}{5}}}\right) Q_{i,j}^{-\frac{2}{5}} \frac{Q_{i,j+1} - Q_{i,j}}{\Delta t} = 0 \qquad (3.3.11)$$

Index *i* is used for the space dimension and *j* for the time. Given an initial situation, Eq. 3.3.11 can be solved with respect to $Q_{i,j+1}$ to give a formula for the discharge at a node as a function of the discharges at the nodes in the previous time step:

$$Q_{i,j+1} = Q_{i,j} - \left[\frac{5}{3}\frac{I_0^{\frac{3}{10}} M^{\frac{3}{5}}}{P^{\frac{2}{5}}} Q_{i,j}^{\frac{2}{5}} \frac{(Q_{i+1,j} - Q_{i-1,j})}{2\Delta x}\Delta t\right] \qquad (3.3.12)$$

The equation can be solved numerically using a spreadsheet, if there exist simple formulas for *P* as a function of the discharge. One axis in the spreadsheet is the distance *x*, and the other axis is the time.

Example: Solution by differentials.

Compute the water discharge at cross-section 5 at time step 11 minutes, when water discharge at time step 10 minutes are given as:

Cross-section 4: Q=203 m^3/s
Cross-section 5: Q=195 m^3/s
Cross-section 6: Q=188 m^3/s.

Assume a time step of one minute, and that the cross-sections are 200 meters apart. The bed slope is 1:400 and the Manning-Stricklers coefficient is 66. The wetted perimeter is 54 meters at cross-section 5 for this discharge.

Solution: We give the numbers to equation 3.3.12:

$$Q_{5,11} = 195 - \left[\frac{5}{3}\left[\frac{\left(\frac{1}{400}\right)^{\frac{3}{10}} x 66^{\frac{3}{5}}}{54^{\frac{2}{5}}}\right] 195^{\frac{2}{5}} \frac{(188 - 203)}{2x200}(60)\right]$$

The disharge is 208 m3/s.

Discussion

One simplification for the kinematic wave is assuming uniform flow on a reach. The water level is then a unique function of the water discharge. A rating curve showing the water levels at a gauging station during the passing of a flood, will get different values for the rising and the falling limb of the hydrograph. This is shown in Fig. 3.3.1. However, because of the simplifications, the kinematic wave method is not able to model this effect.

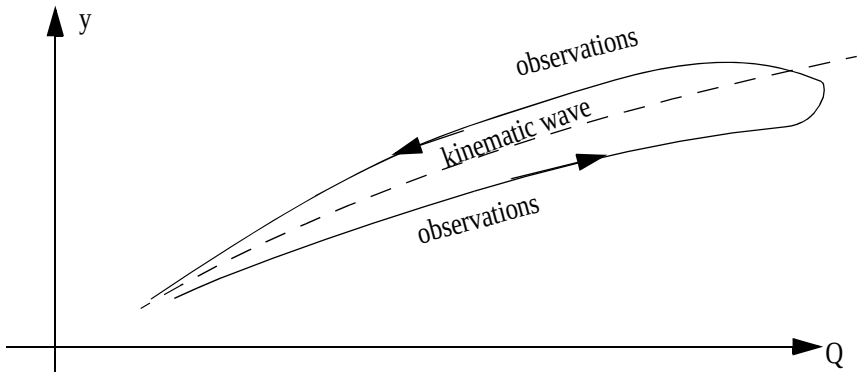

Figure 3.3.1. Rating curve during passing of a flood wave. The kinematic wave model gives the same values for the rising and falling of the hydrograph. The observations give different stage/discharge observations in the rising and falling of the hydrograph.

Another point to note is that the differential solution method introduces some errors, causing the maximum discharge for a wave to be **dampened**. This is not observed in the quasi-analytical solution method. However, it is noticed in field data. The damping of a real flood wave must not be confused with the damping introduced by inaccuracies in the numerical algorithm.

3.4 Unsteady flow - Saint-Venant equations

Solving the full Saint-Venant equations is done for dam-break modelling and other flood problems where there is a rapid change in the water depth over time, and the water discharge is significantly higher than the available calibration data.

The approach to solving the Saint-Venant equations is more involved than solving the kinematic wave equation. There exist a number of different solution methods, which can be divided in two groups:

- Explicit methods
- Implicit methods

Implicit/Explicit method

When the differences in space are to be computed, the question is if the values in time step *j* or time step *j*+1 should be used. If the values in time step *j* is used, an explicit solution is given. If the values at time step *j*+1 are used, an implicit solution is given. An implicit solution is more stable than an explicit solution, and longer time step can be used. An explicit solution is simpler to program.

The explicit computational molecule is seen in Fig. 3.4.1.

Often, the gradients are computed as a combination of values at time step *j* and time step *j*-1. A weighting factor, θ, is then used, where the final solution is θ times the gradients at time step *j*, plus (1-θ) times the gradients at time step *j*-1. This means if θ is 1, an implicit solution is given, and if θ is 0 the solution is explicit. If θ is between 0 and 1, the values at both time steps will be used. The method is then still said to be

implicit. The DAMBRK program uses a default value of 0.6 for θ, equivalent of using 60 % of the value at time step *j* and 40 % of the value at time step *j*-1.

Both the explicit and the implicit method are described in the following.

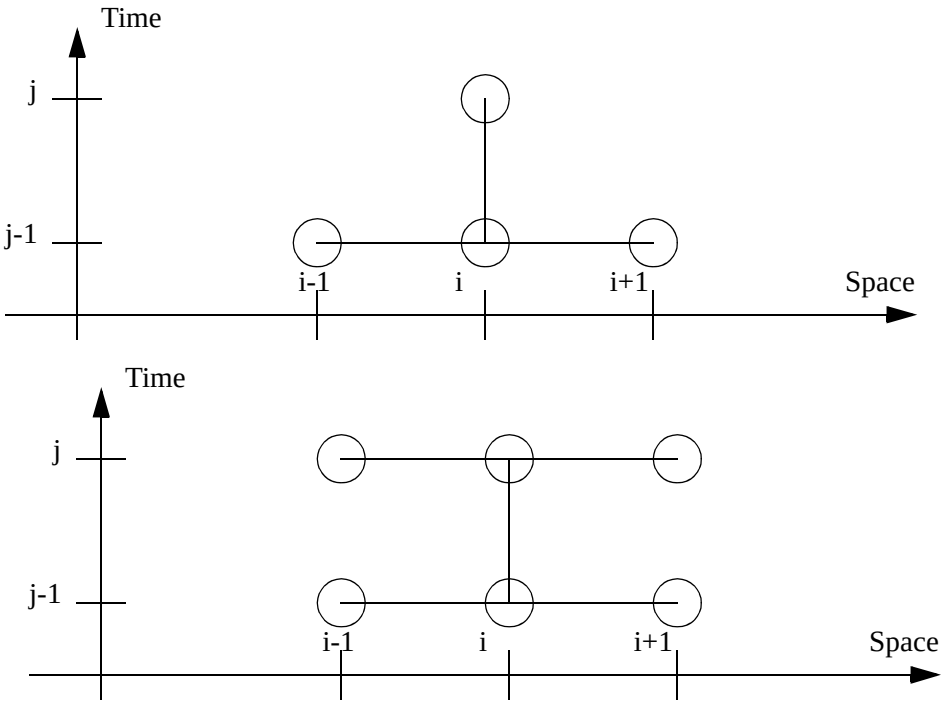

Figure 3.4.1 Nodes for computation molecule. The upper figure shows an explicit molecule and the lower figure shows an implicit molecule. For the explicit molecule, the value at node (*i,j*) is computed from nodes at the previous time step, *j*-1. The *i* nodes in the space direction is the different cross-sections.

Explicit method

The explicit solution is easier to solve than the implicit method. This can be seen from Fig. 3.4.1. The initial water discharge in the river is known, so the first computation starts with the next time step. For each cross-section, *i*, the discharge can be computed from the discharges at the previous time step. This is repeated for all cross-sections, and the discharges at the time step *j* is computed by one sweep. Then the computation proceeds to the next time step.

What is needed is a formula for the water discharge at time step *j* as a function of the discharges at time step *j*-1. This is obtained by discretizing Eq. 3.2.1 and Eq. 3.2.2. For a rectangular channel with depth *y* and width *B*, the continuity equation, Eq. 3.2.1, becomes

$$B\frac{\partial y}{\partial t} + B\frac{\partial (yU)}{\partial x} = B\frac{\partial y}{\partial t} + B\left(U\frac{\partial y}{\partial x} + y\frac{\partial U}{\partial x}\right) = 0 \qquad (3.4.1)$$

The *B*'s are eliminated and *y* and *U* is taken to be the value at the previous time step. The following differentials are used:

$$\frac{\partial U}{\partial x} = \frac{U_{i+1,j-1} - U_{i-1,j-1}}{2\Delta x} \qquad (3.4.2)$$

$$\frac{\partial y}{\partial x} = \frac{y_{i+1,j-1} - y_{i-1,j-1}}{2\Delta x} \tag{3.4.3}$$

$$\frac{\partial y}{\partial t} = \frac{y_{i,j} - y_{i,j-1}}{\Delta t} \tag{3.4.4}$$

$$\frac{y_{i,j} - y_{i,j-1}}{\Delta t} + \left(U_{i,j-1} \frac{y_{i+1,j-1} - y_{i-1,j-1}}{2\Delta x} + y_{i,j-1} \frac{U_{i+1,j-1} - U_{i-1,j-1}}{2\Delta x} \right) = 0 \tag{3.4.5}$$

The equation is solved with respect to the water depth at time step j:

$$y_{i,j} = y_{i,j-1} - \frac{\Delta t}{2\Delta x}[U_{i,j-1}(y_{i+1,j-1} - y_{i-1,j-1}) + y_{i,j-1}(U_{i+1,j-1} - U_{i-1,j-1})] \tag{3.4.6}$$

In a similar way, the Saint-Venant equation itself (Eq. 3.2.2) can be discretized as:

$$\frac{U_{i,j} - U_{i,j-1}}{\Delta t} + U_{i,j-1} \frac{(U_{i+1,j-1} - U_{i-1,j-1})}{2\Delta x} + g \frac{y_{i+1,j-1} - y_{i-1,j-1}}{2\Delta x} = g(I_0 - I_f) \tag{3.4.7}$$

where

$$I_f = \frac{|U_{i,j-1}| U_{i,j-1}}{M^2 r_i^{\frac{4}{3}}} \tag{3.4.8}$$

The source code in C for the explicit solution of Saint-Venant equations is given in Appendix I.

is taken from Mannings equation.
Eq. 3.4.6 can be solved with respect to $U_{i,j}$:

$$U_{i,j} = U_{i,j-1} - U_{i,j-1} \frac{(U_{i+1,j-1} - U_{i-1,j-1})\Delta t}{2\Delta x} - \frac{g\Delta t(y_{i+1,j-1} - y_{i-1,j-1})}{2\Delta x} + g\Delta t(I_0 - I_f) \tag{3.4.9}$$

The explicit procedure then becomes:

1. Guess starting values of *U* and *y* along the channel.
2. Determine inflow values of *U* and *y*
3. Repeat for each time step
   4. Repeat for each cross-section of a time
      5. Compute the water level, *y*, from Eq. 3.4.6
      6. Compute I_f from Eq. 3.4.8
      7. Compute the water velocity, *U*, from Eq. 3.4.9
   End of repetition 4

End of repetition 3

The explicit procedure will become unstable if the time step is chosen too large. The Courant criteria says the time step should be smaller than what would be required to make a water particle pass from one cross-section to another:

$$\Delta t < \frac{\Delta x}{(|U| + c)} \tag{3.4.10}$$

This criteria is only theoretical. Sometimes it is necessary to use an even smaller time step. Fig. 3.4.2 shows a numerical simulation of antidunes (described in more details in Chapter 9). The upper figure shows the correct result with a time step of 0.5 milliseconds. The lower figure shows the result with a time step of 1 milliseconds.

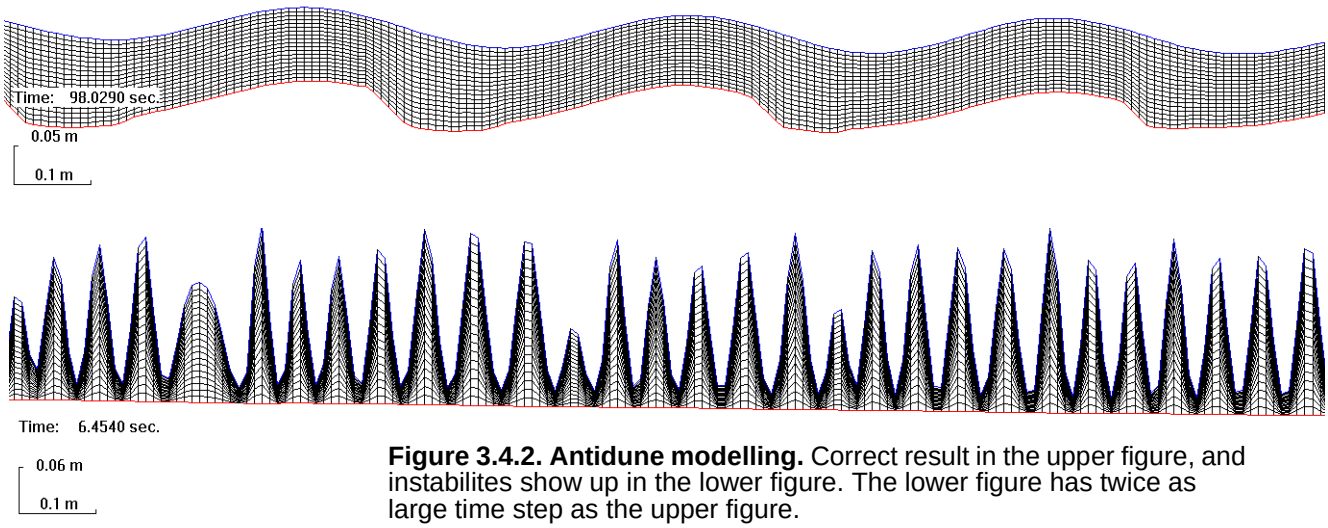

Figure 3.4.2. Antidune modelling. Correct result in the upper figure, and instabilites show up in the lower figure. The lower figure has twice as large time step as the upper figure.

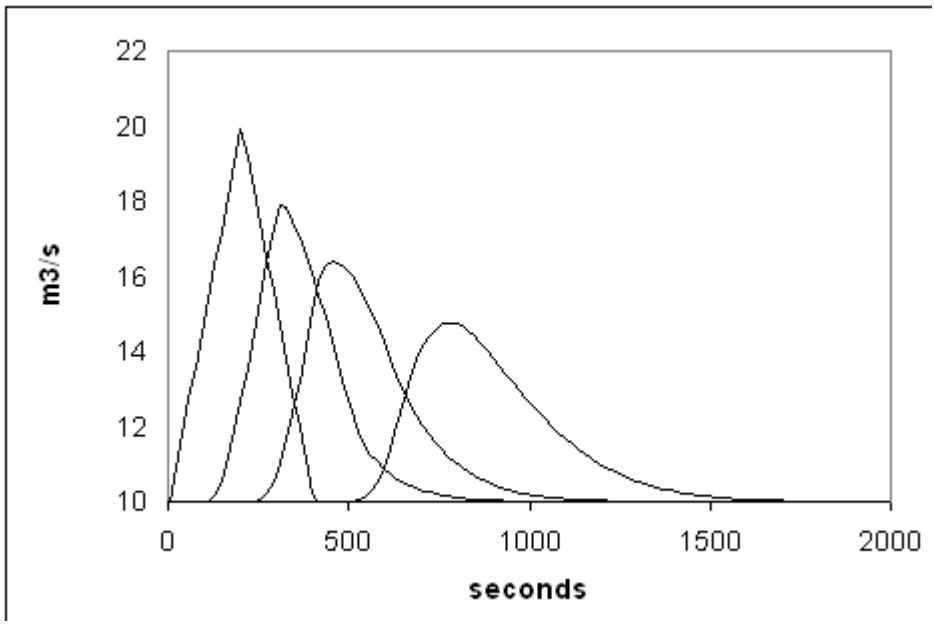

Figure 3.4.2 Example of a flood wave routed downstream a channel using the full Saint-Venant equations and an explicit solver. The channel has a slope of 1:200, and a Manning's M value of 30 was used. The vertical axis is the water discharge, and the horizontal axis is the time in seconds. The different curves show the hydrograph at 0, 1250, 2500 and 5000 meters downstream. The initial hydrograph has the triangular shape. A time step of 3 seconds was used. The source code written in *C* to generate this figure is given in Appendix I.

Control volume approach

The explicit procedure is still fairly unstable in the form given above. An improvement in stability can be obtained by considering a control volume approach when discretizing the continuity equation:

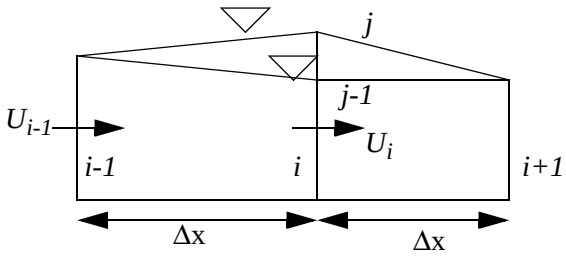

Fig. 3.4.3. Figure for control volume approach to discretization of continuity equation

Fig. 3.4.3 shows a longitudinal part of the river, with three cross-sections: *i*-1, *i* and *i*+1. It also shows two water surfaces. One surface is at time step *j*-1, and the other is at time step *j*. The purpose of the algorithm is to compute the water level at section *i*, for time step *j*. This is done on the basis of the fluxes in and out of the volume upstream of *i*:

Inflow: $I = \overline{U}_{i-1} * \overline{y}_{i-1}$ or

$$I = \frac{(U_{i-1,j-1} + U_{i-1,j})}{2}\frac{(y_{i-1,j-1} + y_{i-1,j})}{2} \qquad (3.4.11)$$

Outflow: $O = \overline{U}_i * \overline{y}_i$ or

$$O = \frac{(U_{i,j} + U_{i,j-1})}{2}\frac{(y_{i,j} + y_{i,j-1})}{2} = \overline{U}_i\frac{(y_{i,j} + y_{i,j-1})}{2} \qquad (3.4.12)$$

The overbar denotes average values over the time step.

The difference between the inflow and outflow is equal to the volume of the water between the surfaces at time *j* and *j*-1, during one time step. This gives:

$$\left[I - \overline{U}_i \frac{(y_{i,j} + y_{i,j-1})}{2}\right]\Delta t = 0.5(y_{i,j} - y_{i,j-1})2\Delta x \qquad (3.4.13)$$

or

$$y_{i,j} = \frac{I - y_{i,j-1}\left(\frac{\overline{U}_i}{2} - \frac{\Delta x}{\Delta t}\right)}{\frac{\Delta x}{\Delta t} + \frac{\overline{U}_i}{2}} \qquad (3.4.14)$$

This equation can be used to compute the water level at section *i*, starting from the upstream end going downstream. Then the values of *I* and U_i are known. This can be done after computing the velocities by solving the Saint-Venant equation. This procedure is implemented in the source code given in Appendix I

Implicit method

The procedure starts with discretization of each differential terms of Eq. 3.2.1 and Eq. 3.2.2 in space and time according to the figure below:

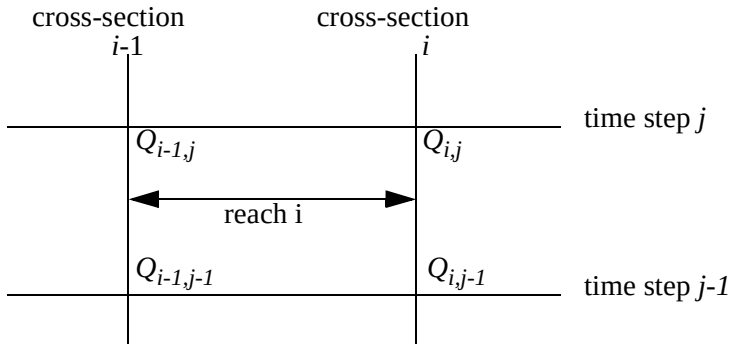

Figure 3.4.4. Discretization of terms between cross-section i and *i*-1, computing for time step *j*. Time step j-1 is the previous time step. This is called a four-point difference scheme.

The choice of using the water discharge instead of the velocity as a variable has been reported to give better stability.

The equations are transformed so that all the terms only have the two independent variables, *Q* and *y*. The rating curve where the cross-sectional area is given as a function of the water depth (Fig. 3.2.2) is also used.

After multiplication with *A*, the first term in Eq. 3.2.2 becomes:

$$A\frac{\partial U}{\partial t} = \frac{Q_{i,j} + Q_{i-1,j} - Q_{i,j-1} - Q_{i-1,j-1}}{2\Delta t} \qquad (3.4.15)$$

Using the chain rule and the continuity equation, the second term becomes:

$$AU\frac{\partial U}{\partial x} = \frac{A}{2}\frac{\partial (U)^2}{\partial x} = \frac{1}{2}\frac{\partial\left(\frac{Q^2}{A}\right)}{\partial x} \qquad (3.4.16)$$

Using finite differences, the term is transformed to:

$$AU\frac{\partial U}{\partial x} = \theta\frac{\left(\frac{Q^2}{A}\right)_{i,j} - \left(\frac{Q^2}{A}\right)_{i-1,j}}{2\Delta x} + (1-\theta)\frac{\left(\frac{Q^2}{A}\right)_{i,j-1} - \left(\frac{Q^2}{A}\right)_{i-1,j-1}}{2\Delta x} \qquad (3.4.17)$$

Note the weighting factor, θ, described below Fig. 3.4.1. The third term becomes:

$y = \theta y_j + (1-\theta)y_{j-1}$

$$Ag\frac{\partial y}{\partial x} = Ag\theta\frac{y_{i,j} - y_{i-1,j}}{\Delta x} + Ag(1-\theta)\frac{y_{i,j-1} - y_{i-1,j-1}}{\Delta x} \qquad (3.4.18)$$

The friction loss term is discretized by solving the Manning's equation:

$$gAI_f = \frac{\theta gAQ_j|Q_j|}{M^2A^2R^{\frac{4}{3}}} + \frac{(1-\theta)gAQ_{j-1}|Q_{j-1}|}{M^2A^2R^{\frac{4}{3}}} \qquad (3.4.19)$$

The variables are here averaged between section *i* and *i*-1.

The same procedure is used for the continuity equation (3.2.1). The transient term becomes:

$$\frac{\partial A}{\partial t} = \frac{A_{i,j} + A_{i-1,j} - A_{i,j-1} - A_{i-1,j-1}}{2\Delta t} \qquad (3.4.20)$$

The second term:

$$\frac{\partial Q}{\partial x} = \theta\frac{Q_{i,j} - Q_{i-1,j}}{\Delta x} + (1-\theta)\frac{Q_{i,j-1} - Q_{i-1,j-1}}{\Delta x} \qquad (3.4.21)$$

Additionally, there may be lateral inflow/outflow.

Evaluation of the equations

After the terms in the continuity and momentum equations are replaced by Eq. 3.4.18 and 3.4.19, the two equations will be in the form:

$$f_c(Q,y) = A_cQ_i + B_cQ_{i-1} + C_cy_i + D_cy_{i-1} + E_c = 0 \qquad (3.4.22)$$

$$f_m(Q,y) = A_mQ_i + B_mQ_{i-1} + C_my_i + D_my_{i-1} + E_m = 0 \qquad (3.4.23)$$

where *A, B, C, D* and *E* are functions of constants and variables at the previous time step and the indexes *c* and *m* denote the continuity and momentum equation, respectively. Note, all variables at time step *j-1* are known. The variables at time step *j* are unknown. The momentum equation and the continuity equation are applied to all reaches in the river between the cross-sections. Given boundary conditions, there are the same number of unknown as equations.

There are a number of methods for solving the equations. The two main groups are direct methods and iterative methods. In direct methods, the equations are set up in a matrix, which is inverted to get the solution (Brunner, 2010). In iterative methods, guesses are made for the variables, and Equations 3.4.7 and 3.4.8 are modified to get formulas for improvement of the guessed values.

Stability problems

or all values of the time step. However, a mixture of an explicit and a fully implicit solution as described in Fig. 3.4.1 will contain some elements an explicit solution and be unstable for large time steps. It may be possible to get a stable solution for Cournant numbers above 1, but seldom above 10. Then the explicit solution may still be preferred above the added complexity of an implicit solution.

As recommended by Brunner (2010), the user should always recompute a case with different time steps and distances bewtween the cross-sections, to assess the influence of these parameters.

Experience with solving the equations shows that convergence problems occur where there is supercritical flow. Many computer programs therefore implement special algorithms to deal with this situation. Some are more successful than others. If the algorithm in a given program fails, it is possible to avoid the problem by modifying the friction factor, *M*, so that only subcritical flow is present in the problematic area. The flood wave will then get a slower translation speed as the velocities are reduced. This must be taken into consideration when evaluating the results.

Boundary conditions

The upstream and downstream cross-section will need boundary conditions. There are several options:

1. User-specified values

This could typically be results from a dam break computation, which gives the water discharge as a function of time at the upstream boundary. Or if the downstream value is located in a lake or in the ocean, then the water elevation there is known.

2. A rating curve

This can be used if for example a weir is present at the downstream boundary, giving a unique relationship between discharge and water level.

3. Uniform flow approximation

The Mannings formula can be used to find the discharge if uniform flow is assumed.

4. Zero gradient boundary condition.

This is typically used at the downstream boundary. The depth and/or discharge are assumed to be the same at the downstream boundary cross-section as the second most downstream cross-section.

The choise of boundary conditions must be made based on the available data and the hydraulic conditions in the river.

3.5 Hydrologic routing

A simplified river routing method is the Muskingum algorithm. It is derived from the water continuity equation and some assumptions about the volume of the water in the river:

The volume, V_0, of water in the reach is assumed to be proportional to the steady water discharge, Q^o, flowing out of the reach:

$$V_0 = KQ^o \tag{3.5.1}$$

where K is a proportionality coefficient, with units [sec].

For unsteady flow, the water discharge **into** the reach is not always equal to the discharge **out of** the reach. If the inflow is denoted Q^i, the water continuity defect is assumed to take up a volume equal to:

$$V_D = KX(Q^i - Q^o) \tag{3.5.2}$$

X is another geometrical proportionality coefficient (dimensionless).

The total volume of water in the reach is therefore: $V=V_0+V_D$

$$V = KQ^o + KX(Q^i - Q^o) = K(XQ^i + (1-X)Q^o)) \tag{3.5.3}$$

The change in water volume in a reach between one time step j, and the next time step j+1 becomes:

$$V_{j+1} - V_j = K\{[XQ^i_{j+1} + (1-X)Q^o_{j+1}] - [XQ^i_j + (1-X)Q^o_j]\} \tag{3.5.4}$$

From the continuity equation, the volume change can also be written:

$$V_{j+1} - V_j = \frac{1}{2}(Q^i_j + Q^i_{j+1})\Delta t - \frac{1}{2}(Q^o_j + Q^o_{j+1})\Delta t \tag{3.5.5}$$

Combining the two equations and solving with respect to Q^o_{j+1}, the following equation is obtained:

$$Q^o_{j+1} = C_1 Q^i_{j+1} + C_2 Q^i_j + C_3 Q^o_j \tag{3.5.6}$$

Expressions for the C's as functions of X, K and Δt are:

$$C_1 = \frac{\Delta t - 2KX}{2K(1-X) + \Delta t} \quad (3.5.7)$$

$$C_2 = \frac{\Delta t + 2KX}{2K(1-X) + \Delta t} \quad (3.5.8)$$

$$C_3 = \frac{2K(1-X) - \Delta t}{2K(1-X) + \Delta t} \quad (3.5.9)$$

By combining Eq. 3.5.4 and 3.5.5, the following expression for K is obtained:

The parameters in the Muskingum method are based on observed discharges. If floods higher than the observed values are to be computed, the coefficients may not be correct. The Muskingum method can then not be used.

$$K = \frac{0.5\Delta t[(Q_j^i + Q_{j+1}^i) - (Q_j^o + Q_{j+1}^o)]}{X(Q_{j+1}^i - Q_j^i) + (1-X)(Q_{j+1}^o - Q_j^o)} \quad (3.5.10)$$

The Muskingum method determines the *C* values from observed hydrographs. The numerator and denominator in Eq. 3.5.10 is computed and plotted for each time interval for different values of *X*. The value giving the straightest line is chosen, and *K* is then the slope of this line. From these values of *K* and *X*, Eq. 3.5.7-9 are used to compute $C_{1\text{-}3}$. When the *C*'s are given, the water discharge can be determined from Eq. 3.5.6.

3.6 HEC-RAS

HEC is an abbreviation for **H**ydrologic **E**ngineering **C**enter. RAS is an abbreviation for **R**iver **A**nalysis **S**ystem. HEC is a part of US Army Corps of Engineers. Over the years, the organization has made several computer programs for water flow problems, named HEC1, HEC2 etc. HEC2 computed the water surface profile for a steady water flow in a natural river in one dimension. The solution procedure followed the theory in Chapter 3.2.

HEC-RAS is freeware, and can be downloaded from the Internet. It is much used by Norwegian consulting companies and water authorities.

The original HEC2 program did not have a user interface. It read an ASCII input file with all the necessary information about water discharge, friction factors, geometry etc. The result was an output file with the computed water levels. Later, a graphic user interface for the program was made, with interactive input of data and visualization of results. This version is called HEC-RAS. The most recent version of HEC-RAS includes algorithms for computing unsteady flow, including mixed flow regime between supercritical and subcritical flow. It also has a dam break analysis module, and connection to GIS programs. Version 4 came out in 2008 and has sediment transport with movable bed and water quality computations. A 2D version came in 2016, and very fast became popular in Norway.

3.7 Commercial software

Because the initial HEC2 program was limited in functionality and graphics, there was a period of time in the 1990's where there were a market for commercial software for hydraulic engineering. The purpose was often analysis of flooding and dam-breaks. Several commercial programs were developed, and some are briefly described below.

DAMBRK

DAMBRK is made by the US National Weather Service. It consist of two parts:

- A program for computing the outflow hydrograph from a reservoir where the dam is breaking
- Routing of the hydrograph downstream, by solving the Saint-Venant equations.

The program is in principle freeware, and the source code is publicly available. The original version did not have a user interface, but commercial companies have made user interfaces and these are sold together with the program. An example is BOSS DAMBRK.

There also exist two programs for separate computations of the dam break hydrograph and the flood routing, made by the same organization. The program computing the hydrograph is called BREACH. The program computing only the routing of the flood wave is called DWOPPER.

MIKE11

MIKE 11 is used by Norwegian consulting companies and The Norwegian Water Resources and Energy Directorate for flood zone mapping.

MIKE 11 is made by the Danish Hydraulic Institute. It is a one-dimensional program with both steady state water surface profile computation and solution of the full Saint-Venant equations. The program has a graphical user interface, and program includes connections with GIS systems. MIKE 11 has a number of different add-on modules, computing for example:

- rainfall/runoff
- water quality
- sediment transport
- groundwater

The modules makes MIKE 11 very well suited for a solving a number of different hydraulic river problems.

ISIS is the most used tool by consulting companies in the UK for river flow computatitons.

ISIS

ISIS is made by Hydraulic Research Wallingford, in the UK. It is similar in functionality to MIKE11, with a graphical user interface and computational modules for one-dimensional steady and unsteady flow. It also has a number of add-on modules.

3.8 Problems

Problem 1. Coefficients

Derive formulas for the coefficients C_1, C_2, and C_3 in Eqs. 3.5.7-9. This is done by combining Eq. 3.5.4 and 3.5.5, eliminating the volumes V, and solving with respect to Q^o_{t+1}, The resulting equation is compared with Eq. 3.5.6, giving the coefficients.

Problem 2. Flood wave

Water is released from a dam, with the outflow hydrograph given in the figure below. The river downstream is 50 m wide, and has stones with d_{90} of 0.2 meter. The river slope is 1:300. A town is located 2 km downstream of the dam. When will the water start to rise in the town? And when will the peak of the flood wave reach the town?

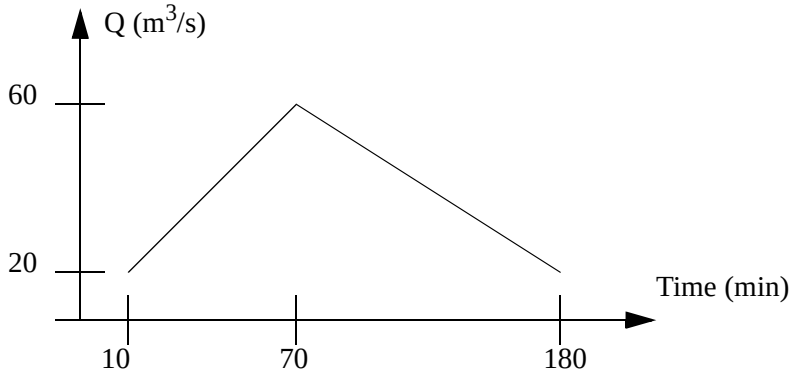

Use a computer program solving the Saint-Venant equation to compute the maximum water discharge at the town.

4. Dispersion of pollutants

4.1 Introduction

Numerical algorithms for solving the water velocity equations in 3D can be difficult to learn. It is sometimes easier to learn the algorithms when looking at dispersion of a pollutant than computing the water velocity. This is the reason why the dispersion processes are described before the computation of the water flow.

Dispersion is a combination of the two processes: convection and diffusion. Convection is pollutant transport by the time-averaged water velocity. This is relatively straightforward to compute. For our purposes, diffusion is caused by turbulence and velocity gradients, which are more complicated.

The most common method of modelling diffusion is by use of a turbulent diffusion coefficient, Γ, defined as:

$$\Gamma = \frac{\frac{F}{A}}{\left(\frac{dc}{dx}\right)} \qquad (4.1.1)$$

F is the flux of a pollutant with concentration *c*, passing through an area *A*, and *x* is the direction of the flux transport.

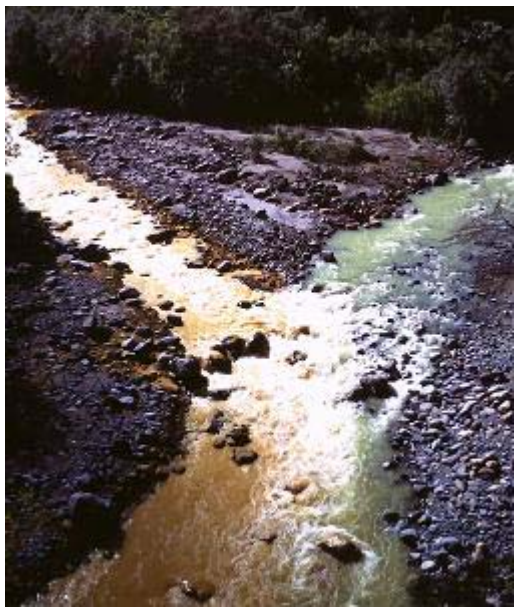

The picture shows the confluence of two small rivers in Costa Rica with different water quality. The branch on the left part of the picture comes from an area with volcanic activity. (Photo: N. Olsen)

4.2 Simple formulas for the diffusion coefficient

The diffusion coefficient, Γ, for diffusion of a toxic substance, can be set equal to the eddy-viscosity, ν_T, of the water. The relationship between the variables are given by the following formula:

$$\Gamma = \frac{\nu_T}{Sc} \qquad (4.2.1)$$

Sc is the Schmidt number. This has been found to be in the range of 0.5-1.0, but more extreme values have been used. In the following, we assume a value of 1.0, meaning the turbulent diffusion coefficient is equal to the eddy-viscosity.

Classical hydraulics give a number of empirical and semi-analytical formulas for the eddy-viscosity in rivers or lakes. For a river, the eddy-viscosity, ν_T, is used in the definition of the shear stress in a fluid:

$$\tau = \nu_T \rho \frac{dU}{dy} \qquad (4.2.2)$$

The equation can be solved with respect to ν_T:

$$\nu_T = \frac{\tau}{\rho \frac{dU}{dy}} \tag{4.2.3}$$

For a wide rectangular channel, Schlichting's wall laws (Eq. 2.1.2) gives the variation of the velocity with the depth. The vertical velocity gradient can be obtained by derivation of Eq. 2.1.2, with respect to the distance above the bed, *y*:

$$\frac{dU}{dy} = \frac{u_*}{\kappa y} \tag{4.2.4}$$

For a wide, rectangular channel, the shear stress increases linearly from the surface to the bed:

$$\tau = \tau_0 \left(1 - \frac{y}{h}\right) \tag{4.2.5}$$

The water depth is denoted *h*. Using the definition of the shear velocity, the equation can be rewritten:

$$\tau = \rho u_*^2 \left(1 - \frac{y}{h}\right) \tag{4.2.6}$$

Inserting Eq. 4.2.4 and Eq. 4.2.6 into Eq. 4.2.3:

$$\nu_T = \kappa u_* y \left(1 - \frac{y}{h}\right) \tag{4.2.7}$$

The average value over the depth is obtained by integrating Eq. 4.2.7 over the depth:

$$\overline{\nu_T} = \frac{1}{h} \int_0^h \frac{\kappa u_*}{h} (hy - y^2) dy = \frac{\kappa}{6} u_* h = 0.067 u_* h \tag{4.2.8}$$

Equation 4.2.8 is derived for an idealized case, with a wide straight channel with rectangular cross-section. Naas (1977) measured the eddy-viscosity in a number of natural rivers, and suggested the following formula instead:

$$\nu_T = 0.11 u_* h \tag{4.2.9}$$

Note that this formula is based on the vertical velocity gradients, so this gives the eddy-viscosity in the vertical direction.

The shear stress on a lake will also introduce turbulence in the water. A similar approach can be used as for a river, but now the shear stress is acting on the water surface instead of the bed. The result is a formula similar to Eq. 4.2.8 and 4.2.9, but a different empirical coefficient may be used.

4.3 One-dimensional dispersion

A typical example of a one-dimensional dispersion problem is pollution from a point-source into a river where the vertical and lateral mixing is large. Typical concentration profiles at several points in the river downstream of the spill is given in Fig. 4.3.1:

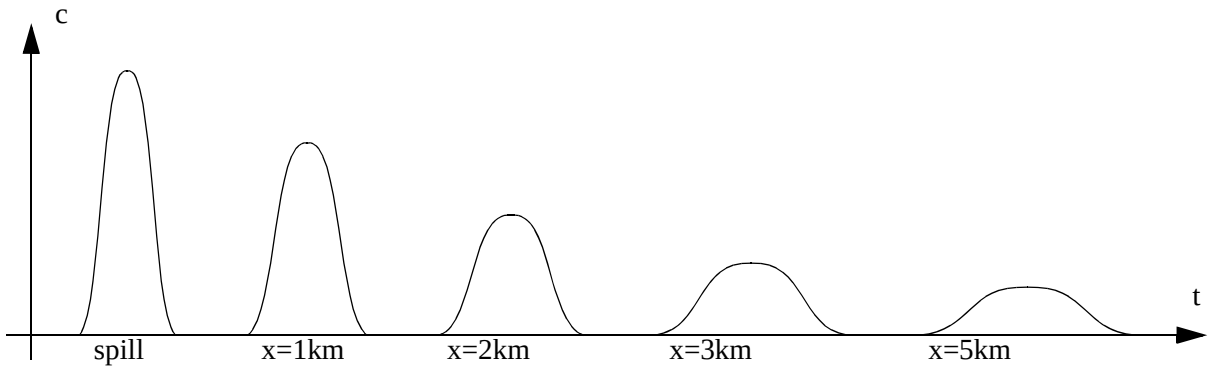

Figure 4.3.1 Time-series of concentrations at several locations downstream of a spill

The figure shows the two main processes:

- Convective movement of the point of maximum concentration
- Diffusion of the spill, with reduction of the maximum concentration

The transport can be described by a convection-diffusion equation for the pollutant concentration, *c*:

$$\frac{dc}{dt} + U\frac{dc}{dx} = \frac{d}{dx}\left(\Gamma\frac{dc}{dx}\right) \qquad (4.3.1)$$

The problem is to find the correct value of the longitudinal diffusion coefficient, Γ. The coefficient is not a function of small-scale turbulent processes. Instead, mixing in the longitudinal direction is often caused by convective movements due to lateral velocity gradients. The diffusion coefficient for a one-dimensional model of a river will be much larger than the small-scale turbulent diffusion used in multi-dimensional models.

Some researchers have developed empirical formulas for the longitudinal dispersion coefficient:

McQuivey and Keefer (1974):

$$\Gamma = 0.058\frac{Q}{IB} \qquad (4.3.2)$$

Fisher et. al. (1979)

$$\Gamma = 0.011\frac{(UB)^2}{Hu_*} \qquad (4.3.3)$$

Ahmad et al (1999)

$$\frac{\Gamma}{q} = 0.4\left(\frac{B}{R}\right)^{2.12}\left(\frac{U}{u_*}\right)^{-0.72} I^{0.19} \qquad (4.3.4)$$

Q is the water discharge in the river, with slope I, width B, hydraulic radius, R and depth H. U is the water velocity and u_* is the shear velocity. The discharge pr. unit width is denoted q.

The convection-diffusion equation can be solved analytically, assuming constant values of velocity and diffusion coefficient, giving (Chapra, 1997, p.182):

$$c(x,t) = \frac{c_0 L}{2\sqrt{\pi\Gamma t}} e^{-\frac{(x-Ut)^2}{4\Gamma t}} \qquad (4.3.5)$$

The initial concentration is denoted c_0, and the length of the spill in the river is denoted L.

Eq. 4.3.5 is derived based on simplifications that reduce the accuracy of the result. The equation may give a rough estimate of the concentration, but to get better accuracy it is necessary to solve the convection-diffusion equation numerically.

Looking at measurements of pollution concentration in a river, the profiles in Fig. 4.3.1 have an additional feature: a prolonged tail. It is caused by storage of pollution in recirculation zones and dead waters along the river. This effect is difficult to take into account using one-dimensional models. Instead, it is possible to model the river using a three-dimensional model, where the water flow field is modelled, including recirculation zones. This approach also have the advantage that the uncertainty with the longitudinal diffusion coefficient is eliminated. It is computed as a part of the solution of the equations. Research is ongoing in this area.

4.4 Jets and plumes

Jets and plumes are water entering a reservoir or a lake, for example from a river or a wastewater outlet. For an idealized case, there exist formulas for the dispersion of jets and plumes. The formulas can be derived analytically based on the momentum equation, but empirical coefficients are required when computing dispersion because of turbulence.

Close to the outlet, the momentum of the water will be a dominating force determining the flow field. This is then called a jet. Fig. 4.4.1 shows a jet close to the outlet:

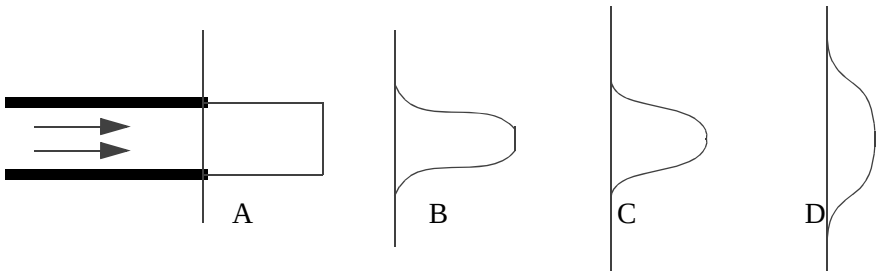

Figure 4.4.1 Velocity profiles at the core of a jet outlet. The entrance profile is denoted A, the core region ends at profile C. Profile B has uniform distribution at the core, but curved distribution at the edge. Profile D has reduced maximum velocity, as it is located after the core region.

Assuming a uniform velocity profile at the outlet, the jet will have a core where the velocity distribution changes. The length of the core is approximately 6 times the diameter of the outlet. In the core, the maximum velocity is constant. The water from the jet is mixed with the surrounding water, reducing the velocity in this area. The reduction of the velocity will finally take place also at the center of the jet. This point forms the end of the core.

After the core, the jet may moves in various directions, depending on:

- The geometry around the plume
- The density difference between the inflowing and the surrounding water
- The density stratification in the surrounding water
- The velocity field in the surrounding water
- The turbulence in the surrounding water.

A flow situation dominated by the **momentum** of the inflowing water is often called a **jet**. If the flow situation is dominated by the **density difference** between the inflowing and receiving water, this is often called a **plume**.

If the velocity of the surrounding water is very strong, this may also affect the jet in the core region.

For an idealized case, it is possible to derive formulas for the velocity and effective discharge after the outlet. Assuming the receiving water has no velocity, turbulence or density stratification, and its density is the same as the water in the jet, the momentum of the water stays the same in a cross-section of the jet. It is also assumed the jet will not interact with any geometry. The momentum equation, together with experiments then give the following equations for a jet from a circular pipe (Carstens, 1997):

$$\frac{u}{u_{max}} = \left(1 + \frac{r^2}{0.016x^2}\right)^{-2} \tag{4.4.1}$$

$$\frac{u_{max}}{u_0} = 6.4\left(\frac{x}{d_0}\right)^{-1} \tag{4.4.2}$$

$$\frac{Q}{Q_0} = 0.42\frac{x}{d_0} \tag{4.4.3}$$

The velocity is denoted u, r is the distance from the centerline of the plume, x is the distance from the pipe outlet, d_0 is the diameter of the pipe and Q_0 is the water discharge out of the pipe. Because the surrounding water will be mixed into the plume, the total water discharge, Q, in the jet will increase with the distance from the outlet.

The formulas are empirical. Fischer et al (1979) came up with slightly different coefficients: 6.2 instead of 6.4 in Eq. 4.4.2, and 0.28 instead of 0.42 in Eq. 4.4.3.

If the receiving water does not have the same density as the water from the pipe, the plume will rise or sink. A densimetric Froude number, *Fr'*, is often used to derive formulas for the plume.

Figure 4.4.2. A plume of hot smoke rises from a fire in the city of Trondheim. (Photo: N. Olsen)

$$Fr' = \frac{u_0}{\sqrt{\left(\frac{\rho_{res} - \rho_0}{\rho_{res}}\right) g d_0}} \tag{4.4.4}$$

It is assumed that plume water density, ρ_0, has a lower value than the recipient water density, ρ_{res}. The formulas below are given by Rouse et. al. (1952) from experiments:

$$\frac{u}{u_0} = 4.3 Fr'^{-\frac{2}{3}} \left(\frac{z}{d_0}\right)^{-\frac{1}{3}} e^{\left[-96\frac{r^2}{z^2}\right]} \tag{4.4.5}$$

$$\frac{\rho - \rho_{res}}{\rho_0} = 9 Fr'^{-\frac{2}{3}} \left(\frac{z}{d_0}\right)^{-\frac{5}{3}} e^{\left[-71\frac{r^2}{z^2}\right]} \tag{4.4.6}$$

$$\frac{Q}{Q_0} = 0.18 Fr'^{-\frac{2}{3}} \left(\frac{z}{d_0}\right)^{\frac{5}{3}} \tag{4.4.7}$$

It is assumed the pipe releases the water in the vertical direction.

Detailed derivations of the formulas, together with equations for more jet/ plume cases are given by Fisher et. al. (1979).

4.5 Problems

Problem 1. Dispersion in a river

Two thousand litres of a toxic chemical is spilled from a factory into a river during ten minutes. The river has a water discharge of 20 m^3/s, an average depth of 2 meters, and average width of 30 meters and a slope of 1:63. Ten kilometer downstream of the factory is a city. Compute the concentration of the chemical in the river at the city as a function of time.

Problem 2. Dispersion of a plume

A plume rises from a hydropower plant outlet into the sea. The sea water has a salinity of 3 %, and a density of 1023 kg/m^3. The water discharge is 50 m^3/s from a tunnel with diameter 3 meters. The water from the tunnel has a density of 1000 kg/m^3. The lake is 30 meters deep at the outlet point. What is the velocity of the water 20 meters right above the outlet? Assume no initial water currents or vertical stratification.

What will happen if there are currents in the lake?

5. Dispersion modelling in 2D and 3D

Dispersion modelling in 2D or 3D is conducted using a science called computational fluid dynamics, or CFD. This chapter gives an introduction to CFD, applied to modelling dispersion of pollutants.

5.1 Grids

A basic concept of CFD is to divide the fluid geometry into elements or cells, and then solve an equation for each cell. In the following text, the word cell will be used instead of element, to avoid confusion with the finite element method. The algorithms described in the following chapters are based on the finite volume method.

Grid classifications

Grids can be classified according to several characteristics:

shape
orthogonality
structure
blocks
grid movements
nesting
outblocking

The **shape** of the cells is usually triangular or quadrilateral:

Fig. 5.1.1. Grid shapes

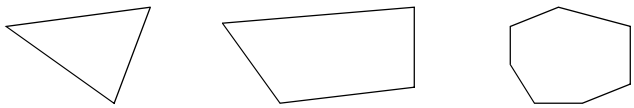

Triangular, quadrilateral and polyhedral shapes

The **orthogonality** of the grid is determined by the angle between crossing grid lines. If the angle is 90 degrees, the grid is orthogonal. If it is different from 90 degrees, the grid is non-orthogonal.

Fig. 5.1.2. Grid orthogonality

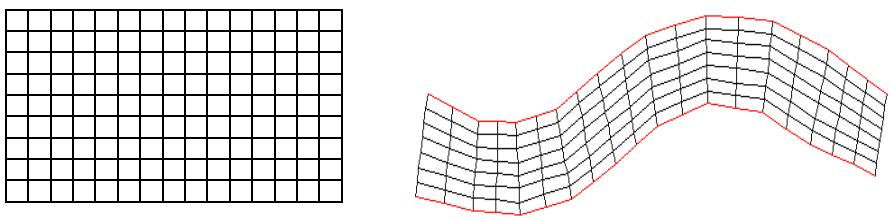

Orthogonal grid *Non-orthogonal grid*

Pronounciation of the Greek letters:

ξ : ksi
ψ: psi
ζ: zeta

For non-orthogonal grids, a non-orthogonal coordinate system is often used to derive terms in the equations. The coordinates then follow the grid lines of a structured grid. The three non-orthogonal coordinate lines are often called ξ,ψ,ζ, corresponding to x,y and z in the orthogonal coordinate system. Fig. 5.1.3 shows the two systems in 2D. Additionally, the third direction will be *z* in the cartesian system and ζ in the computational domain.

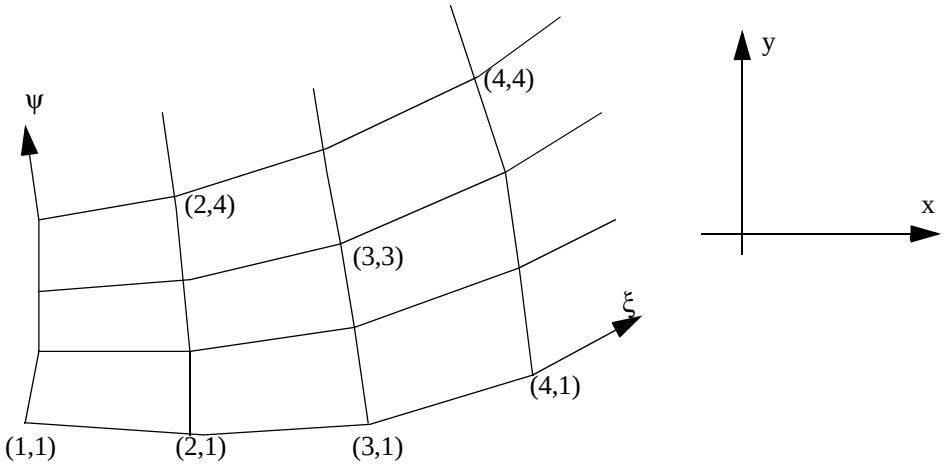

Figure 5.1.3 Body-fitted coordinate system. The two coordinate systems are shown in two dimensions, where some values of ξ and ψ are given in brackets

The directions along the computational domain are often called (ξ,ψ) in 2D as shown in the figure above, or (ξ,ψ,ζ) in 3D, where the last index is the vertical direction. In the computational domain, the distance between the grid lines are often set to unity, so it is easy to calculate gradients of variables. It means all δξ will be unity.

An important definition is the notation of the variables at a cell. Instead of using *x*,*y* and *z* directions, the non-orthogonal cell now uses the directions north, south, east, west, bottom and top. Another definition is to use indexes, as in tensor notation. Then direction 1 is east-west, direction 2 is north-south and direction 3 is vertical. Using tensor notation, (ξ,ψ,ζ) can also be written (ξ^1,ξ^2,ξ^3).

Grid structure

Grids can be **structured** or unstructured. In the last century, a structured grid was often used in finite volume methods and an unstructured grid was used in finite element methods. However, modern finite volume methods also uses unstructured grids. The figure below shows a structured and an unstructured grid. In a structured grid it is possible to make a two-dimensional array indexing the grid cells. If this is not possible, the grid is unstructured.

Figure 5.1.4 Grid structure

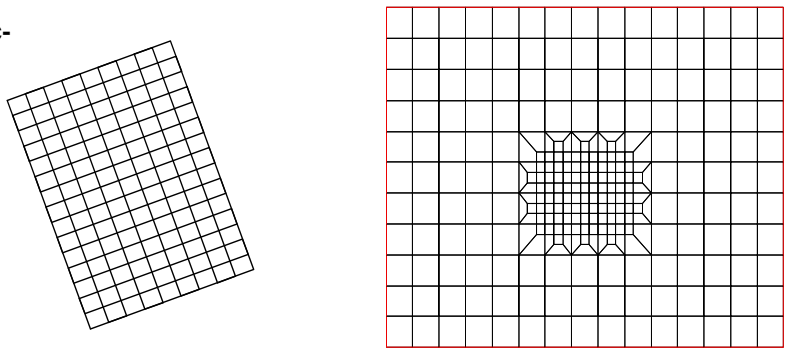

Structured grid *Unstructured grid*

Almost all grids using triangular cells are unstructured.

It is possible to connect several structured grids. Each grid is then called a block, and the result is called a **multi-block** grid.

Adaptive grid

The grid may also **move** during the computations. A grid that moves according to the solution of the equations is called an **adaptive** grid.

Typical examples are vertical movements due to changes in water levels, or changes in bed levels due to erosion or sedimentation. The grid may also move laterally, for example modelling a meandering river. Examples are given in Chapter 9. All these movements are due to changes in the geometry of the computational domain. Grid movements can also be internal. Often, a higher grid density is wanted in large gradients, and algorithms have successfully been used to change the internal grid structure to change the cell sizes according to for example velocity gradients.

High gradients may also necessitate the use of a **nested** grid. This means that a grid with small cells are located inside a coarser grid. A typical example is computation of pollutants from a point source in a lake. The lake itself is modelled with a coarse grid, while the concentration around the point source is modelled with a finer grid, nested inside the coarse grid. Another example is local scour, where a fine grid is made around the bridge pier and a coarser grid is made of the river (Baranya et al, 2014)

Outblocking is a procedure where cells in a structured grid are made inactive. This makes it easier to generate structured grids in a complex geometry.

Grid Qualities

The accuracy and convergence of a finite volume calculation depends on the quality of the grid. Three grid characteristics are important:

Grid qualities

- non-orthogonality
- aspect ratio
- expansion ratio

The non-orthogonality of the grid line intersections is the deviation from 90 degrees. If the grid line intersection is below 45 degrees or over 135 degrees, the grid is said to be very non-orthogonal. This is a situation one should avoid. Low non-orthogonality of the grid leads to more rapid convergence, and in some cases better accuracy.

The aspect ratio and expansion ratio is described in the figure below:

Figure 5.1.5 Expansion/aspect ratio definition:

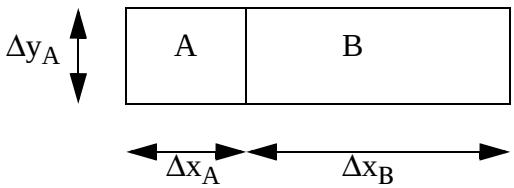

The figure shows two grid cells, *A* and *B*. The length of the cells are Δx_A and Δx_B.

The **expansion ratio** of the grid at these cells is $\Delta x_A/\Delta x_B$.

The **aspect ratio** of the grid at cell *A* is $\Delta x_{A/}\Delta y_A$.

The expansion ratio and the aspect ratio of a grid should not be too great, in order to avoid convergence problems and inaccuracies. Aspect ratios of 2-3 should not be a problem if the flow direction is parallel to the longest side of the cell. Experience shows that aspect ratios of 10-50 will give extremely slow convergence for water flow calculations. Expansion ratios under 1.2 will not pose problems for the solution. Experience also shows that expansion ratios of around 10 can give very unphysical

results for the water flow calculation.

Grid generation

Some kind of geographical information is required to make a grid of a natural river or lake. Often a map can be used. The first step is usually to determine the points at the edges of the grid. Then the internal grid intersections are made.

Two of the most commonly used methods to generate internal points in a structured grid are called *Transfinite interpolation* and *Elliptic grid generation*. These are described in the following.

Transfinite interpolation

In a transfinite interpolation, the grid lines on two opposing edges are connected with straight lines. An example is given in Fig. 5.1.6. The method is well suited for modelling rivers, as the straight lines can be cross-sections. Note that the straight lines are only generated in one direction. For the right figure in Fig. 5.1.6, the lines in the longitudinal direction are not straight.

Fig. 5.1.6. Grid generated with transfinite interpolation.

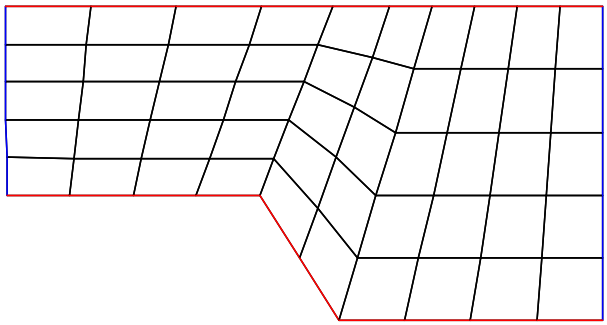

Elliptic grid generation

Some times a smoother grid is required, than the result of the Transfinite interpolation. The elliptic grid generation solves a differential equation for the location of the grid intersections:

$$\nabla^2 \xi_i = 0$$

The grid given in Fig. 5.1.7 is made by this method.

Fig. 5.1.7. Grid made by an elliptic grid generation.

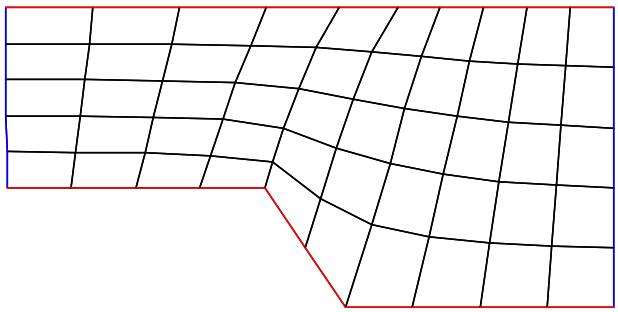

5.2 Discretization methods

The discretization described here is by the control volume method.

Steady state dispersion is governed by the convection-diffusion equation for the concentration, *c*, of the pollutant:

$$U_i \frac{\partial c}{\partial x_i} = \frac{\partial}{\partial x_i}\left(\Gamma \frac{\partial c}{\partial x_i}\right) \qquad (5.2.1)$$

The left side of the equation is the convective term, and the right side of the equation is the diffusive term.

The main point of the discretization is:

Discretization is: *To transform the partial differential equation into a new equation where the variable in one cell is a function of the variable in the neighbour cells*

The new function can be thought of as a weighted average of the concentration in the neighbouring cells. For a two-dimensional situation, the following notation is used, according to directions north, south, east and west:

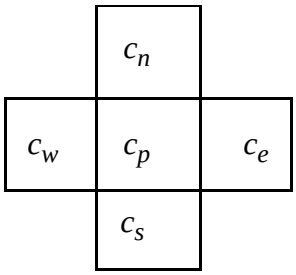

Figure 5.2.1 Discretization molecule. Computation of concentration, *c*, in the center cell, *p*, as a function of the concentration in the neighbouring cells *n*, *s, e* and *w*.

a_e : weighting factor for cell *e*
a_w : weighting factor for cell *w*
a_n : weighting factor for cell *n*
a_s : weighting factor for cell *s*
$a_p = a_e+a_w+a_n+a_s$

The formula becomes:

$$c_p = \frac{a_w c_w + a_e c_e + a_n c_n + a_s c_s}{a_p} \qquad (5.2.2)$$

The weighting factors for the neighbouring cells a_e, a_w, a_n and a_s are often denoted a_{nb}

What we want to obtain are formulas for a_{nb}.

In a three-dimensional computation, the same principles are involved. But two more neighbouring cells are added: t (top) and b (bottom), resulting in six neighbour cells. The simple extension from 2D to 3D is one of the main advantages of the finite volume method.

There are a number of different discretization methods available for the control-volume approach. The difference is in *how the concentration on a cell surface is calculated*. Some methods are described in the following.

Note that the methods are based on the physics of the dispersion and flow processes. They are not mathematically based, or derived from the convection-diffusion equation (5.2.1).

5.3 The First-Order Upstream Scheme

Development of CFD algorithms was initially done in aeronautics. The fluid was air, and the methods were then called upwind instead of upstream. Both expressions are used, meaning the same.

For a non-staggered grid, the values of the variables are given in the center of the cells. Using the finite volume method, it is necessary to estimate variable values on the cell surfaces. The main idea of the upstream methods is to estimate the surface value from the *upstream* cell. The first order method uses information in only one cell upstream of the cell surface. In other words: the concentration at a cell surface for the first-order upstream method is the same as the concentration in the cell on the upstream side of the cell side.

The control volume method is based on continuity of sediments. The basis of the calculation is the fluxes on a cell surface. The surface area is denoted *A*; the velocity at the surface, normal to it, is denoted *U*; c is the concentration at the surface, and Γ is the turbulent diffusion at the surface.

The convective flux is calculated as: $U * A * c$ (5.3.1)
The diffusive flux is calculated as: $\Gamma * A * dc / dx$ (5.3.2)

The term *dc/dx* is calculated as the concentration difference between the cells on each side of the surface, divided by the distance between the centres of the cells. Looking at the west side of cell *p*, Fig. 5.3.1 explains the variable locations and the fluxes in the center cell.

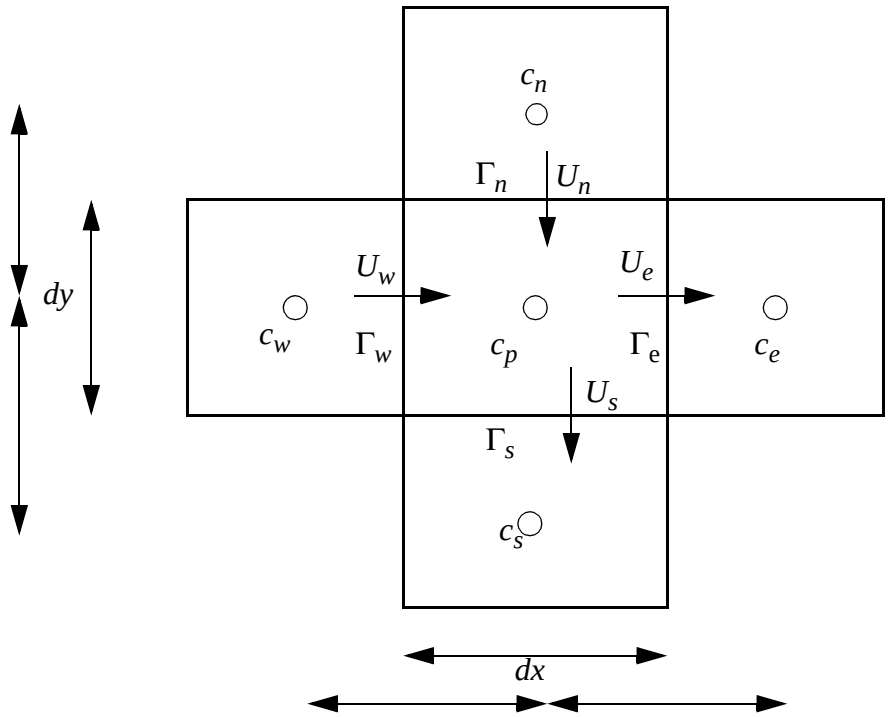

Figure 5.3.1 Fluxes through the walls of the center cell in a computational molecule. The cells have a width of *dx* and a height of *dy*. Note, the diffusion coefficient and the velocities are given on the boundary between the cells. The concentrations are computed in the centre of each cell. Also note that this is a two-dimensional situation. The area of a cell surface is therefore equal to *dx* or *dy*, multiplied with a unit depth in the third dimension.

The flux, F_w, through the west side of cell *P* then becomes:

$$F_w = U_w A_w c_w + \Gamma_w \frac{A_w (c_w - c_p)}{dx} \qquad (5.3.3)$$

where A_w is the area of the cell wall on the west side, equal to Δy times the height of the wall. For the other sides, the following fluxes are obtained:

$$F_e = U_e A_e c_p + \Gamma_e \frac{A_e (c_p - c_e)}{dx} \quad (5.3.4)$$

$$F_s = U_s A_s c_p + \Gamma_s \frac{A_s (c_p - c_s)}{dy} \quad (5.3.5)$$

$$F_n = U_n A_n c_n + \Gamma_n \frac{A_n (c_n - c_p)}{dy} \quad (5.3.6)$$

Sediment continuity means the sum of the fluxes is zero, in other words:

$$F_w - F_e + F_n - F_s = 0 \quad (5.3.7)$$

This gives the following equation:

$$\left(\Gamma_w \frac{A_w}{dx} + U_e A_e + \Gamma_e \frac{A_e}{dx} + U_s A_s + \Gamma_s \frac{A_s}{dy} + \Gamma_n \frac{A_n}{dy}\right) c_p = \left(U_w A_w + \Gamma_w \frac{A_w}{dx}\right) c_w + \left(\Gamma_e \frac{A_e}{dx}\right) c_e + \left(U_n A_n + \Gamma_n \frac{A_n}{dy}\right) c_n + \left(\Gamma_s \frac{A_s}{dy}\right) c_s \quad (5.3.8)$$

When we compare Equation 5.2.2 with Equation 5.3.8, we see they are the same. The concentration in Cell *P* is a function of the concentration in the neighbouring cells. The resulting weighting factors are:

$$a_p = \Gamma_w \frac{A_w}{dx} + U_e A_e + \Gamma_e \frac{A_e}{dx} + U_s A_s + \Gamma_s \frac{A_s}{dy} + \Gamma_n \frac{A_n}{dy} \quad (5.3.9)$$

$$a_w = U_w A_w + \Gamma_w \frac{A_w}{dx} \quad (5.3.10)$$

$$a_e = \Gamma_e \frac{A_e}{dx} \quad (5.3.11)$$

$$a_s = \Gamma_s \frac{A_s}{dy} \quad (5.3.12)$$

$$a_n = U_n A_n + \Gamma_n \frac{A_n}{dy} \quad (5.3.13)$$

The water continuity equation for the grid cell is:

$$U_w A_w - U_e A_e + U_n A_n - U_s A_s = 0 \quad (5.3.14)$$

or:

$$U_w A_w + U_n A_n = U_e A_e + U_s A_s \quad (5.3.15)$$

If the above equation is inserted into the expression for a_p, the equation

$$a_p = a_e + a_w + a_s + a_n \quad (5.3.16)$$

is verified to be correct.

Note that the equations above are only valid if the velocity flows in the

same direction as given on the arrows in Fig. 5.3.1.

Example:

Particles are deposited in a river with constant width and depth. A 2D situation is assumed, averaged over the width. The north-south direction is used as the vertical direction, so the indexes *s* and *n* are replaced by *b* and *t*. Further simplifications are:

- uniform the water flow
- negligible horizontal diffusion

Then the vertical velocity is equal to the sediment particle fall velocity, w. Also, the grid can be made orthogonal and two-dimensional, so $A_e = A_w = dy$, and $A_b = A_t = dx$. The weighting factors then become:

$$\begin{aligned} a_e &= 0.0 \\ a_w &= U\,dy \\ a_b &= \Gamma\,dx/dy \\ a_t &= w\,dx + \Gamma\,dx/dy \\ a_p &= U\,dy + w\,dx + 2\,\Gamma\,dx/dy \end{aligned} \qquad (5.3.17)$$

If for example, U is 2 m/s, w is 0.01 m/s, Γ is 0.01 m^2/s, and the river depth is 4 meters, we may assume 10 cells in the vertical direction, giving dy = 0.4 m. Modelling a reach of 1 km with 100 cells, gives dx=10 m. The coefficients becomes:

$$\begin{aligned} a_e &= 0.0 \\ a_w &= 0.8 \\ a_b &= 0.25 \\ a_t &= 0.35 \\ a_p &= 1.4 \end{aligned} \qquad (5.3.18)$$

The numbers can be inserted in a spreadsheet and the problem solved. This is described in the next chapter.

The Power-Law Scheme

The Power-Law Scheme is a first-order upstream scheme where the diffusive term is multiplied with the following reduction factor:

$$f = (1 - 0.1|Pe|)^5 \qquad (5.3.19)$$

where *Pe* is the Peclet number, given by:

$$Pe = \frac{U\Delta x}{\Gamma} \qquad (5.3.20)$$

The Peclet number is the ratio of convective to diffusive fluxes. The factor f is always between 1 and 0. The diffusive term will be reduced for flows where the convection is large compared with the diffusion.

5.4 Spreadsheet programming

Given formulas for the water flow field and the turbulence, it is possible to make a spreadsheet for calculation of the pollutant concentration. One

application is to calculate the trap efficiency of a sand trap. Then a two-dimensional width-averaged approach is used. A structured orthogonal grid is used, where each cell in the grid is simulated by a cell in the spreadsheet. If a uniform water velocity and turbulence field can be assumed in the vertical direction, then the same a_{nb} coefficients can be used for all the cells. A more advanced approach is to use a logarithmic velocity distribution, and a given distribution of the eddy-viscosity.

If the simpler approach is used, the coefficients a_{nb} can be calculated before the programming starts. This is based on the formulas given previously, and a chosen number of grid cells. The grid is structured, orthogonal and all cells have the same size.

A figure of this spreadsheet is given below, with 8 cells in the vertical direction, and 9 cells in the horizontal direction. The size of the grid can of course be changed according to the dimensions of each problem.

	A	B	C	D	E	F	G	H	I	J	K
1		0	0	0	0	0	0	0	0	0	0
2	*X*										*Y*
3	*X*										*Y*
4	*X*										*Y*
5	*X*										*Y*
6	*X*										*Y*
7	*X*										*Y*
8	*X*										*Y*
9	*X*										*Y*
10	*X*	*Z*	*Z*	*Z*	*Z*	*Z*	*Z*	*Z*	*Z*	*Z*	*Y*

The cells marked *X* are inflow boundary conditions. These are the *A2..A10* cells. A concentration value is given in these cells. A constant value can be given, or it is possible to use a formula for the vertical distribution of the concentration.

The cells marked *0* is the boundary condition at the water surface. This is zero.

The cells marked *Y* is the outflow boundary condition. If the horizontal diffusion is assumed to be zero, the values in these cells will not affect the computation. If the horizontal diffusion is non-zero, a zero gradient boundary condition can be used. Then the formula in these cells should be:

Cell *K2: =J2*
Cell *K3: =J3*
...
Cell *K10: =J10*

The cells marked *Z* is the bed boundary condition. A formula for the equilibrium sediment concentration can be used, for example van Rijn's formula, given in Chapter 9.6. However, often the shear stress is below critical at the bed of the sand trap, giving zero concentration. This will not be correct, as the sediment concentration at the bed will always be higher than the cell above. Therefore, the concentration can be set equal to the concentration in the cell above.

(Note that a more detailed calculation will give a very low diffusion coefficient close to the bed of the sand trap, meaning the concentration in the cell above the bed is independent of the concentration in the bed boundary. For a simplified calculation, the diffusion coefficient is significant. Then the same result is obtained if zero gradient boundary condition is used.)

Cell *B10*: =*B9*
Cell *C10*: =*C9*
...
Cell *J10*: =*J9*

The discretized formula now has to be given in all the remaining interior cells. As an example, the following data is assumed:

a_w = 0.1
a_n = 0.2
a_s = 0.006
a_e = 0.002
a_p = 0.308

Starting in cell *B2*, we give the following formula:

+(0.1**A2*+0.2**B1*+0.006**B3*+0.002*C*2*)/0.308

The method of invoking more iterations is dependent on the particular spreadsheet program. For Lotus 123, use *F9* on the keyboard repeatedly. For MS Excel, use the menu *Tools, Options, Calculations*, and cross off *Iterations*, and give a number in the edit-field, for example 50.

This formula is copied to all the interior cells, from cell *B2* to *J9*. Afterwards, the calculation has to be repeated some times to get convergence.

The trap efficiency is calculated by first summing the inflow and the outflow:

Inflow: sum of cells *A2..A10*
Outflow: sum of cells *K2..K10*

Trap efficiency = (Inflow-Outflow)/Inflow

Running this case with varying number of grid cells will give different result for the trap efficiency. The next chapter explains why.

5.5 False diffusion

False diffusion is due to the approximations in the convective terms in the discretization schemes. More specifically, how the concentration on the cell side is calculated. The effect is best shown with a coarse grid and steep gradients, for example the following situation:

A sand trap is calculated with 5 x 5 cells in the vertical and horizontal direction, respectively. The cells are 1 meter high and 5 meters long. The water velocity is 0.3 m/s, and the sediment fall velocity is 6 cm/s. The sediments are added from a point source at the water surface, over a

length of 5 meters. There is **no** turbulence! This gives the following theoretical concentration profile in the flow:

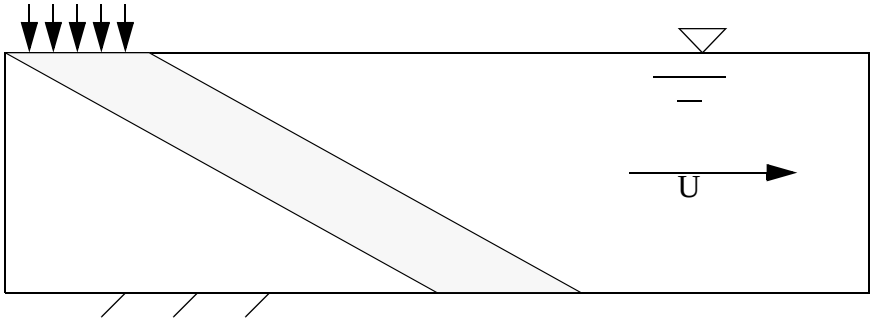

Figure 5.5.1. Profile of the real concentration in the geometry

The concentration is unity along a band in the flow. The concentration is zero elsewhere.

The first-order upstream scheme is used to calculate the concentration. The following coefficients are obtained:

$a_n = 0.06 * 5 = 0.3$
$a_w = 0.3 * 1 = 0.3$
$a_s = 0.0$
$a_e = 0.0$
$a_p = 0.6$

This gives $a_n/a_p = 0.5$ and $a_w/a_p = 0.5$. In other words, the concentration in a cell is the average of the concentration in the cell above and in the cell upstream. The boundary condition is a concentration of unity in one cell at the surface, and zero concentration in the other surface cells and the inflow cells. The following result is obtained:

1.0

0.0 →

0.5	0.25	0.125	0.0625	0.0313	0.0156
0.25	0.25	0.188	0.125	0.0781	0.0469
0.125	0.188	0.188	0.156	0.117	0.0820
0.0625	0.125	0.156	0.156	0.137	0.109
0.0313	0.0781	0.117	0.137	0.137	0.123

Figure 5.5.2. Grid with computed concentration values

The maximum concentration has decreased from unity to 0.137 at the bed. It has also been smeared out over several cells at the bed.

False diffusion can be avoided by:

- aligning the grid with the flow direction
- increasing the number of grid cells
- using higher order schemes

The last option is described in the following chapter.

5.6 The Second Order Upstream Scheme

The Second-Order Upstream (SOU) method is based on a second-order accurate method to calculate the concentration on the cell surfaces. The method only involves the convective fluxes, and the diffusive terms are calculated as before. The following figure shows the calculation of the concentration on the west side of cell *p*: side *W*:

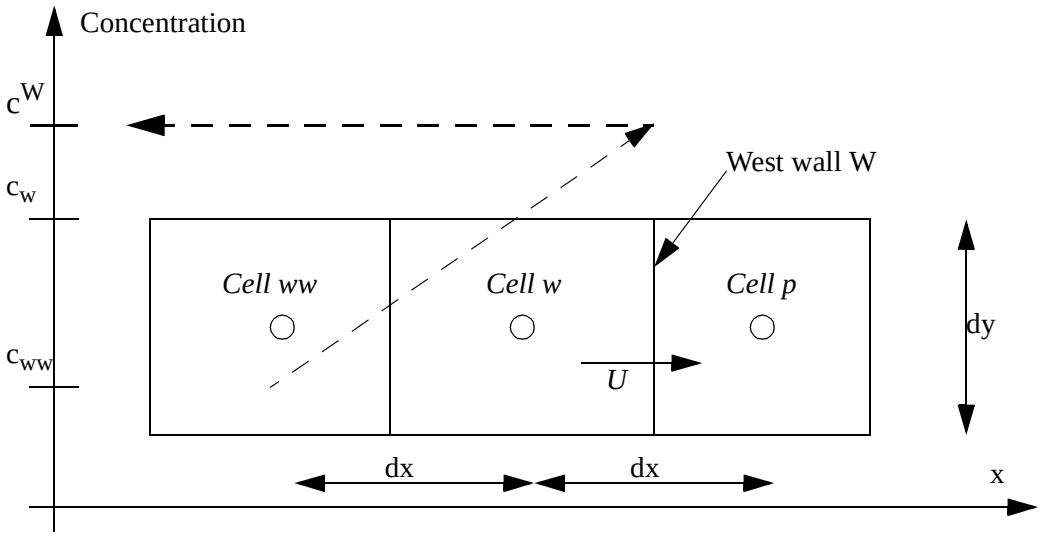

Figure 5.6.1 Definition sketch for concentration estimation at the wall, *W*, for the SOU scheme.

The cell on the west side of cell *w* is called cell *ww*. The concentration in this cell is denoted c_{ww}. The concentration in cell *w* is denoted c_w and the concentration on side *W* of cell *p* is denoted c^W. The SOU scheme uses the concentration in cell *ww* and cell *w* to extrapolate linearly to side *W*. Given the width of the cell in the x-direction is *dx*, and the height in the y-direction is *dy*, it is possible to derive a formula for the concentration on side *W* by triangulation:

$$\frac{c^w - c_{ww}}{dx + 0.5dx} = \frac{c_w - c_{ww}}{dx} \qquad (5.6.1)$$

or

$$c^w = \frac{3}{2}c_w - \frac{1}{2}c_{ww} \qquad (5.6.2)$$

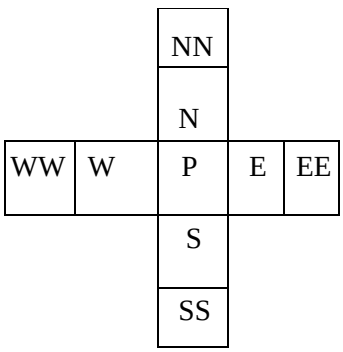

Figure 5.6.2 SOU nine-point calculation molecule

Equation 5.6.1 is only valid if the cells are of equal size. If the expansion ratio is different from unity, a separate formula needs to be applied, where the coefficients 3/2 and ½ are given as a function of the expansion ratio.

The calculation molecule now gets nine cells, as shown in the figure to the left

The flux through the west side of Cell *P* then becomes:

$$F_w = U_w A_w\left(\frac{3}{2}c_w - \frac{1}{2}c_{ww}\right) + \Gamma_w \frac{A_w(c_w - c_p)}{dx} \qquad (5.6.3)$$

For the other sides, the following fluxes are obtained:

$$F_e = U_e A_e\left(\frac{3}{2}c_p - \frac{1}{2}c_w\right) + \Gamma_e\frac{A_e(c_p - c_e)}{dx} \quad (5.6.4)$$

$$F_s = U_s A_s\left(\frac{3}{2}c_p - \frac{1}{2}c_n\right) + \Gamma_s\frac{A_s(c_p - c_s)}{dy} \quad (5.6.5)$$

$$F_n = U_n A_n\left(\frac{3}{2}c_n - \frac{1}{2}c_{nn}\right) + \Gamma_n\frac{A_n(c_n - c_p)}{dy} \quad (5.6.6)$$

Again, the equations are only valid if the velocity vectors are in the same direction as in Fig. 5.3.1. The weighting factors become:

$$a_w = \frac{3}{2}U_w A_w + \Gamma_w\frac{A_w}{dx} + \frac{1}{2}U_e A_e \quad (5.6.7)$$

$$a_{ww} = -\frac{1}{2}U_w A_w \quad (5.6.8)$$

$$a_e = \Gamma_e\frac{A_e}{dx} \quad (5.6.9)$$

$$a_{ee} = 0 \quad (5.6.10)$$

$$a_n = \frac{3}{2}U_n A_n + \Gamma_n\frac{A_n}{dy} + \frac{1}{2}U_s A_s \quad (5.6.11)$$

$$a_{nn} = -\frac{1}{2}U_n A_n \quad (5.6.12)$$

$$a_s = \Gamma_s\frac{A_s}{dy} \quad (5.6.13)$$

$$a_{ss} = 0 \quad (5.6.14)$$

For the SOU scheme, Equation 5.3.1 now becomes:

$$c_p = \frac{a_w c_w + a_e c_e + a_n c_n + a_s c_s + a_{ww} c_{ww} + a_{nn} c_{nn}}{a_p} \quad (5.6.3)$$

The formula is used for a two-dimensional situation. In 3D, the terms for top and bottom is also added, giving four extra coefficients: a_t, a_{tt}, a_b, a_{bb}.

5.7 Time-dependent computations and source terms

The derivations given previously has been made under the assumption of a steady state condition. Often, it is necessary to compute the concentration changes over time. In Chapter 5.3, the fluxes into cell P was equal to the fluxes out of the cell. In a time-dependent situation, this may not be the case. To derive an equation for this problem, we look at what happens during a time step Δt, between time t and t-1. The mass change, m, in cell P would then be:

$$m = (c_{p,t} - c_{p,t-1})V_p \quad (5.7.1)$$

The volume of cell *P* is then denoted V_p

The fluxes in and out of cell P can then be computed as previously, but it is necessary to multiply with the time step, to get the mass instead of the flux. Equation 5.3.7 becomes:

$$\Delta t F_w - \Delta t F_e + \Delta t F_n - \Delta t F_s = m \tag{5.7.2}$$

Combining Eqs. 5.7.1 and 5.7.2, we obtain:

$$\sum_{nb} a_{nb} c_{nb} - a_p c_p = F_w - F_e + F_n - F_s = \frac{(c_{p,t} - c_{p,t-1}) V_p}{\Delta t} \tag{5.7.3}$$

The left side of the equation is similar to the steady state situation. For a time-dependent computation, the term on the right hand side emerges. The equation can be rewritten:

$$a_p c_p = a_w c_w + a_e c_e + a_n c_n + a_s c_s - \frac{(c_{p,t} - c_{p,t-1}) V_p}{\Delta t} \tag{5.7.4}$$

The a_{nb} and a_p coefficients are now the same as for the steady equation. The additional term on the right side is called a **source term**. In a computer program these has to be calculated. The most commonly way of doing this for Eq. 5.7.4 is by dividing the source term in two, according to:

$$S_C - S_P c_{p,t} = \frac{(c_{p,t} - c_{p,t-1}) V_p}{\Delta t} \tag{5.7.5}$$

The source terms are:

$$S_C = \frac{c_{p,t-1} V_p}{\Delta t} \tag{5.7.6}$$

This term only depends on known variables, as the concentration at the previous time step is known.

$$S_P = \frac{V_p}{\Delta t} \tag{5.7.7}$$

The final equation can then be written in the following way, where the a_{nb} and a_p coefficients are the same as for the steady case:

$$c_p = \frac{a_w c_w + a_e c_e + a_n c_n + a_s c_s + S_C}{(a_p + S_P)} \tag{5.7.8}$$

The equation can be solved similarly as for a steady case. However,

because of the new dimension, time, it is difficult to do this in a spreadsheet. A computer program is often necessary.

The transient convection-diffusion equation can be written:

$$\frac{\partial c}{\partial t} + U_i \frac{\partial c}{\partial x_i} = \frac{\partial}{\partial x_i}\left(\Gamma \frac{\partial c}{\partial x_i}\right) \qquad (5.7.9)$$

5.8 Grid independency tests

The choise of grid layout and number of grid cells in the domain is often the most important parameters for the quality of the result from a numerical computation. To assess if the number of grid cells is sufficient, there exist several grid independency tests. One common test is called the Grid Convergence Index (GCI). The results from the same calculation is here compared, but done with two grids of different size: Grid 1 is the finer grid, and Grid 2 is the coarser grid. The GCI indeis is then computed with the following formula (Celik et al, 2008):

$$GCI^{21} = \frac{1.25 e^{21}}{r^{21} - 1} \qquad (5.8.1)$$

The index 21 denotes the two grids: 1 and 2. The deviation, e_{21}, in the result between the two grids is given from the following formula:

$$e^{21} = \left| \frac{\varphi_1 - \varphi_2}{\varphi_1} \right| \qquad (5.8.2)$$

The parameter f is a result from one grid. This could for example be the trap efficiency for a sand trap, or the discharge for a spillway computation. The parameter r^{21} in Eq. 5.8.1 is the ratio of the grid cell lengths in the two grids. This can be computed from the following equation:

$$r^{21} = \frac{h_2}{h_1} \qquad (5.8.3)$$

The charachteristic grid cell length is denoted *h*. If the grid is three-dimensional, and the cells have different size in more than one direction, the charachteristic cell length can be computed from the following formula:

$$h = \left(\frac{1}{M} \sum_{j=1}^{M} V_j \right)^{\frac{1}{3}} \qquad (5.8.4)$$

V is the volume of each cell *j*, and *M* is the number of cells in the grid.

Example:

A CFD program computes the discharge over a spillway. Two grids are used. The finer grid has 1 million cells, and the coarser grid has 0.7 million cells. The finer grid gives a discharge of 30 m3/s, and the coarser

grid gives a disharge of 31 m3/s. Compute the GCI for the case:

Solution:

First, compute the deviation: $e^{21} = \left|\frac{30-31}{30}\right| = 0.0333$

Then, compute the h *indexes. The total volumes of the two grids must be the same. The ratio,* r*, then becomes:*

$$r^{21} = \frac{h_2}{h_1} = \frac{\left(\frac{1}{M_2}\sum_{j=1}^{M_2} V_j\right)^{\frac{1}{3}}}{\left(\frac{1}{M_1}\sum_{j=1}^{M_1} V_j\right)^{\frac{1}{3}}} = \left(\frac{M_1}{M_2}\right)^{\frac{1}{3}} = \left(\frac{1000000}{700000}\right)^{\frac{1}{3}} = 1.126$$

This is inserted into the definition of the GCI index:

$$GCI^{21} = \frac{1.25(0.0333)}{1.126-1} = 0.33 = 33\ \%$$

There are also a number of other indexes for computing the grid independency.

5.9 Problems

The following three line styles are used in the sketches in the problems 1-6:

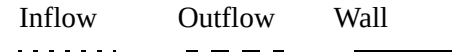

Problem 1. Grid for reservoir

Make a sketch of a 2D structured non-orthogonal grid with 300 cells for the geometry given below.

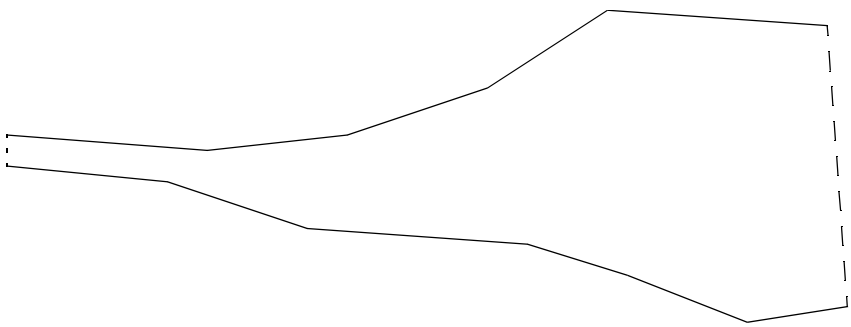

Problem 2. Structured grid for groyne

Make a sketch of a 2D structured non-orthogonal grid with 300 cells for the geometry given below, without using outblocking.

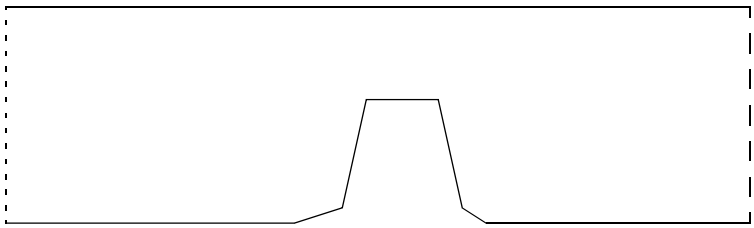

Problem 3. Grid with outblocking

Make a sketch of a structured non-orthogonal grid with 300 cells for the geometry given below, but use outblocking for the groyne.

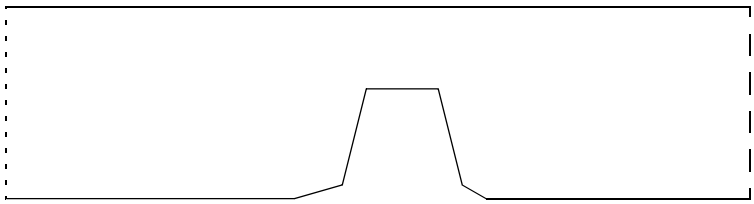

Problem 4. Grid for bay

Make a sketch of a structured non-orthogonal grid with 600 cells for the geometry given below.

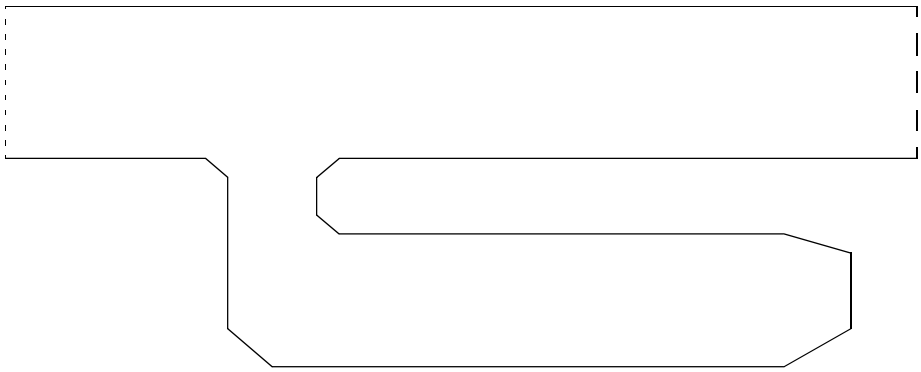

Problem 5. Cylinder grid

Make a paper sketch of a structured non-orthogonal grid with 2400 cells for a circular cylinder with diameter 1.0 meters placed vertically in the centre of a 4 meter wide and 7 meter long flume.

Problem 6. Dispersion of particles

Particles are dumped in a river with depth 2 meters, velocity 1 m/s and a slope of 1/300. The particles have a fall velocity of 0.01 m/s. A water intake is located 1 km downstream of the dumping place. What is the percentage of particles passing the intake? Assume no resuspension of the particles, and that the particles are added close to the water surface.

6. Numerical modelling of water velocity in 2D and 3D

This chapter describes the solution procedures for the Navier-Stokes equations. These equations describe the water velocity and turbulence in a river or a hydraulic system.

Claude Louis Marie Henri Navier was professor at École Polytecnique in Paris from 1819 to 1831. He derived the Navier-Stokes equations in 1822, 23 years before Stokes. Prof. Navier also worked on road and bridge constructions, and derived theories for suspension bridges.

6.1 The Navier-Stokes equations

The Navier-Stokes equations describe the water velocity, *U*. The equations are derived on the basis of equilibrium of forces on a small volume of water in laminar flow:

$$\frac{\partial U_i}{\partial t} + U_j\frac{\partial U_i}{\partial x_j} = \frac{1}{\rho}\frac{\partial}{\partial x_j}\left(-P\delta_{ij} + \rho\nu\left(\frac{\partial U_i}{\partial x_j} + \frac{\partial U_j}{\partial x_i}\right)\right) \qquad (6.1.1)$$

The pressure is denoted *P*, ν is the kinematic viscosity and ρ is the water density. For turbulent flow, it is common to use the Reynolds' averaged versions of the equations. The Reynolds' averaging is described first.

We are looking at a time series of the velocity at a given location in turbulent flow:

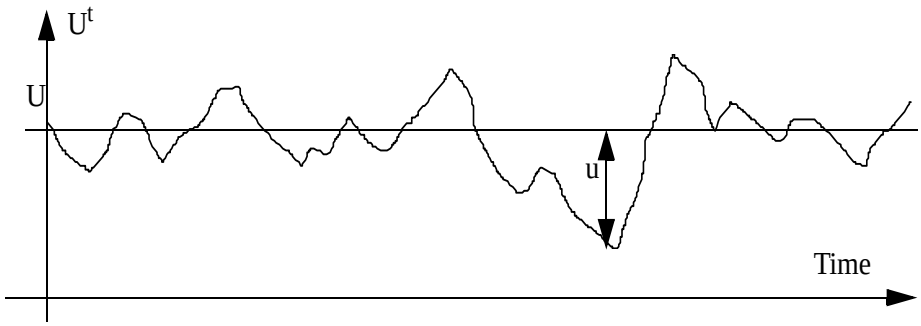

Figure 6.1.1 Time series of water velocity, for definition of velocity fluctuations, u.

The velocity, U^t is divided into an average value *U*, and a fluctuating value *u*. The two variables are inserted into the Navier-Stokes equation for laminar flow, and after some manipulations and simplification the Navier-Stokes equation for turbulent flow emerges:

$$\frac{\partial U_i}{\partial t} + U_j\frac{\partial U_i}{\partial x_j} = \frac{1}{\rho}\frac{\partial}{\partial x_j}(-P\delta_{ij} - \rho\overline{u_i u_j}) \qquad (6.1.2))$$

"*Big whirls have little whirls that feed on their velocity,*

and little whirls have lesser whirls and so on to viscosity."

L. R. Richardson

(Richardson number, Chapter 7.3).

P is the pressure and δ_{ij} is the Kronecker delta, which is 1 if *i=j* and 0 otherwise. The last term is the Reynolds stress term, often modelled with the Boussinesq' approximation:

$$-\rho\overline{u_i u_j} = \rho\nu_T\left(\frac{\partial U_i}{\partial x_j} + \frac{\partial U_j}{\partial x_i}\right) - \frac{2}{3}\rho k\delta_{ij} \qquad (6.1.3)$$

The variable *k* is the turbulent kinetic energy. This is further described in Chapter 6.3. Inserting Equation 6.1.3 into Equation 6.1.2 and regrouping the variables:

$$\frac{\partial U_i}{\partial t} + U_j \frac{\partial U_i}{\partial x_j} = \frac{1}{\rho}\frac{\partial}{\partial x_j}\left[-\left(P + \frac{2}{3}k\right)\delta_{ij} + \rho\nu_T\frac{\partial U_i}{\partial x_j} + \rho\nu_T\frac{\partial U_j}{\partial x_i}\right] \quad (6.1.4)$$

There are basically five terms: a transient term and a convective term on the left side of the equation. On the right side of the equation there is a pressure/kinetic energy term, a diffusive term and a stress term.

Important note:

The convective and diffusive term are solved with the same methods as the solution of the convection-diffusion equation for dispersion modelling in Chapter 5. The difference is that the pollution concentration is replaced by the velocity.

The stress term is sometimes neglected, as it has very little influence on the solution for many cases. The pressure/kinetic energy term is solved as a pressure term. The kinetic energy is usually very small, and negligible compared with the pressure.

A difference between Eq. 6.1.4 and the convection-diffusion equation for sediments is the diffusion coefficient. Eq. 6.1.4 includes an eddy-viscosity instead of the diffusion coefficient. The relationship between these two variables is:

$$\nu_T = Sc\ \Gamma \quad (6.1.5)$$

where *Sc* is the Schmidt number. This is usually set to unity, meaning ***the eddy-viscosity is the same as the turbulent diffusivity.***

This leaves the problem of solving the pressure term. Several methods exist, but with the control volume approach, the most commonly used method is the SIMPLE method. This is described in the next chapter.

6.2 The SIMPLE method

SIMPLE is an abbreviation for Semi-Implicit Method for Pressure-Linked Equations. The purpose of the method is to find the unknown pressure field. The main idea is to guess a value for the pressure and use the continuity defect to obtain an equation for a pressure-correction. When the pressure-correction is added to the pressure, water continuity is satisfied.

Modern CFD using the finite volume method, the SIMPLE method and the k-ε turbulence model was pioneered by a group of researchers in the early 1970's at Department of Mechanical Engineering, Imperial College, London. The group included researchers as D. B. Spalding, B. E. Launder, S. V. Patankar and W. Rodi. The algorithms are used in most commercial CFD programs today.

To derive the equations for the pressure-correction, a special notation is used. The initially calculated variables do not satisfy continuity and are denoted with an index *. The correction of the variables is denoted with an index '. The variables after correction do not have a superscript. The process can then be written:

$$P = P^* + P' \quad (6.2.1)$$
$$U_k = U_k^* + U_k' \quad (6.2.2)$$

P is the pressure and *U* is the velocity. The index *k* on the velocity denotes direction, and runs from 1 to 3 for a 3D calculation.

Given guessed values for the pressure, the discretized version of the

Navier-Stokes equations is:

$$a_p U_{k,p}^* = \sum_{nb} a_{nb} U_{k,nb}^* + B_{u_k} - \left(A_k \frac{\partial P^*}{\partial \xi} \right) \qquad (6.2.3)$$

The convective and diffusive terms have been discretized as described in Chapter 3. The variable *B* contains the rest of the terms besides the convective term, the diffusive term and the pressure term. In the pressure term, A_k is the surface area on the cell wall in direction *k*, and ξ is an index for the grid, described in Chapter 5. Looking at a pressure difference between two neighbour cells, ξ will be unity.

The discretized version of the Navier-Stokes equations based on the corrected variables can be written as:

$$a_p U_{k,p} = \sum_{nb} a_{nb} U_{k,nb} + B_{u_k} - \left(A_k \frac{\partial P}{\partial \xi} \right) \qquad (6.2.4)$$

If this equation is subtracted from Equation 6.2.3, and the two Equations 6.2.2 and 6.2.3 are used, the following equation can be made for the velocity correction in cell *P*:

Exam suggestions from students on what SIMPLE stands for:

$$U_k' = -\left(\frac{A_k}{a_p} \frac{\partial P'}{\partial \xi} \right) \qquad (6.2.5)$$

Semi-Implicit Multiple Pressure Loss Equation

A simplification has then been made to neglect the first term on the right side of Eq. 6.2.4. The SIMPLEC method instead uses the following formula:

Surface IMplied Pressure Level Elements

Semi-Imperfect Pressure Link Estimation

$$U_k' = -\left(\frac{A_k}{\left(a_p - \sum_{nb} a_{nb} \right)} \frac{\partial P'}{\partial \xi} \right) \qquad (6.2.6)$$

Equations 6.2.5 and 6.2.6 give the velocity-corrections once the pressure-corrections are known. To obtain the pressure-corrections, the continuity equation is used for cell *P*, where the water fluxes through each cell side are summed up:

$$\sum_{nb} A_k U_k = \sum_{nb} A_k U'_k + \sum_{nb} A_k U^*_k = 0 \quad (k=1,2,3) \qquad (6.2.7)$$

The term $\sum_{nb} A_k U^*_k$ is equal to the water continuity deficit in each cell, from the previous iteration. We denote this expression to be ΔV.

The expression for the velocity correction from Equation 6.2.5 is inserted into Equation 6.2.7, eliminating it as unknown. Summing up over each side of the cell, the pressure correction gradient can be discretized for one side as follows:

Side east: $A_e U'_e = -A_e\left(\frac{A_e}{a_p}\frac{\partial P'}{\partial \xi}\right) = \frac{A_e^2}{a_p}(P'_p - P'_e)$ (6.2.8)

Using this formula for four sides in a 2D situation, Eq. 6.2.7 can be written:

$$\frac{A_w^2}{a_p}(P'_w - P'_p) + \frac{A_s^2}{a_p}(P'_s - P'_p) + \frac{A_e^2}{a_p}(P'_e - P'_p) + \frac{A_n^2}{a_p}(P'_n - P'_p) + \Delta V = 0 \quad (6.2.9)$$

The result is an equation where only the pressure-correction is unknown:

$$a^\circ_p P'_p = \sum_{nb} a^\circ_{nb} P'_{nb} + b \quad (6.2.10)$$

The index ^{0} is used to indicate the new set of a^0_{nb} coefficients. The source term, b, in Eq. 6.2.10 will be the water continuity deficit ΔV from the guessed velocity field. When water continuity is satisfied, this term is zero, and there are no more corrections to the pressure.

The following formula is derived for a^0_e:

$$a^\circ_e = \frac{A_e^2}{a_{p,e}} \quad (6.2.11)$$

A similar equation holds for the other a^0_{nb} coefficients. The index *e* is then replaced by *w, n, s, t* or b. The $a_{p,e}$ factor is the average a_p value in cell *p* and cell *e*.

Equation 6.2.10 is solved in the same way as the other equations.

The procedure is therefore:

Guess a pressure field, *P**
Calculate the velocity *U** by solving Equation 6.2.3
Solve equation 6.2.10 and obtain the pressure-correction, *P'*
Correct the pressure by adding *P'* to *P**
Correct the velocities *U** with *U'* using equation 6.2.5.
Iterate from point 2 to convergence

An equation for the pressure is not solved directly, only an equation for the pressure-*correction.* The pressure is obtained by accumulative addition of the pressure-correction values.

The SIMPLE method can give instabilities when calculating the pressure field. Therefore, the pressure-correction is often multiplied with a number below unity before being added to the pressure. The number is a relaxation coefficient. The value 0.2 is often used. The optimum factor depend on the flow situation and can be changed to give better convergence rates. Relaxation coefficients are further described in Chapter 6.5.

Regarding the difference between the SIMPLE and the SIMPLEC

The book **Numerical Heat Transfer and Fluid Flow**, by S. V. Patankar, is one of the most readable texts on CFD, and provides an excellent introduction to this science.

Patankar taught CFD at the Norwegian University of Science and Technology in 1977.

method, the SIMPLEC should be more consistent in theory, as a more correct formula is used. Looking at Equations 6.2.5 and 6.2.6, the SIMPLE method will give a smaller correction than the SIMPLEC method, as the denominator will be larger. The SIMPLE method will therefore move slower towards convergence than the SIMPLEC method. If there are problems with instabilities, this can be an advantage.

A more detailed description of the SIMPLE method is given by Patankar (1980).

Most pressure-correction methods for incompressible flow follows algorithms similar to SIMPLE. There are algorithms involving more correction steps, for example SIMPLER and PISO. Note that the different method will only affect the convergence speed and the stability of the solution. The accuracy of the results will not be directly affected, as long as the methods are based on water continuity.

6.3 Advanced turbulence models

The following chapter is a brief overview of advanced turbulence models. The reader is referred to White (1974) and Rodi (1980) for more detailed description of turbulence and turbulence models.

In chapter 6.1, the Boussinesq approximation was introduced for finding an expression for the Reynolds' stress term:

The kinematic viscosity is a fluid property, while the turbulent eddy-viscosity depends of the velocity field.

$$-\rho\overline{u_i u_j} = \rho\nu_T\left(\frac{\partial U_i}{\partial x_j}+\frac{\partial U_j}{\partial x_i}\right)-\frac{2}{3}\rho k\delta_{ij} \qquad (6.3.1)$$

ν_T is the turbulent eddy viscosity.

Some simpler turbulence models were described in Chapter 3. These models require calibration before being used on new cases. They are also based on algebraic relations, and no differential equations are solved when computing the eddy-viscosity. The models are then often called zero-equation models.

Komogorov micro scale:

$$l = \left(\frac{\nu^3}{\varepsilon}\right)^{\frac{1}{4}}$$

A more advanced approach is to use more complex methods to computed the eddy-viscosity. One option is to use a partial differential equation for ν_T. One of the more popular approaches is the Spalart-Allmaras model:

The Spallart-Allmaras model

The model (Spallart and Allmaras, 1994) is essentially a convection-diffusion equation for the eddy-viscosity, where different terms are included to take special physical phenomena into account.

$$\frac{\partial \nu_T}{\partial t}+U_j\frac{\partial \nu_T}{\partial x_j} = c_{b1}S\nu_T+\frac{1}{\sigma}\left[\frac{\partial}{\partial x}\left(\nu_T\frac{\partial \nu_T}{\partial x_j}\right)+c_{b2}\left(\nu_T\frac{\partial \nu_T}{\partial x_j}\right)^2\right]-c_{w1}f_w\left[\frac{\nu_T}{d}\right]^2 \qquad (6.3.2)$$

The first term on the right side is the production of turbulence. There are several ways this can be modelled. One is:

$$S = \frac{\partial U_j}{\partial x_i}\left(\frac{\partial U_j}{\partial x_i} + \frac{\partial U_i}{\partial x_j}\right) \tag{6.3.3}$$

The next term on the right side of Eq. 6.3.2 is the diffusion of turbulence. The last term is related to damping of turbulence close to the wall. The distance to the wall is given as *d*. Spalart and Allmaras suggested the following function for f_w:

$$f_w = g\left[\frac{1 + c_{w3}^6}{g^6 + c_{w3}^6}\right]^{\frac{1}{6}} \qquad g = r + c_{w2}(r^6 - r) \qquad r = \frac{\nu_T}{S\kappa^2 d^2} \tag{6.3.4}$$

The remaining parameters are constants:

c_{b1} = 0.1355, c_{b2} = 0.622, σ = 2/3, c_{w1} = 3.28, c_{w2} = 2, c_{w3} = 0.3, κ=0.4

The k-ε model

Instead of solving only one equation for the eddy-viscosity, it is possible to use two partial differential equations. The most popular two-equation model is the *k*-ε model (Jones and Launder, 1973). The *k*-ε model computes the eddy-viscosity as:

$$\nu_T = c_\mu \frac{k^2}{\varepsilon} \tag{6.3.5}$$

k is turbulent kinetic energy, defined by:

$$k \equiv \frac{1}{2}\overline{u_i u_i} \tag{6.3.6}$$

k is modelled as:

$$\frac{\partial k}{\partial t} + U_j \frac{\partial k}{\partial x_j} = \frac{\partial}{\partial x_j}\left(\frac{\nu_T}{\sigma_k}\frac{\partial k}{\partial x_j}\right) + P_k - \varepsilon \tag{6.3.7}$$

where P_k is the production of turbulence, given by:

$$P_k = \nu_T \frac{\partial U_j}{\partial x_i}\left(\frac{\partial U_j}{\partial x_i} + \frac{\partial U_i}{\partial x_j}\right) \tag{6.3.8}$$

The dissipation of *k* is denoted ε, and modelled as:

$$\frac{\partial \varepsilon}{\partial t} + U_j \frac{\partial \varepsilon}{\partial x_j} = \frac{\partial}{\partial x_j}\left(\frac{\nu_T}{\sigma_\varepsilon}\frac{\partial \varepsilon}{\partial x_j}\right) + C_{\varepsilon 1}\frac{\varepsilon}{k}P_k + C_{\varepsilon 2}\frac{\varepsilon^2}{k} \tag{6.3.9}$$

The constants in the *k*-ε model have the following standard values:

$$
\begin{aligned}
c_\mu &= 0.09 \\
C_{\varepsilon 1} &= 1.44 \\
C_{\varepsilon 2} &= 1.92 \\
\sigma_\kappa &= 1.0 \\
\sigma_\varepsilon &= 1.3
\end{aligned}
\qquad (6.3.10)
$$

The main advantage of the k-ε model is the almost universal constants. The model can thereby be used on a number of various flow situations without calibration. For river engineering this may not always be the case, because when friction along the bed is influencing the flow field, the roughness of the bed also needs to be given. If the roughness can not be obtained from direct measurements, it has to be calibrated with measurements of the velocity.

As seen from Equation 6.3.1, the eddy-viscosity is isotropic, and modelled as an average for all three directions. Schall (1983) investigated the eddy-viscosity in a laboratory flume in three directions. His work shows that the eddy-viscosity in the streamwise direction is almost one magnitude greater than in the cross-streamwise direction. A better turbulence model could therefore give more accurate results for many cases.

More advanced turbulence models

To be able to model non-isotropic turbulence, a more accurate representation of the Reynolds stress is needed. Instead of using the Boussinesq approximation (Equation 6.3.1), the Reynolds' stress can be modelled with all terms:

$$
-\rho\overline{u_i u_j} = -\rho\begin{bmatrix} \overline{uu} & \overline{vu} & \overline{wu} \\ \overline{uv} & \overline{vv} & \overline{wv} \\ \overline{uw} & \overline{vw} & \overline{ww} \end{bmatrix} \qquad (6.3.11)
$$

The following notation is used: u is the fluctuating velocity in direction 1, v is the fluctuating velocity in direction 2 and w is the fluctuating velocity in direction 3.

The nine terms shown on the right hand side of Equation 6.3.8 can be condensed into six different terms, as the matrix is symmetrical. A Reynolds' stress model will solve an equation for each of the six unknown terms. Usually, differential equations for each term are solved. This means that six differential equations are solved compared with two for the k-ε model. It means added complexity and computational time.

An alternative is to use an Algebraic Stress Model (ASM), where algebraic expressions for the various terms are used. It is also possible to combine the k-ε model with an ASM to obtain non-isotropic eddy viscosity (Rodi, 1980).

An even more advanced method is to resolve the larger eddies with a very fine grid, and use a turbulence model only for the smaller scales. This is called Large-Eddy Simulation (LES). If the grid is so fine that subgrid eddies do not exist because they are dissipated by the kinematic viscosity, the method is called a Direct Solution (DS) of the Navier-Stokes equations.

Note that both LES and especially DS modelling require extreme computational resources, presently not available for engineering purposes.

6.4 Boundary conditions

Boundary conditions for the Navier-Stokes equations are in many ways similar to the solution of the convection-diffusion equation. In the following text, a division in four parts is made: Inflow, outflow, water surface and bed/wall.

Inflow

Dirichlet boundary conditions have to be given at the inflow boundary. This is relatively straightforward for the velocities. Usually it is more difficult to specify the turbulence. It is then possible to use a simple turbulence model, like Equation 3.4.1 to specify the eddy-viscosity. Given the velocity, it is also possible to estimate the shear stress at the entrance bed. Then the turbulent kinetic energy *k* at the inflow bed is determined by the following equation:

$$k = \frac{\tau}{\rho\sqrt{c_\mu}} \qquad (6.4.1)$$

This equation is based on equilibrium between production and dissipation of turbulence at the bed cell.

Given the eddy-viscosity and *k* at the bed, Equation 6.3.2 gives the value of ε at the bed. If *k* is assumed to vary linearly from the bed to the surface, with for example half the bed value at the surface, Equation 6.3.2 can be used together with the profile of the eddy-viscosity to calculate the vertical distribution of ε.

Outflow

Zero gradient boundary conditions can be used at outflow boundaries for all variables. A boundary condition where the gradient is specified is often called a von Neumann condition.

Water surface

Zero gradient boundary conditions are often used for ε. The turbulent kinetic energy, *k*, can set to zero. Rodi (1980) gives an alternative expression for computing *k* at the water surface. Symmetrical boundary conditions are used for the water velocity, meaning zero gradient boundary conditions are used for the velocities in the horizontal directions. The velocity in the vertical direction is calculated from the criteria of zero water flux across the water surface.

Bed/wall

The flux through the bed/wall is zero, so no boundary conditions are given. However, the flow gradient towards the wall is very steep, and it would require a significant number of grid cells to dissolve the gradient sufficiently. Instead, a wall law is used, transformed by integrating it over the cell closest to the bed. Using a wall law for rough boundaries (Schlichting, 1980)

$$\frac{U}{u_*} = \frac{1}{\kappa}\ln\left(\frac{30y}{k_s}\right) \qquad (6.4.2)$$

also takes the effect of the roughness, k_s, on the wall into account. The velocity is denoted *U*, u_* is the shear velocity, κ is a coefficient equal to 0.4 and *y* is the distance from the wall to the centre of the cell.

The wall law is used both for the velocities and the turbulence parameters. The use on turbulence parameters is described in more detail by Rodi (1980). For the velocities, the wall shear stress is a force on a cell, and it is computed as a sink term in the Navier-Stokes equation. The

force is computed by rearranging Eq. 6.4.2:

$$F = \tau A = \rho u_*^2 A = \rho A \left(\frac{U}{\frac{1}{\kappa}\ln\left(30\frac{y}{k_s}\right)} \right)^2 \qquad (6.4.3)$$

The area of the cell at the bed is denoted *A*, while *y* is the distance from the center of the cell to the bed. The velocity in the bed cell is denoted *U*.

6.5 Stability and convergence

The solution method described previously are iterative. The principle is to guess a starting value for the variables and then iterate to get a better solution. The procedure is illustrated in Fig. 6.5.1.:

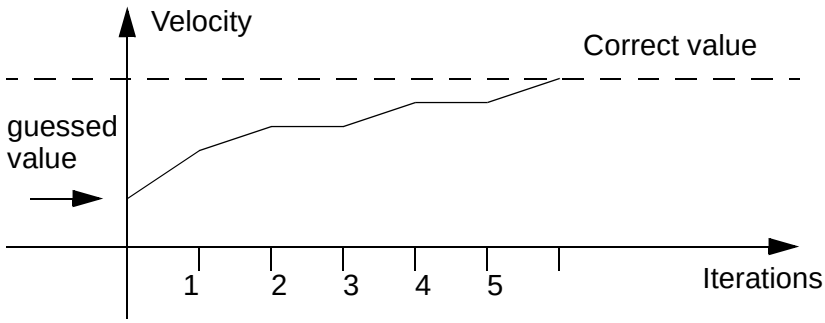

Figure 6.5.1 Convergence graph for the velocity in one cell.

Convergence criteria

In an iterative procedure, some criteria has to be met to decide if the solution is converged. Several different criteria exist, based on computation of a residual. The residual is a measure of how large the deviation is between the correct value and the values in the current iteration. A low residual indicates that convergence is reached.

One formula for the residual, *r*, is given in Eq. 6.5.1:

$$r = \frac{\sum^{n} \left| a_p U_p - \sum a_{nb} U_{nb} - Source_p \right|}{nF_c U_c} \qquad (6.5.1)$$

F_c is a characteristic flux, and U_c is a characteristic velocity. The values at the inflow boundary are often used. The total number of cells in the grid is denoted *n*.

Example: We are looking at one 2D cell with the following parameters:

$a_w = 2.0$, $U_w = 1.0$
$a_e = 0.5$, $U_e = 0.3$
$a_n = 1.0$, $U_n = 0.4$
$a_s = 0.3$, $U_s = 0.7$

For simplicity, we assume that the source term is zero.

The first time cell p is computed, the following values are obtained:

$a_p = 3.8.\ U_p = 0.73$

The velocity in cell P is computed from Eq. 5.2.2, where the concentration is replaced by the velocity.

After the cell is computed, the east and north cells are recomputed and get different values. They now have values:

$U_e = 0.35$
$U_n = 0.45$

The contribution of this cell to the residual of Eq. 6.5.1 becomes:

$$a_p U_p - \sum a_{nb} U_{nb} = 3.8x0.73 - 2x1 + 0.5x0.35 + 1x0.45 + 0.3x0.7$$

$$= 0.075$$

Note that the values from the previous iteration is not used.

Another convergence criteria is based on the difference in the values between two iterations:

$$r = \frac{\sum^{n} |U_i - U_{i-1}|}{nU_c} \qquad (6.5.2)$$

The disadvantage with using Eq. 6.5.2 is that the residual can go to zero even if the solution is not converged. This is illustrated in Fig. 6.5.2:

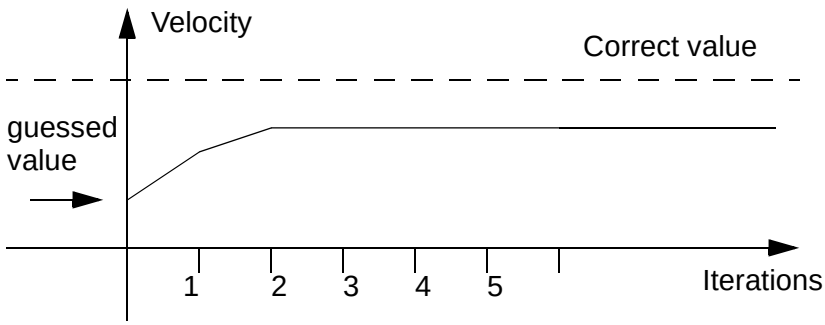

Figure 6.5.2 Convergence graph for the velocity in one cell. The correct value is not obtained, but still the new values in the iterations are the same as in the previous iteration.

The reason for this can be that the velocity-correction equation from the SIMPLE method may change the velocities back to what they were before the application of the solver. Also, possible bugs in the program can give the same problem. Many CFD programs therefore prefer to use Eq. 6.5.1 instead of Eq. 6.5.2.

Instabilities

It is not always that the iterative solution method is successful in obtaining convergence. The system of equations may be unstable. The con-

vergence graph for one cell may then look like what is given in Fig. 6.5.3. The values may oscillate, and more and more extreme values are produced. Often, one defines a solution crash as the residuals becoming above a high value, for example 10^{10}.

There are several methods to prevent instabilities and accelerate convergence. Some are further described in the following.

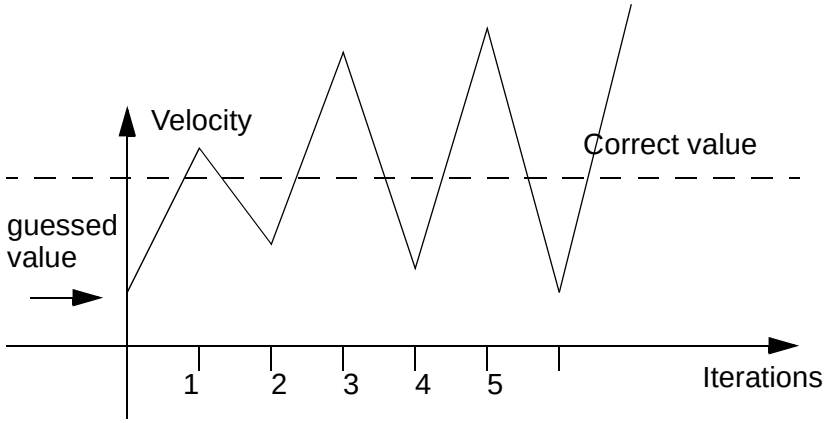

Figure 6.5.3 Convergence graph for the velocity in one cell, where there are instabilities and non-convergence..

Relaxation

The main principle in the solution of the equations are to obtain an improvement of a guessed velocity field. Starting with the guessed values, several iterations are done to improve the result. For each iteration, a new guess is made. Let us say that we have finished iteration *i*-1 and *i*, and we are looking at what variables, *v*, we should use when starting iteration *i*+1. An obvious choice is of course the variables at iteration *i*. However, introducing the relaxation coefficient, *r*, instead we use:

$$v = r * v_i + (1-r) * v_{i-1} \qquad (6.5.3)$$

The relaxation coefficients should normally be between 0 and 1.

Relaxation will give a slower convergence speed towards the final solution, but there will be less instabilities. If the solution diverges or does not converge because of instabilities, a normal measure is to lower the relaxation coefficients.

Multigrid and block-correction

The purpose of the multigrid methods is to speed up the convergence of the solution. The main principle is a division of the grid several coarser sub-grids. This is shown in Figure 6.5.4. The discretized equations on the fine grid are transferred to the medium grid and then to the coarser grid. This procedure is called **restriction.** The equations are solved on the coarse grid, and the solution is transferred to the medium grid, where a finer solution is made. The procedure is repeated to the fine grid, where the solution is made. The transfer from coarse grid to finer grid is called **prolongation**. The sequence can be repeated. Both for the restriction and prolongation process, interpolation and extrapolation formulas are used.

Figure 6.5.4 Grid structure for multi-grid method

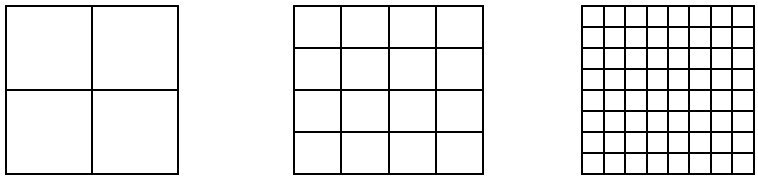

In the example in Fig. 6.5.4, only three levels of grid resolutions are shown. For very fine grids, there may be many more layers.

Usually, the equation variables themselves are not moved between the grids, only the **residuals** of the first solution in the fine grid.

A version of the multigrid method is called **block-correction**. For a two-dimensional situation, the grids then look like this:

Figure 6.5.5 Grid structure for multi-block method. Original grid to the left.

The iterations are started on the original grid. Then all variables are summed in a slice of the grid, so that a one-dimensional grid emerges. This is solved, and the result is used to correct the original values. This is repeated in all directions, shown here with two coarse grids, for a two-dimensional situation.

The Rhie and Chow interpolation

Using a non-staggered variable location, all variables are calculated in the centre of the cells. This causes oscillations in the solution and instabilities. The staggered grid was invented to avoid these oscillations. Then the pressure is calculated between the centres of the grid cells. There are several problems with this variable arrangement, especially for non-orthogonal grids. The Rhie and Chow interpolation was invented to avoid the instabilities and still use a non-staggered grid. The interpolation gives the velocity on the cell surface. This velocity is used to calculate the flux on the cell surface.

A derivation of the Rhie and Chow interpolation procedure is fairly involved, and the reader is referred to Rhie and Chow (1983). The main idea is to use information about pressure gradients in staggered and non-staggered positions. The resulting interpolation formula is a function of the linearly interpolated velocity plus a term dependent on the pressure gradients, cell areas and the a_p coefficient.

The Rhie and Chow interpolation can be interpreted as an addition of 4^{th} order artificial diffusion. However, no adjustment coefficients are used.

The Rhie and Chow interpolation is used in most CFD programs using the finite volume method, the SIMPLE algorithm and non-staggered grids.

Note that the Rhie and Chow interpolation has given problems for some cases where there are large source terms in the Navier-Stokes equations (Olsen and Kjellesvig, 1998b). In these cases there are significant forces on the water in addition to the pressure, for example from gravity.

Upstream methods and artificial diffusion

The discretization schemes given in Chapter 5 are all fairly stable for the calculation of sediment concentration. However, other schemes developed earlier were not so stable. The classical example is the central-difference scheme. In this method, the flux on a cell wall is calculated by interpolation between the cells on the two sides. The figure below shows the estimation.

Figure 6.5.6 Estimation of concentration for the central scheme

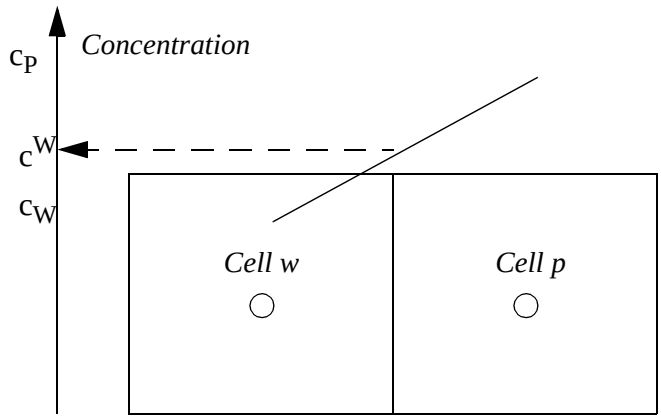

The fluxes through the sides are then:

$$F_w = 0.5U_wA_w(c_w + c_p) + \Gamma_w\frac{A_w(c_w - c_p)}{dx} \quad (6.5.2)$$

$$F_e = 0.5U_eA_e(c_p + c_e) + \Gamma_e\frac{A_e(c_p - c_e)}{dx} \quad (6.5.3)$$

$$F_s = 0.5U_sA_s(c_p + c_s) + \Gamma_s\frac{A_s(c_p - c_s)}{dy} \quad (6.5.4)$$

$$F_n = 0.5U_nA_n(c_n + c_p) + \Gamma_n\frac{A_n(c_n - c_p)}{dy} \quad (6.5.5)$$

Applying the continuity equation (Eq. 5.3.7), and the same method as in Chapter 5.3, the coefficients become:

$$a_w = 0.5U_wA_w + \Gamma_w\frac{A_w}{dx} \quad (6.5.6)$$

$$a_e = -0.5U_eA_e + \Gamma_e\frac{A_e}{dx} \quad (6.5.7)$$

$$a_n = 0.5U_nA_n + \Gamma_n\frac{A_n}{dy} \quad (6.5.8)$$

$$a_s = -0.5U_sA_s + \Gamma_s\frac{A_s}{dy} \quad (6.5.9)$$

$$a_p = -0.5U_wA_w + \Gamma_w\frac{A_w}{dx} + 0.5U_eA_e + \Gamma_e\frac{A_e}{dx} + 0.5U_sA_s + \Gamma_s\frac{A_s}{dy} - 0.5U_nA_n + \Gamma_n\frac{A_n}{dy} \quad (6.5.10)$$

Applying continuity, the following simplification can be done for a_p:

$$a_p = \Gamma_w\frac{A_w}{dx} + \Gamma_e\frac{A_e}{dx} + \Gamma_s\frac{A_s}{dy} + \Gamma_n\frac{A_n}{dy} \quad (6.5.11)$$

Looking at for example a_e, if the diffusivity is low compared with the velocity, there is a chance that a_e can become negative. Also, the effective weighting factor is actually a_e/a_p. When the diffusion becomes small, the effective factor becomes very large, as a_p is only a function of the diffusion. A large negative number for the weighing factor is not physically realistic, and this causes instabilities.

The minimum value of the diffusivity before instability occur can be calculated by setting the weighting factor to zero.

$$a_e = -0.5U_eA_e + \Gamma_e\frac{A_e}{dx} = 0 \quad (6.5.12)$$

This gives the following theoretical minimum viscosity to avoid instabilities:

$$\Gamma_{e,\,min} = 0.5U_e dx \quad (6.5.13)$$

Artificial/false diffusion: Many people confuse the difference between artificial and false diffusion. Artificial diffusion can be seen as a kind of fudging factor, to get a stable solution. False diffusion is due to inaccurate approximation in the discretization method.

Schemes based on the central-difference scheme or similar ill-formulated numerical schemes may require adding extra diffusivity to the solution in order to become stable. This is called **artificial diffusion**, and comes in addition to the physical diffusivity. The disadvantage with adding artificial diffusivity is that the increased diffusivity it may give a different final result than what the natural diffusion would give.

6.6 Free surface algorithms

The ability to compute flow with a free surface is important in hydraulic engineering. The free surface algorithms can be classified according to how many dimensions are used. For two-dimensional depth-averaged computations, similar algorithms as described in Chapter 3 can be used. However, there exist a large number of different algoritms for computing the free surface in 2D.
For computing the free surface in 3D, the different algorithms can be classified according to if an adaptive grid is used or not.

Fixed grid algorithms

The fixed grid algorithms will in general compute a two-phase flow. The two phases will be water and air. The algorithms must determine where the location of the free surface is within the grid. Some cells will be completely filled with water, and others completely filled with air. The remaining cells will be partially filled with water and air.

One of the most commonly used algorithms is called a Volume Of Fluid (VOF) method. The method introduces a variable called the volume of

fluid, defined as:

$$F = \frac{V_w}{V_a + V_w}$$

V_w is the volume of water in a cell and V_a is the volume of air in the cell. The parameter r will therefore be 1 when the cell is completely filled with water and 0 if a cell is completely filled with air.

The VOF ratio is computed by solving a convection-diffusion equation:

$$\frac{\partial F}{\partial t} + U_i \frac{\partial F}{\partial x_i} = \frac{\partial}{\partial x_i}\left(\Gamma \frac{\partial F}{\partial x_i}\right) \qquad (6.6.2)$$

Based on the *F* values in all the cells, the location of the free surface must be determined. The reconstruction of the surface is not trivial, and there are several different methods that can be used.

The VOF method is used in Flow-3D.

A more recent method that has attracted attention in research communities is the Level Set method. Instead of solving an equation for the volume of fluid, an equation for the distance, *L* [m], to the water surface is used. A convection equation for this distance is given as:

$$\frac{\partial L}{\partial t} + U_i \frac{\partial L}{\partial x_i} = 0 \qquad (6.6.2)$$

The equation is solved with similar methods as given in Chapter 5, as this is a convection-diffusion equation where the diffusive term is omitted.

The advantage of using the level set method instead of the volume of fluid method is that it is easier to compute the location of the free water surface once the equations are solved.

Adaptive grid algorithms

Adaptive grid algorithms will change the grid so that the free surface always is aligned with its top. All the cells will thereby always be filled with water. No cells are thereby wasted by filling it with air. The method therefore needs less cells than the fixed grid algorithms. Another advantage is that inaccuracies can occur when the cells are partially filled with water. Also, the grid close to the surface will be aligned with the flow, reducing false diffusion.

A disadvantage with the adaptive grid methods is that they may be more unstable than the fixed grid methods.

In an adaptive grid algorithm, the free surface is given an initial value. The algorithms will compute changes in the free surface, and adjust the grid accordingly. The adjustments are done in small steps, to prevent instabilities.

The adaptive grid methods can be further classified from which equations are solved to compute the changes in the water levels. One method uses the water continuity equation in the cells close to the surface (Olsen and Kjellesvig, 1998). Normally, the water continuity defect

is used in the SIMPLE algorithm to compute the pressure. Instead, the pressure is computed by linear interpolation between the cell below and the surface. This approach also introduces the gravity in the Navier-Stokes equations. The gravity is a large source term, causing instabilities in the solution. Therefore, a very short time step has to be used. An example is given in Fig. 6.6.1, where the coefficient of discharge for a spillway is computed.

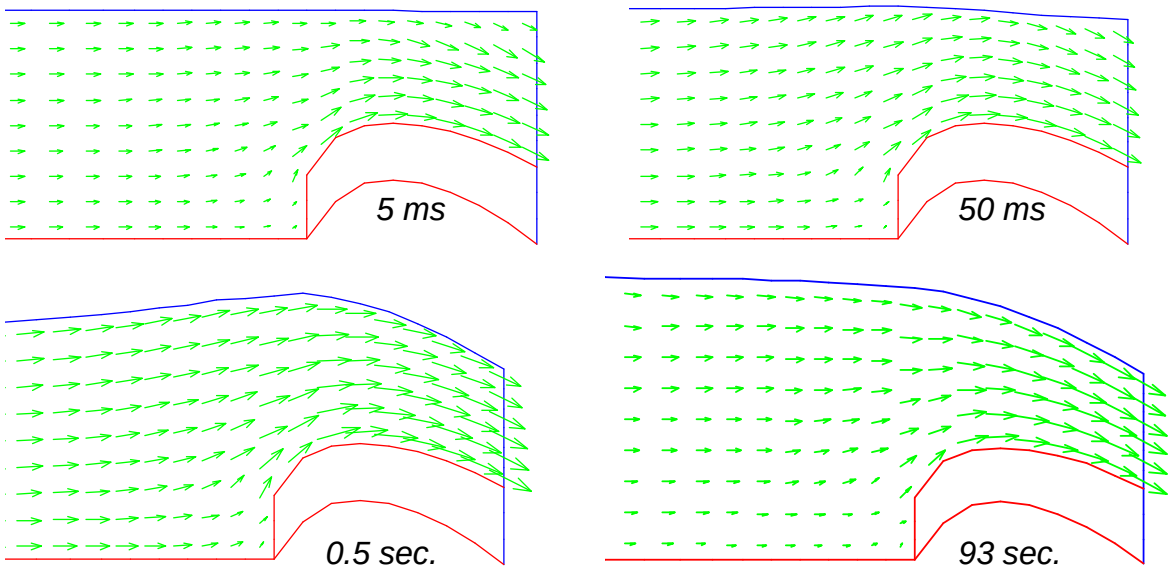

Figure 6.6.1 *Longitudinal profile of the water level and velocities for computation of coefficient of discharge for a spillway. The numbers show the computed time.*

The main problems with the method is the stability and the need for extremely short time steps. When modelling a river over several weeks, it is necessary to use longer time steps. Then the gravity can not be used in the Navier-Stokes equation. The alternative is to use the Energy equation instead of the continuity equation to compute the changes in the free surface. Then the computed pressure field is used to estimate the location of the surface, according to the following equation:

$$dh = \frac{dp}{\rho g} : \qquad (6.6.3)$$

It is then assumed that one location in the grid is kept at a known elevation. The elevation difference, *dh*, between this location and another cell in the grid can be computed from Eq. 6.6.3, given the pressure difference *dp* between the cells. The method is very stable and can be used with large time steps. However, the water close to the surface must have a hydrostatic pressure for Eq. 6.6.3 to be valid. Therefore, very steep surface slopes, like in Fig. 6.6.1 can not be computed. The location in natural rivers and channels can be computed.

More details about free surface algorithms are given by Olsen (2015).

6.7 Errors and uncertainty in CFD

As shown in previous chapters, there are a number of uncertainties in CFD modelling, and approximations in the algorithms leads to some

errors in the results. The European Research Community on Flow, Turbulence and Combustion (ERCOFTAC) published Best Practice Guidelines for CFD, where the errors are classified according to the following list:

1. Modelling errors
2. Errors in the numerical approximations
3. Errors due to not complete convergence
4. Round-off errors
5. Errors in boundary conditions and input data
6. Human errors due to inexperience of the user
7. Bugs in the software

Modelling errors are errors introduced when modelling the real world with a number of mathematical equations. Typical modelling errors are using a one-dimensional formulation if there are three-dimensional effects affecting the problem. Another example is the assumption of an isotropic turbulent eddy-viscosity made for example in the standard k-e model. Non-isotropic effects may affect the results in some cases.

Errors due to numerical approximations are often introduced when discretization the equations. False diffusion is a typical error in the numerical approximations.

Many times an iterative solver is used for the equations. Sometimes the results are used even if the solution is not fully converged. This could be the case if proper convergence criteria are not used. Also, for time-dependent computations, convergence may not be reached for each time step.

Round-off errors are due to limitations in the accuracy of the microprocessors of the computers. Most numerical programs nowadays use 64 bits floating point numbers with 12 digits accuracy, and then this is usually not a serious problem. However, earlier 32 bits programs often used numbers with only 6 digits accuracy, and then round-off errors could be significant.

Errors in the boundary conditions is one of the most common problems in CFD modelling. Computing flow in complex geometries the grid has to follow the water level and river bed completely. This is sometimes difficult. Also there may be problems with deciding boundary conditions for example for the roughness. Inflow boundary conditions are also uncertain. This applies for the distribution of the velocity at the inlet cross-section and the turbulence there. For sediment computations, the amount of sediment inflow may be uncertain. Also, the empirical formula for sediment concentration close to the bed is often not very accurate.

Human errors due to inexperience of the user is often a likely problem. Experience on CFD modelling is scarce, and it is easy to make errors when choosing among different parameters and algorithms in the CFD model.

There will always be bugs in every software. An estimate often used is one bug pr. 1000-10 000 lines for a commercial program. A typical CFD program may have 100 000 - 1 million lines of code. It is therefore likely that most CFD program has a fair number of bugs. A CFD program is usually improved relatively frequently. Every time a new algorithm is made in the program, it is possible that bugs are introduced. This may be problematic to detect, as it is often difficult to predict how the new algorithm with interact with the older algorithms.

6.8 SSIIM

SSIIM is an abbreviation for **S**ediment **S**imulation **I**n **I**ntakes with **M**ulti-block option. The program solves the Navier-Stokes equations in a three-dimensional non-orthogonal grid, using the k-ε turbulence model and the SIMPLE method to compute the pressure. The program also solves convection-diffusion equations for various water quality constituents, like sediments, temperature, algae, nutrients, pollutants etc. Time-dependent changes in bed and surface levels are computed.

There exist a large number of CFD programs. Some are tailor-made for hydraulic engineering, for example **TELEMAC**, **SSIIM** and **HEC-RAS 5** (made by US Army Corps of Engineers). Others are general-purpose programs, that can be used for gas, oil, multiphase flow etc. Some of the most used general-purpose programs are **FLUENT**, **OpenFOAM, CFX**, **FLOW3D**, and **STAR-CCM**. Web addresses to more information about the programs can be found at: **folk.ntnu.no/nilsol/cfd**

The program was originally designed to compute sediment transport for hydropower intakes. Later it has been expanded to areas of river morphology, hydraulic structures like spillways, head loss in contractions etc.; general water quality, density stratification, wind-induced currents, special algae algorithms etc.

The program has a graphical user interface with an interactive grid editor, containing several algorithms simplifying the constructions of the grid. The main program contains graphical presentation of results in multiple dimensions, which can be run simultaneously with the solution of the differential equations. The program writes result files that can be read by the ParaView program. ParaView is freeware and has powerful 3D graphics.

The SSIIM program runs on Windows, and can be down loaded from the Internet: http://folk.ntnu.no/nilsol/ssiim. The User's Manual gives more details, and can be downloaded from the same web page.

6.9 OpenFOAM

OpenFOAM is an acronym for "Open source Field Operation And Manipulation". The program was made by Henry Weller from Imperial College i London in the 1980's. It was launched as open source in 2004, with a business model where the users would pay for support and maintenance instead of a program license. Since then, several companies have emerged that sells support for OpenFOAM.

Being open source means that the OpenFOAM program is free. This is an advantage compared with commercial CFD programs, as the license cost can be substantial. Binary versions of the program also exist, so most users will not need to work with the source code. However, the source code can be downloaded and changed by anyone. This means that anyone has the possibility to modify the program. For advanced research in CFD this is a major advantage compared with commercial CFD programs. PhD students can make new algorithms for the program, which is impossible for a commercial CFD program. New algorithms is necessary to advance research in CFD. OpenFOAM is therefore very popular in leading research groups in the world.

OpenFOAM has earlier been relatively difficult to use, but over the last years improvements have been made with respect to installation, graphical user interface and platform. OpenFOAM is developed for Linux, but several companies have made Windows version which are relatively easy to install on a PC. Graphical user interfaces for OpenFOAM has also been made. Several companies sells support and gives courses for OpenFOAM. OpenFOAM is still more difficult to use than the commercial CFD programs, for example in making the grid. However, the program is not considered to be slower or less accurate than commercial programs.

OpenFOAM has been used to compute the coefficient of discharge for spillways. Olsen (2015) computed the water surface elevations over a broad-crested weir and got good results compared with a physical model test. Jacobsen (2014) also obtained reasonable results for computation of flow over a standard ogee spillway.

OpenFOAM uses the ParaView program as post-processor, similar to SSIIM.

6.10 Problems

Problem 1. Navier-Stokes solver

Apply the *SSIIM* model to the example with the sand trap: Tutorial 1 in the User's Manual. Note how many iterations are required for convergence of the Navier-Stokes equations, and how long time it takes on your PC.

Problem 2. Multigrid

Repeat the calculation in Problem 1, but this time use block-correction for all equations. How many iterations are now needed, and how long time does this take?

Problem 3. Relaxation coefficients

Repeat the calculation as in Problem 1, but this time change the relaxation factors first to 1.0 for all the equations. How many iterations are needed?

Again, change the relaxation coefficients to 0.5 for all equations. How many iterations are needed?

Change the relaxation coefficients to 0.3 for velocity, 0.1 for pressure and 0.2 for k and ε. How many iterations are needed?

Problem 4. The Rhie and Chow interpolation

Repeat the calculation in Problem 1, but this time reduce the influence of the Rhie and Chow interpolation by the using the *F 21* data set. Set this to 0.5 for one run and 0.0 for the next run. How does the Rhie and Chow interpolation affect the resulting trap efficiency? And how many iterations are needed?

Problem 5. Upstream boundary conditions

Repeat the calculation in Problem 1, but this time use uniform upstream and downstream velocity profile. This is done by using the *G 7* data sets. How does this affect the convergence rate and the resulting trap efficiency? What are the reasons for the change?

Problem 6. Bed roughness

Repeat the calculation in Problem 1 twice, using a roughness of 2 cm and 0.1 mm. This is done by giving the roughness in the F 16 data set. How does the roughness affect the trap efficiency and calculation time? What is the reason for the change?

Problem 7. Initial values

Calculate the water flow for the fish farm tank example with SSIIM. How many iterations are needed? Remove the G 8 data set with initial velocities in the control file. What happens in the calculations and why? How is it possible to make the calculations converge without lowering the initial water velocities?

Problem 8. Stability

Implement the central scheme for Problem 1. Vary the amount of diffusion, and see how the result changes. What is the minimum amount of diffusion to get a stable solution? How does this compare with the real diffusion?

7. Physical limnology

7.1 Introduction

Limnology is the science of processes in lakes, including water quality, temperature, ice, water currents etc. A large number of words explaining the processes has been made. Also various classification systems have been developed. This chapter focuses on the hydraulic and temperature processes. Biological processes and classification systems for lakes are given in Chapter 8.

7.2 Circulation in non-stratified lakes

The term **circulation** is often used for water currents in a lake. Velocities in a lake are often wind-induced. The water will then follow a circulation pattern, moving with the wind at the water surface and a return current is formed close to the bed. However, the term circulation is also used if the water currents are due to inflow/outflow, and the water moves in almost straight lines. Fig. 7.2.1 shows a typical profile of wind-induced velocity in a shallow lake:

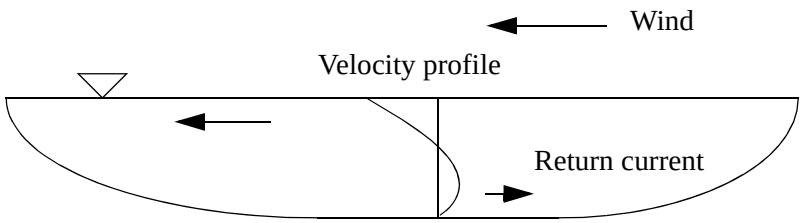

Figure 7.2.1. Longitudinal profile of a lake with wind-induced currents. The velocity profile is shown, where the water close to the surface moves with the wind, and a return current is formed close to the bed.

The magnitude of the wind-induced currents will depend on the wind speed. The most common approach to calculate the currents is to compute a shear stress from the wind on the surface of the lake. And then use this shear stress to calculate the currents. The wind-induced shear is given by:

$$\tau = c_{10}\rho_a U_a^2 \qquad (7.2.1)$$

The wind speed is denoted U_a, ρ_a is the air density (around 1.2 kg/m^3) and c_{10} is an empirical coefficient. The coefficient will be different depending on which elevation the wind is measured. The c_{10} coefficient is given for wind speeds taken 10 meters above the water surface. There are a number of empirical formulas for c_{10}, for example as given by Bengtsson (1973)

$$c_{10} = 1.1*10^{-3} \qquad (7.2.2)$$

"Circulation is when water flows in circles". -Exam answer from student

If the wind persist for a long time, the water surface will not be horizontal any more. The slope, I, can be computed from equilibrium forces on a water element, similar to what was done for a river in Chapter 2. The slope becomes:

$$I = \frac{\tau}{\rho g h} \tag{7.2.3}$$

where h is the water depth.

The wind will also induce velocity gradients and turbulence in the lake. Classical hydraulics will give the following formula for the turbulent mixing coefficient, Γ (derivation given in Chapter 4.2):

$$\Gamma = \alpha u_* h \tag{7.2.4}$$

The shear velocity is denoted u_*, h is the water depth and α is an empirical coefficient. For rivers, α has been found to be 0.11. This value was used successfully for lakes by Olsen et. al. (2000) modelling a small reservoir in Wales, UK. However, when modelling Loch Leven in Scotland (Olsen et. al. 1998), the formula gave too high diffusion.

7.3 Temperature and stratification

Table of water density as a function of temperature:

Temp (^{0}C)	Density (kg/m^3)
0	999.87
2	999.97
4	1000.0
6	999.97
8	999.88
10	999.73
12	999.52
14	999.27
16	998.97
18	998.62
20	998.23
22	997.80
24	997.33
26	996.81
28	996.26
30	995.68

The water density in freshwater lakes and reservoirs is mainly a function of the temperature, as long as the sediment concentration is reasonably low. Maximum density is at 4^oC, with lower densities at higher and lower temperatures. Stratification of the lake/reservoir will therefore occur for some vertical temperature distributions.

The specific heat for water is 4182 W/(kg^{0}Cs) The temperature changes in the water close to the surface can be computed from the energy balance across the water surface. The sources/sinks of energy are:

- solar short-wave radiation
- atmospheric longwave radiation
- longwave black radiation from the water
- conduction
- evaporation

The formula for the surface flux, I, in Watt/m^2, can be written according to Chapra (1997) and Henderson-Sellers (1984):

temperature flux $I =$

short-wave irradiance IrB

long-wave irr. from atm. $+ \sigma(T_{air} + 273)^4 (A + 0.003\sqrt{e_{air}})(1 - R)$

long-wave irr. from water $- \varepsilon\sigma(T_w + 273)^4$

conduction $- 0.136 c_1 (1 + 0.437 U_2)(T_w - T_{air})$

evaporation $- 0.136(1 + 0.437 U_2)(e_w - e_{air})$

(7.3.1)

In the formula, *Ir* is the irradiance, *B* is a reduction factor and *T* is the temperature. The irradiance terms follow Stefan-Bolzmanns law, where σ is the Stefan-Bolzman's constant 5.67x10^{-8} W/(m^{2}K^4) and ε is the emissivity of water (~0.97). The emissivity is a correction factor for the water not being a perfect emitter of radiation. *A* is an empirical coefficient between 0.5 and 0.7 and e_{air} is the vapour pressure in the air. *R* is a

reflection coefficient, which usually is very small (around 0.03). The parameter c_1 is Bowen's coefficient (62 Pa/^{o}C), U_2 is the wind speed 2 meters above the water surface and e_w is the saturation vapour pressure at the water surface. The subscript *w* denotes water and *air* the air.

Short-wave irradiance intensity is usually measured in μmol-photons/m^2/s, or W/m^2. The conversion between the units is: 1 μmol photons/s = 0.3 W

The **short-wave irradiance** is from the sun, and depends on several factors:

- Variation over the year
- Variation over the day
- Latitude of lake
- Shading by clouds
- Reflection from the water surface

All these parameters can be estimated and put into the factor *B*. The first three factors can be taken from tables. The cloud shading is determined by the weather conditions. And the reflection from the water surface depends mostly of the solar altitude. If this is above 20^o, the reflection is less than 10 %.

The **long-wave irradiance** is black-body heat emission from the atmosphere and the water. The term contains attenuation from the atmosphere and reflection.

The **conduction and convection** term describes physical processes at the water surface. The processes are similar to convection and diffusion, as described in Chapter 4. Eq. 7.3.1 gives an empirical formula for these processes.

Evaporation/condensation at the water surface affect the temperature, as the specific energy of a certain mass of water is different depending on if it is in liquid or gas form. The term in Eq. 7.3.1 also gives an empirical estimate of the amount of evaporation, as it is a function of the wind speed.

Limnological classifications

The temperature profile of a lake will vary over the year, depending on the heat flux at the water surface. In different climates, there will be different types of stratification. The science of limnology has given several definitions to classification of lakes and stratification layers.

In a temperate climate with warm summers and cold winters, the vertical temperature profiles are given in Fig. 7.3.1.

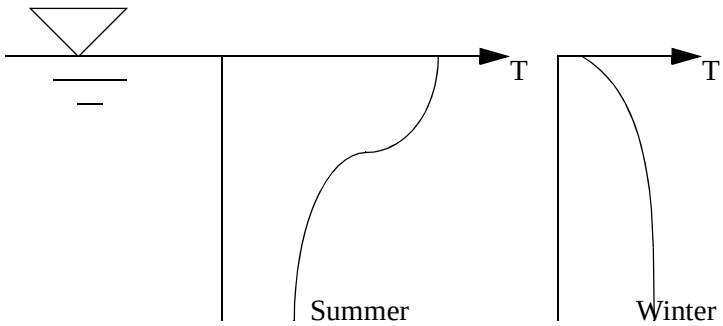

Figure 7.3.1. Vertical temperature profiles for a dimitic lake in the summer and the winter

The upper layer close to the water surface is called **epilimnion**. The layer close to the bed is called **hypolimnion**. In deep lakes, the hypolim-

nion will hold a temperature of 4^oC throughout the year. The layer between the epilimnion and hypolimnion is called the **metalimnion**. During the summer, the vertical temperature gradient is usually large in this layer. The **thermocline** is located in this layer, marking the difference between the warm upper water and the cold water close to the lake bottom.

In temperate climates, the winter is cold and the summer is warm. The stratification will follow Fig. 7.3.1. In the summer, the warm water close to the surface is lighter than the cold bottom water. In the winter, the water close to the surface is below 4^oC, and is lighter than the bottom water. These two situations give a stable water body, and the stratification prevents mixing from taking place. However, during spring and fall, the water temperature will at some point in time be 4^oC over the whole depth of the lake. Then vertical circulation may occur. The water from the bottom may rise to the surface, if wind-induced currents are present. This process is called a spring/fall **overturn**.

The science of limnology has also provided classifications of the lakes according to the overturns. If there is no overturn due to the surface water being too cold the whole year, the lake is called **amictic**. If only one overturn occur during the year, the lake is called **monomictic**. This may be due to the lake being so warm that no winter stratification is formed. The lake is then called **warm monomictic**. If the lake is so cold that no stable summer stratification occur, and only one overturn takes place in the summer, the lake is called **cold monomictic**. The cycle described in Fig. 7.3.1 with two overturns is present in **dimictic** lakes. There are also lakes with multiple overturns, called **polymictic** lakes. This is due to small changes in seasonal temperature and strong winds.

Turbulence damping

When horizontal water currents occur in a lake, there will be velocity gradients producing turbulence. In a stratified lake, the turbulent eddies will be dampened by the stratification. A formula for the damping of the turbulence is often given by the following formula for the turbulent diffusion coefficient, Γ (Rodi, 1980):

$$\Gamma = \Gamma_0(1 + \beta Ri)^{\alpha} \tag{7.3.2}$$

Γ_0 is the original turbulent diffusion, when not taking the stratification into account. *Ri* is the Richardson number, given by:

$$Ri = -\frac{g}{\rho}\frac{\frac{\partial \rho}{\partial z}}{\left(\frac{\partial U}{\partial z}\right)^2} \tag{7.3.3}$$

The formula is often used in numerical models (Olsen and Tesaker, 1995; Olsen et. al. 1999; Olsen and Lysne, 2000)

Various values of the constants a and b are used by different reserachers. Rodi (1980) recommends the values given by Munk and Anderson (1948):

α = -0.5 and β = 10.0, computing the diffusion for the velocity.
α = -1.5 and β = 3.33, computing the diffusion for other variables.

Olsen and Lysne (2000), however, found better correspondence with measurements when using the values:

α = -1.3 and β = 10.0, for all variables.

More advanced methods of taking the stratification into account when modelling turbulence is given by Rodi (1980).

7.4 Wind-induced circulation in stratified lakes

Water currents in a stratified lake will be influenced by the density variation in two ways:

1. Vertical velocities will be dampened
2. Turbulence will be dampened

Looking at a deep stratified lake in the summer, where wind-induced currents occur, the circulation pattern given in Fig. 7.4.1 will emerge:

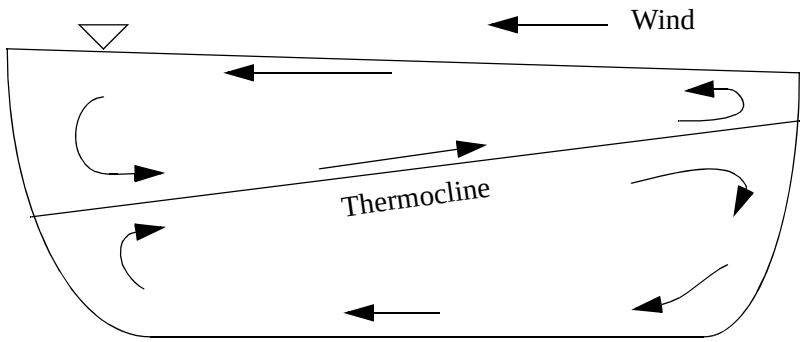

Figure 7.4.1. Wind-induced circulation in a stratified lake. The arrows show the direction of the velocity. Note this is a stationary situation.

The slope of the water surface can be computed by looking at the forces on the water body, as given in Fig. 7.4.2:

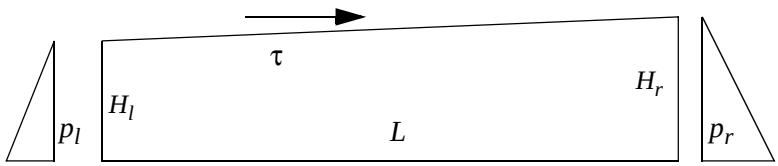

Figure 7.4.2. Forces on a water body. The hydrostatic pressure is denoted *p*, *L* is the length of the reservoir, τ is the shear stress and *H* is the water depth.

The force from the wind is given as:

$$F_w = \tau L \tag{7.4.1}$$

The force from the hydrostatic pressure difference is:

$$F_{pd} = \frac{1}{2}\rho g H_l^2 - \frac{1}{2}\rho g H_r^2 = \rho g \frac{(H_r + H_l)}{2}(H_l - H_r) \tag{7.4.2}$$

We define the average water depth as:

$$H = \frac{(H_r + H_l)}{2} \tag{7.4.3}$$

The surface slope is given as:

$$I = \frac{H_r - H_l}{L} \tag{7.4.4}$$

Combining this equation with Eq. 7.4.3 and Eq. 7.4.2, we obtain:

$$F_{pd} = -\rho g H L I \tag{7.4.5}$$

Setting the sum of the forces (Eq. 7.4.1 and 7.4.5) in the horizontal direction to zero, gives the following equation for the water surface slope:

$$I = \frac{\tau}{\rho g H} \tag{7.4.6}$$

The slope of the thermocline, *I*', can be computed from looking at equilibrium of forces in the horizontal direction on the hypolimnion (Fig. 7.4.3)

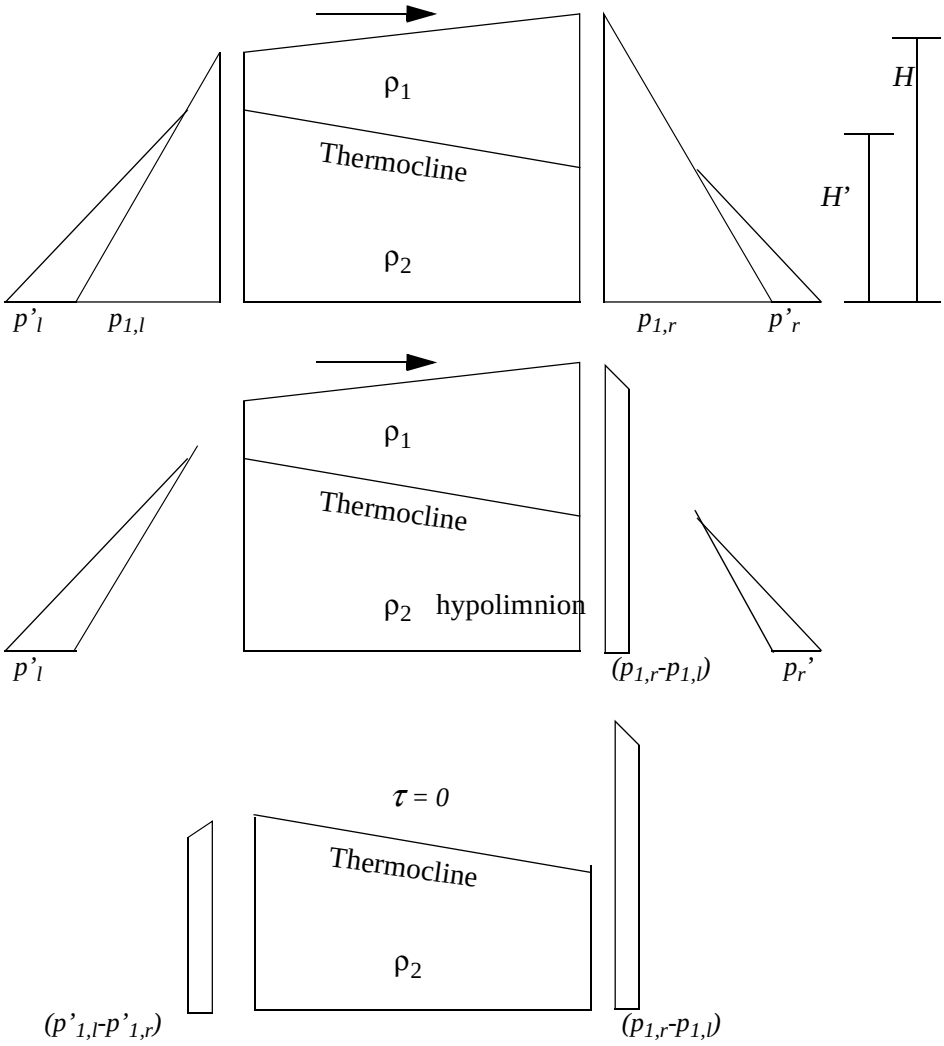

Figure 7.4.3. Forces on the hypolimnion. The left side is denoted *L*, and the right side denoted *R*. The density difference between ρ_1 and ρ_2 is denoted ρ'. The pressure at the bed is denoted *p*. On the upper figure, *p* is equal to $\rho_1 gH$, where *H* is the water depth.

The water below the thermocline is heavier than the water above. The density difference is denoted ρ', and given by:

$$\rho' = \rho_2 - \rho_1 \tag{7.4.7}$$

It is assumed that the shear stress between the epilimnion and the hypolimnion is negligible. The water flow direction above and below the thermocline is the same.

Looking at the forces on the epilimnion only, the situation will be similar to the derivation of the water surface slope. The difference is that the water density is replaced by the density difference, ρ', and the wind force is replaced by the pressure difference p_r-p_l. The force from the pressure difference becomes the same as for a non-stratified lake :

$$F_{pd} = (p_l - p_r)H = -\rho_1 gILH \qquad (7.4.8)$$

The force from the density difference is the same as Eq. 7.4.5, only the density is replaced by the density difference, and the water depth is replaced with *H*', the height of the thermocline.

$$F_{dd} = -\rho' gI'LH' \qquad (7.4.9)$$

Equilibrium of forces means the sum of the forces from Eq. 7.4.8 and 7.4.9 are zero.

$$F_{pd} + F_{dd} = 0 = -\rho_1 gILH - \rho' gI'LH \qquad (7.4.10)$$

Assuming *H/H'* can be approximated to be unity, the following equation is obtained:

$$I' = -I\frac{\rho_1}{\rho'} \qquad (7.4.11)$$

The negative sign indicates that the thermocline slopes in the opposite direction of the lake water surface.

The density difference is much smaller than the water density itself, so the slope of the thermocline is orders of magnitude larger than the water surface slope. During strong winds it may happen that the slope becomes so large that the cold water below the thermocline reaches the water surface.

7.5 Seiches

Assuming we have a situation like given in Fig. 7.4.1, and the wind speed suddenly drops to zero, the thermocline and the water surface will start to oscillate. Fig. 7.5.1 shows the movement:

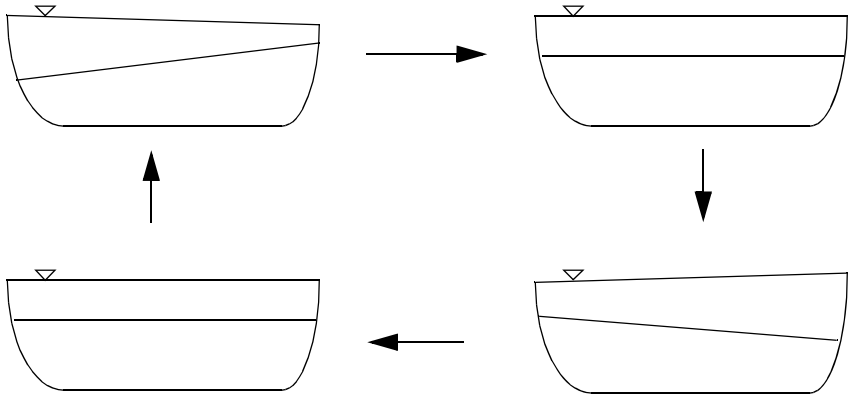

Figure 7.5.1. Surface and internal seiches in a stratified lake. The thermocline is drawn with a line. The slope of the water surface is exaggerated compared to the slope of the thermocline.

The movements of the water surface is called **surface seiches**. The movement of the thermocline is called **internal seiches**.

In Fig. 7.5.1, the thermocline is drawn with a straight line. This will not be the case, as numerical and physical models shows that the water close to the thermocline moves more like a wave, as shown in Fig. 7.5.2:

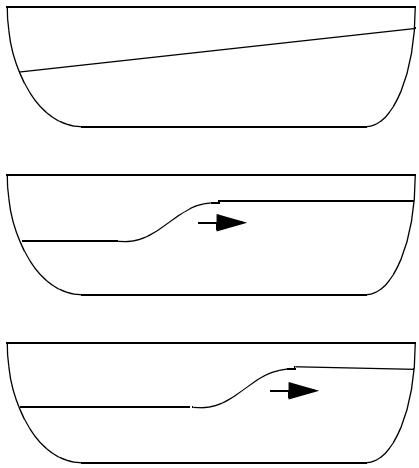

Figure 7.5.2. Movement of the thermocline during an internal seiche. The upper figure shows the initial situation. The middle figure shows the thermocline some time after the wind has stopped. The lower figure shows the situation later.

Speculations: Numerical experiments has shown that under special conditions, an internal seiche may diffuse upwards to the water surface. If this would be the case, a sudden upwelling of water to the water surface would occur, with reasonably high horizontal velocity. Local observations of such phenomena in a lake with otherwise quiet water surface could be interpreted in imaginative ways...

The movement of the internal seiche is associated with considerable horizontal velocities at the thermocline.

7.6 River-induced circulation and Coriolis acceleration

A river feeding water into a lake or a reservoir will create water currents even if there is no wind present. A particular case is an ice-covered lake, where this will be the dominant forcing mechanism for the circulation. If the lake is stratified, the current may form “plume” inside the lake. An example is given in Fig. 7.6.1, showing the velocity pattern close to the water surface in Lake Sperillen in Norway during winter. The plume follows the right (top) side of the lake, due to the Coriolis acceleration.

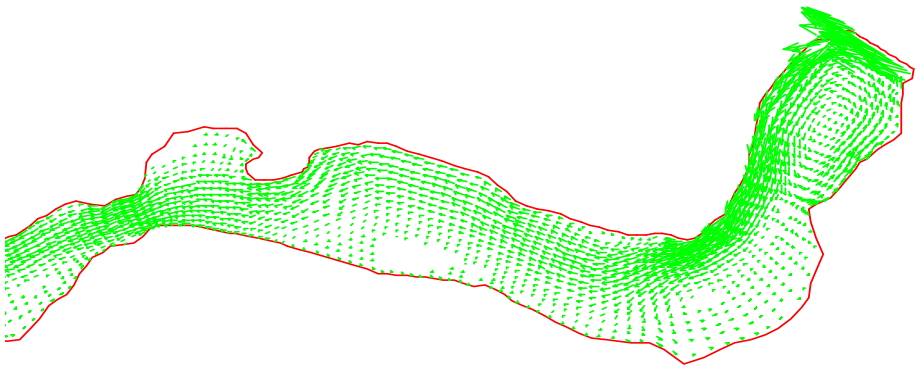

Fig. 7.6.1. Velocity vectors close to the surface in Lake Sperillen, during the winter. The lake is then covered with ice. The river is flowing in from the right and out to the left.

Coriolis

The effect of the earth's rotation is most pronounced for large lakes with stratification. However, the effect may also be present in large non-stratified lakes.

The Coriolis acceleration affect the water movement by the following formula:

$$a = -fU = -\left(\frac{4\pi}{T}\sin\phi\right)U \qquad (7.6.1)$$

T is the time it takes for one earth rotation, i.e. 24 hours or 86 400 sec., ϕ is the latitude of the lake and U is the water velocity. In the northern hemisphere, the acceleration will always be to the right. An example for a lake in southern Norway, the latitude is 60 degrees, and f will be 1.26×10^{-4}.

The formula for the Coriolis acceleration can be derived by looking at the centrifugal force on a particle with velocity U_p, at the surface of the earth that has a velocity U_E in the rotation:

$$a_0 = \frac{U^2}{R} = \frac{(U_E + U_p)^2}{R} = \frac{(U_E)^2}{R} + \frac{2U_E U_p}{R} + \frac{(U_p)^2}{R} \qquad (7.6.2)$$

At the Equator, where the radius, R, is about 6 371 000 meters, the Earth velocity is about 460 m/s. Also for points further away from the Equator, the Earth rotation velocity will be much larger than the water velocity. The last term on the right side of Eq. 7.6.2 is therefore negligible. The first term on the right side is independent of the water velocity. It is actually a fixed acceleration, causing the gravity component to tilt slightly compared with the direction to the centre of the Earth. The second term on the right side of Eq. 7.6.2 is causing the Coriolis force. The Earth velocity at maximum radius is equal to the Earth circumference divided by the time to rotate one time, T. This would be 24 hours. The acceleration is then:

$$a_0 = \frac{2U_E U_p}{R} = \frac{2\left(\frac{2\pi R}{T}\right)U_p}{R} = \frac{4\pi}{T}U_p \qquad (7.6.3)$$

Comparing this formula with Eq. 7.6.1, the sinus of the latitude is miss-

ing. This is because we are only interested in the acceleration term in the direction normal to the gravity direction. This component will be zero at the Equator.

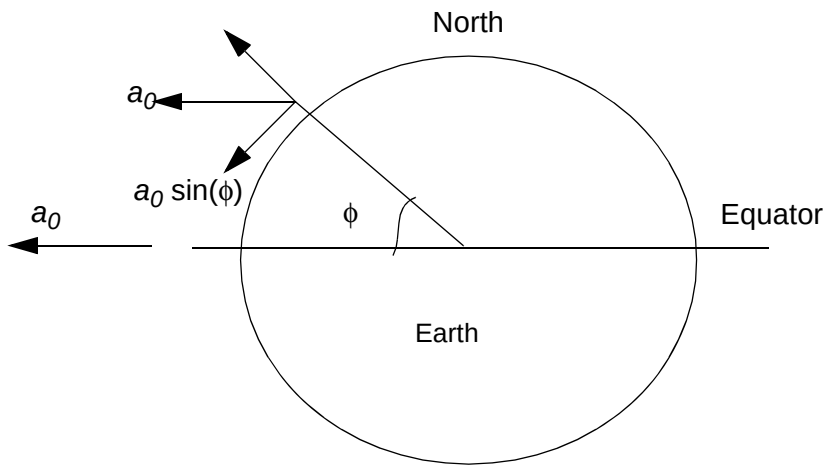

Fig. 7.6.2. Decomposition of the Coriolis accelleration on the Earths surface.

Slope of water surface

For a straight channel, the water surface slope would tilt slightly due to the Coriolis acceleration. The cross-directional slope, I_c, would be equal to the ratio of the Coriolis acceleration to the gravity:

$$I_c = \frac{fU}{g} \tag{7.6.4}$$

The velocity of the current is denoted *U* and *f* is the Coriolis factor. The bottom of the current will also get a cross-directional slope, I_b. Looking at the cross-directional balance of forces, similar to what was done for the thermocline, it is possible to derive a formula for I_b:

$$I_b = \frac{\rho}{\rho'} I_c = \frac{\rho f U}{\rho' g} \tag{7.6.5}$$

As previously, ρ is the water density, and ρ' is the density difference between the water in the current and the water below.

7.7 Density currents

If the water flowing into the lake/reservoir has a different density than the lake water, a density current is formed. The density difference can be due to:

1. Temperature variations
2. Sediment concentration
3. Content of salt in sea water

Combinations of the effects are also observed. If the temperature causes the density of the inflowing water to be lower than in the lake, the current

will move close to the water surface. If the density is higher than the lake water, the current will move along the lake bed. In a stratified lake, it is possible that the current may move down into the water body to a temperature similar to the inflowing water.

A density current caused by high sediment concentrations is called a **turbidity current**. The turbidity current can transport sediment a long way into the reservoir, and even cause deposits in front of an intake of a large reservoir. The process also redistributes sediments from the river mouth to the deeper part of the lake/reservoir.

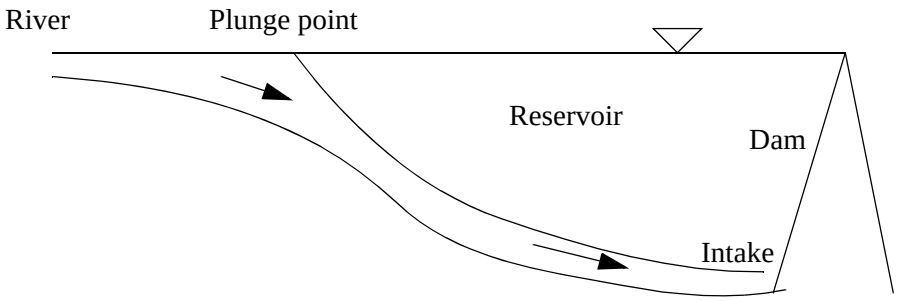

Figure 7.7.1. Turbidity current entering a reservoir. The plunge point is often visible at the water surface, as the river water contains more sediments and has a different colour than the water in the reservoir.

The sediment-laden river water often has a darker colour than the cleaner reservoir water. It is therefore sometimes possible to observe the plunge point at the water surface.

7.8 Intakes in stratified reservoirs

When water is abstracted from a linearly stratified reservoir, the situation given in Fig. 7.8.1 may occur.

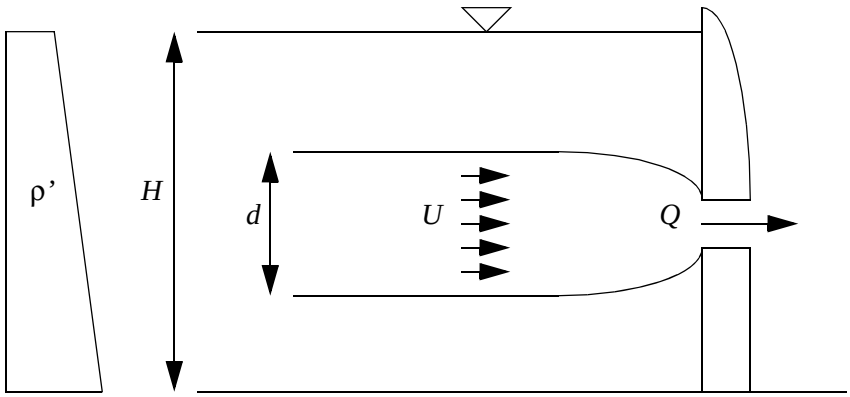

Figure 7.8.1. Water abstraction from a stratified reservoir. The depth is *H*, the discharge is *Q* and *d* is the height of the layer with abstracted water.

Only the water in a layer at the same level as the intake is abstracted. The thickness, *d*, of the layer for a two-dimensional situation with a line abstraction can be computed from:

$$d = k_1 \sqrt{\frac{q}{N}} \qquad (7.8.1)$$

where q is the water discharge/meter width, and k_1 is an empirical constant, between 3 and 5 (Steen and Stigebrandt, 1980). N is the Brunt-Väisälä frequency, given by:

$$N^2 = -\frac{g}{\rho}\frac{d\rho}{dz} \tag{7.8.2}$$

If the water discharge is above a critical value, q_c, then water will be abstracted from the whole depth. The following formula is used to find q_c (Carstens, 1997):

$$q_c = 0.32NH^2 \tag{7.8.3}$$

Eq. 7.8.1 is derived theoretically from an idealized 2D situation. In practice and intake will be limited in width, and 3D effects will be important. Steen and Stigebrandt (1980) developed formulas for a 3D situation where the abstraction gate had a significant size, of width *B* and height *h*:

$$d = k_3\left(\frac{Q^2}{B^2hN^2}\right)^{\frac{1}{3}} \tag{7.8.4}$$

It was assumed that *B* was much smaller than the dam length and h was much smaller than the dam height. The constant, k_3, was found by experiments to be 0.74 (Carstens, 1997) for a gate close to the bed or the water surface, and 1.2 for a gate midway between the water surface and the bed (Carstens, 1997; Steen and Stigebrandt, 1980). Steen and Stigebrandt (1980) also developed more complex formulas for the thickness of the abstraction layer for cases when the outlet size was not relatively small compared to the other dimensions.

7.9 Problems

Problem 1. Thermocline

A lake with depth 100 meters has a thermocline 7 meters below the water surface. The temperature is 15 ^{0}C above the thermocline and 5 ^{0}C below it. A wind from the north lasts for five days. The wind speed is 15 m/s. The lake is 5 km. long in the north-south direction. Compute the depth of the thermocline at the northern and southern side of the lake.

Problem 2. Water intake

Water is taken from a reservoir to a treatment plant to be used for municipal water supply. The intake is located 10 meters below the water surface, with a width of 2 meters and a height of 1 meter. The discharge is 2 m^3/s. The temperature gradient of the reservoir is 0.5 ^{0}C/m, and the temperature at 10 meter is 11 degrees. A pollutant is spilled on the water surface. There is no wind at the time of spill, so on average for the whole lake, the pollutant is only mixed in the upper 1 meter layer. At the intake, water is abstracted from a layer with vertical magnitude Δh. Will this be so large that polluted water enters the intake?

8. Water biology

8.1 Introduction

Water quality in lakes and reservoirs is often of interest for engineering purposes. An example is determination of location of water intakes, to prevent excessive pollutants in the inflowing water. Sometimes algae accumulate on one side of a lake. What is the reason for the variation in the spatial distribution of the algal concentration? Another example is the assessment of the capacity of a lake/reservoir to receive waste water.

The dispersion of the various components was discussed in Chapter 4 and 5, predicting the variation of the concentration as a function of turbulence, water currents etc. The variation of a component can be computed solving the convection-diffusion equation of its concentration. However, the concentration of a component is also a function of biochemical reactions. The biochemical reactions can also affect the variation of a variable. A toxic substance may change as a function of time due to for example sunlight. Or oxygen may be consumed by bacteria or generated by algae. These biochemical reactions are discussed in the following chapters.

8.2 Biochemical reactions

Some atomic weights in units grams/mol:

Hydrogen: 1
Carbon: 12
Nitrogen: 14
Oxygen: 16

Stochiometry

Stochiometry is used to **quantify** the different components in a biological or chemical reaction. An example is the photosynthesis, where carbon dioxide and water are used to produce organic material and oxygen:

$$CO_2 + H_2O \rightarrow C_6H_{12}O_6 + O_2 \qquad (8.2.1)$$

The balanced equation can be written:

$$6CO_2 + 6H_2O \rightarrow C_6H_{12}O_6 + 6O_2 \qquad (8.2.2)$$

The molecular weight of carbon is 12 g/mol and oxygen is 16 g/mol. The weight of a carbon dioxide molecule is then 44 g/mol. The weight of the oxygen molecule is 32 g/mol. So for example 44 grams of carbon dioxide will produce 32 grams of oxygen.

Reaction kinetics

Reaction kinetics is used to describe **how fast** a biochemical process takes place. There are a number of different **rate laws** describing the processes, classified by the order of the kinetics:

The reaction coefficients, *k*, are often given in units 1/day. Remember to convert this to 1/seconds, when using computer programs where this time step is used.

Zero-order kinetics:

$$\frac{dc}{dt} = -k \quad \text{or} \qquad c = c_0 - kt \qquad (8.2.3)$$

First-order kinetics:

$$\frac{dc}{dt} = -kc \quad \text{or} \qquad c = c_0 e^{-kt} \tag{8.2.4}$$

Second-order kinetics:

$$\frac{dc}{dt} = -kc^2 \quad \text{or} \qquad c = c_0 \frac{1}{1 + kc_0 t} \tag{8.2.5}$$

The derivation of the integral version of for example Eq. 8.2.4 is as follows:

$\frac{dc}{dt} = -kc$ separate variables: $\frac{dc}{c} = -kdt$

Integrate on both sides:

$\int \frac{dc}{c} = -\int kdt$ which becomes $\ln c = -kt + K$ or $c = e^{-kt+K}$

The constant, K, is found by the boundary condition $c=c_0$ at $t=0$. This gives

$$c = c_0 e^{-kt}$$

The equations describe variations in only one variable. For some cases there are multiple water quality constituents. The change in one variable may be a function of the concentration of other variables. However, often there is a limiting variable determining which process is taking place. The reaction is then dependent on this variable.

Temperature dependency

Most biochemical processes depend on temperature. For example, algal growth will increase significantly when a lake is heated by the sun during summer. The following formula is often use to estimate the growth increase/decrease as a function of temperature, T:

$$k = k_{20}\theta^{(20-T)} \tag{8.2.6}$$

The reaction rate at 20 ^{o}C, k_{20}, is often used as a basis. The parameter θ is specific for the reaction. Typical values are slightly above unity. Some examples are given in Table 8.7.1. The processes in the table are further described in the following chapters.

Discretization

Biochemical reactions are included in the convection-diffusion equation when computing the dispersion of a water quality parameter. This is done by including the left side of Eq. 8.2.3-5 in the source term. If first-order kinetics is used, the equation can be written:

$$U_i \frac{\partial c}{\partial x_i} = \frac{\partial}{\partial x_i}\left(\Gamma \frac{\partial c}{\partial x_i}\right) - kc \qquad (8.2.7)$$

When the equation is discretized, it becomes:

$$a_p c_p = a_w c_w + a_e c_e + a_n c_n + a_s c_s - k c_p V_p \qquad (8.2.8)$$

V_p is the volume of the cell. The last term on the right side is due to the biochemical reactions. Note that this term is negative, so that it is in principle possible to get a negative concentration. This can lead to instabilities in the solution and unphysical results. To avoid this, the same procedure as in Chapter 5.7 can be used. The equation is then written:

$$(a_p + kV_p)c_p = a_w c_w + a_e c_e + a_n c_n + a_s c_s \qquad (8.2.9)$$

In this way, negative concentrations will be avoided.

The time term can also be added, similarly as described in Chapter 5.7.

8.3 Toxic compounds

Toxic compounds are chemical substances not naturally occurring in the river/lake water, causing a hazard to humans and animals drinking the water.

Individual types of toxics will not be described here, and the dangerous concentrations need to be determined for each component. But a few of the processes affecting the toxic concentration are discussed.

Sorption

Toxic substances often attach to organic and inorganic sediments, suspended in the water. When the sediments settle, some of the toxic substance will be removed. The total concentration of toxics, c, in a water body is therefore the sum of the dissolved toxic concentration, c_d, and the concentration attached to particles, c_p. The fractions of the two components as a function of the total concentration is given by:

In the spring of 1995 there was a large flood in the rivers flowing into Lake Mjøsa in Norway. The flood caused extensive damage to infrastructure. It was also feared it could lead to decreased quality of the water in the lake, which was used for water supply to the main cities in the area. This did not happen, as much of the polluting compounds sorbed to sediments and deposited at the bottom of the lake.

$$F_d = \frac{c_d}{c} = \frac{1}{1 + K_d c_s} \qquad (8.3.1)$$

$$F_p = \frac{c_p}{c} = \frac{K_d c_s}{1 + K_d c_s} \qquad (8.3.2)$$

The index d denotes the dissolved fraction and p denotes the fraction attached to the suspended particles. The particle concentration is denoted c_s. The partition coefficient, K_d, may range between 0.0001 and 1000. The value depends on the type of toxic and the composition of the suspended particles. There exist empirical formulas for K_d for some types of toxics/sediments. Otherwise, the coefficient must be determined by a laboratory analysis.

Translation to Norwegian:

Biodegradation: *Biologisk nedbrytning*
Partition coefficient: *Partisjonskoeffisient*
Reaeration: *Lufting*
Sorption: *Sorpsjon*

Photolysis

Sunlight may cause toxic chemicals to undergo a transformation to other compounds. The decrease in concentration is given by first-order kinetics (Eq. 8.2.4). The reaction rate, k_p, is a function of the specific chemical and the sunlight. There exist tables for k_p at the water surface. But as the light penetrates the water body, it will be dampened. This process must be taken into account when evaluating the effect of the photolysis. The computation of the irradiance damping must also take into account that each photolysis reaction requires light at a specific wavelength. The damping computation must be specific for the particular light frequency.

Hydrolysis

Hydrolysis is a transformation of the toxic to other components, usually by acid or bases in the water. The reaction can be computed by first-order kinetics, and the reaction rate, k_p, is usually in the order of 10^{-7} to 0.1/day. It will be a function of the pH of the water and the chemical composition of the toxic.

Biodegradation

In biodegradation processes, toxic substances are reduced to other compounds by organic material. Usually, different types of bacteria are involved in the process.

8.4 Limnological classifications

Depending on the nutrition inflow to a lake, there may be more or less organic material and processes. A lake with little nutrients and organic material is called **oligotrophic**. If the nutrition inflow is high and large amount of organic material is present in the lake, it is called **eutrophic**. The state in between oligotrophic and eutrophic is called **mesotrophic**. A quantitative distinction between the types are often related to the phosphorous concentration. The mesotropic lake has a concentration between 10 and 30 mg/l. Lower phosphorous concentrations are found in oligotrophic lakes, and higher concentrations in euthropic lakes.

The water body of a lake can be divided in several zones, depending on the biology of the lake. The **littoral zone** is the shallow part of the lake close to land, where plants may grow. Classification also depends on the amount of light penetrating the water body. Since the algae requires light for photosynthesis, the production of organic components only take part in the upper zone. This is called the **euphotic zone**. The **aphotic zone** is below. The light penetration is here so small that photosynthesis is not possible, and only decomposition processes take place.

Water quality is defined from the concentration of various components in the water. For example, the water should have above a certain amount of oxygen, and the concentration of toxic components should be below a threshold value. The component is then a **water quality indicator**. Certain species of algae has also been used for this purpose. The water engineer is faced with the question of determining the concentration of the various water quality constituents.

More details on the typical processes and water quality parameters in a lake is given in the next chapter.

8.5 The nutrient cycle

Most computer programs for water quality models the nutrient cycle in a river/lake using oxygen, phosphorous, nitrogen and algae/bacteria. Fig. 8.5.1 shows a schematic view of the components involved:

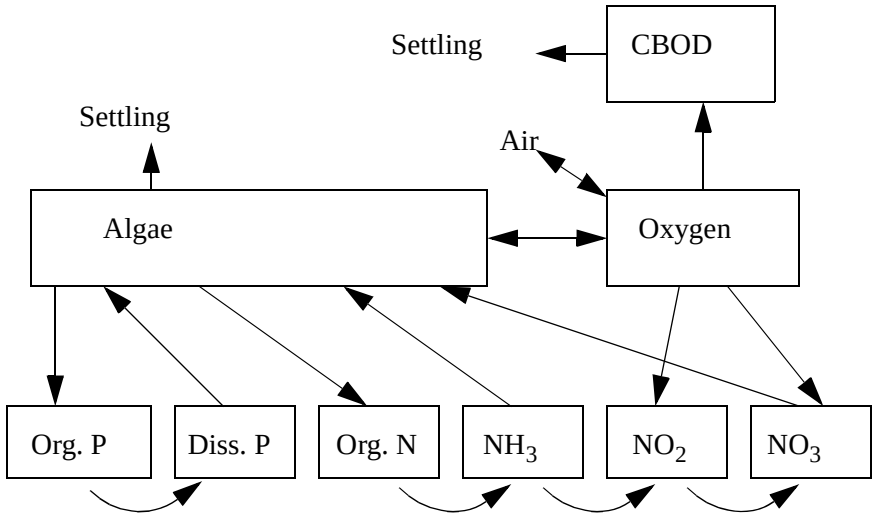

Figure 8.5.1. A model of the components in a river/lake

P is phosphorous, *N* is nitrogen and the oxygen is dissolved in the water.

Oxygen processes

Oxygen dissolved in the water is seen as a main indicator of water quality. The oxygen concentration is often measured as a fraction of the saturation concentration, or a saturation concentration deficit. Clean water will usually have high oxygen concentrations, or close to zero concentration deficit.

One of the most important processes for life is the **photosynthesis**. The process transforms carbon dioxide and water to organic substances and oxygen. In water, the process takes place in chlorophyll of the algae. Algal processes will be further discussed in Chapter 8.7.

Oxygen is used by plants and bacteria in respiration and consumption of nutrients. Usually, there are many types of plants and nutrients, with different types processes taking place. It is therefore difficult to derive analytical formulas for the processes. Instead, an empirical approach is used. A sample is taken from the water, and the oxygen consumption is measured in the laboratory as a **Biochemical Oxygen Demand (BOD)**. The BOD will be dependent on many factors, and empirical coefficients are required when modelling the process. Usually, the oxygen demand is from organic material. Since this is based on carbon, the term **CBOD** is also used. BOD for Nitrogen processes is termed **NBOD**, and this will be discussed later.

The consumption of nutrients by bacteria/algae can be described by first-order kinetics:

Note that this equation is independent of the concentration of bacteria/algae.

$$\frac{dL}{dt} = -k_d L \qquad (8.5.1)$$

L is the concentration of nutrients, and k_d is an empirical reaction coefficient.

If dissolved oxygen is consumed completely from the water, **anaerobic conditions** occur. Then new processes with different types of bacteria will take place. Such processes may create toxic substances and fish deaths. It is therefore important that an oxygen concentration above zero is maintained in rivers and reservoirs/lakes.

The bacteria/algae consuming the oxygen can be floating in the water, or it can be attached to sediments at the river/lake bed. In the last case, the term **Sediment Oxygen Demand (SOD)** is often used instead of BOD. Chapra (1997) developed relatively complex algorithms to compute SOD.

The oxygen in the air above the water surface will be able to replenish the river/lake water if the oxygen concentration, o, is below the saturation concentration o_s. A large number of formulas have been made to quantitatively determine the **reaeration**. The general formula is given as:

$$\frac{do}{dt} = k_a(o_s - o) \qquad (8.5.2)$$

The oxygen saturation concentration is denoted o_s. This is the maximum oxygen concentration in the water. If the concentration goes above this value, gas bubbles are formed, and the oxygen disappears to the atmosphere. The oxygen saturation concentration depends on:

- water temperature
- salinity
- altitude

The development of CFD models enables the estimation of turbulence close to the water surface. Future reaeration formulas will probably be based directly on these turbulence parameters: the turbulent kinetic energy or the eddy-viscosity.

The value of the oxygen saturation concentration will be in the order of 10 mg/liter (Chapra, 1997). Often, the oxygen deficit, D, is modelled instead, where $D=o_s - o$.

The reaeration coefficient, k_a depends on the oxygen flux through the water surface film. It is also influenced by the oxygen mixing by turbulence below the surface. The present empirical formulas contain indirect parameters of the turbulent mixing, for example the water velocity. A formula for the reaeration coefficient for a river is given by O'Connor and Dobbins (1958):

$$k_a = 3.93\frac{U^{0.5}}{h^{1.5}} \qquad (8.5.3)$$

The formula is not dimensionless, and U is given in *m/s* and h is the water depth in meters. The coefficient k_a is given in units day^{-1}.

For lakes, an empirical formula for k_a, has been developed by Broecker et al. (1978).

$$k_a = \frac{0.864U_w}{h} \qquad (8.5.4)$$

U_w is the wind speed 10 meters above the water surface in m/s.

There exist a large number of other empirical formulas for the reaeration process.

Nitrogen

NH_4^+ = ammonium
NH_3 = ammonia

The source of nitrogen in the water is usually organic material. The material decomposes in an **ammonification** process, leading to formation of **ammonium** (**NH_4^+**). The ammonium can react with dissolved oxygen in a **nitrification** process to form **nitrite** (**NO_2^-**). The nitritification process can further transform the nitrite to **nitrate** (**NO_3^-**). Since the nitrificaion process uses oxygen, the process has a nitrogen oxygen demand (**NBOD**). If not, or only small amounts of dissolved oxygen is present, a **denitrification** process can take place. The nitrate is then transformed to nitrite and to nitrogen in gaseous form. The nitrogen gas may be lost to the atmosphere.

There are several implications of the processes on the water quality:

1. If nitrogen is the limiting nutrient for organic growth, abundant nitrogen may cause increased eutrophication.

2. High concentrations of nitrate (above 10mgN/l) in drinking waters can cause disease for very young children.

3. Dissolved ammonia may form ammonia gas (NH_3), which may be toxic to fish. This only happens at high temperatures and high pH in the water. (above 20^0 C and pH above 9).

The nitrogen processes can be modelled by the equations given below, using the following subscripts: *o*=organic, *a*=ammonium, *i*=nitrite and *n*=nitrate.

$$\frac{d}{dt}(N_o) = -k_{o\to a}N_o \qquad (8.5.5)$$

$$\frac{d}{dt}(N_a) = k_{o\to a}N_o - k_{a\to i}N_a \qquad (8.5.6)$$

$$\frac{d}{dt}(N_i) = k_{a\to i}N_a - k_{i\to n}N_i \qquad (8.5.7)$$

$$\frac{d}{dt}(N_n) = k_{i\to n}N_i \qquad (8.5.8)$$

Note that the stochiometry coefficients are not included. The equations can be solved analytically for a simple system of one well-mixed lake/ reservoir. Often, an equation for dissolved oxygen is solved simultaneously.

Phosphorous

Phosphorous is usually the limiting nutrient for plant growth in fresh water. The growth process is then only a function of the phosphorous concentration. The phosphorous may be **dissolved** in the water or it may be present in **organic material**. The organic material consume the dissolved phosphorous and then settle to the bottom of the lake/river. These processes will decrease the concentration of dissolved phosphorous in the water. However, when the organic material decomposes, the phosphorous may again be released and dissolved in the water.

Formulas for depletion of dissolved phosphorous is derived from growth formula for biological material. Stochiometry is used to determine how much the phosphorous concentration is reduced as a function of the organic growth.

$$\frac{d}{dt}(P_{organic}) = -k_{op}P_{organic} \quad (8.5.9)$$

$$\frac{d}{dt}(PO_4) = k_{op}P_{organic} - \alpha k c_A \quad (8.5.10)$$

$P_{organic}$ is the organic phosphorous in the algae, PO_4 is the dissolved phosphorous. The decomposition rate of organic phosphorous is denoted k_{op}, and k is the algae growth factor. The algae concentration is denoted c_A, and the fraction of phosphorous in the algae is α.

In many lakes there is relatively little phosphorous occurring naturally, leading to small concentrations of organic material. Over the last decades there has been an increase in phosphorous inflow into many lakes in Europe. Often, fertilization from agriculture is the cause. The increased phosphorous loading leads to accelerated growth of organic material. This eutrophication has negative effects on the water quality.

8.6 QUAL2E

The QUAL2E program is made by the US Environmental Protection Agency. It is designed to model water quality in rivers in one dimension. The hydraulic computation is based on a steady calculation. The convection-diffusion equation is solved for a number of water quality parameter. Biological reactions are included in the equations, together with interaction between the parameters.

The program models a number of water quality variables: Temperature is modelled with surface fluxes as given in Chapter 7.3. Algae is modelled, including growth, predation, settling and scour. The cycles of nitrogen, phosphorous, carbonaceous BOD and oxygen are modelled, according to the models described in Chapter 8.5.

The program is freeware, and can be downloaded from the Internet, including user's manuals. A Windows user interface is included. Table 8.6.1 gives default values of important input parameters:

Table 8.6.1 Parameters used in QUAL2E

Process	Equation number	Reaction rate name	Default reaction rate (day^{-1})	Max-min. reaction rate (day^{-1})	Temperature coefficient θ
Algal growth	8.7.7	k	2.5	1.0-3.0	1.047
Algal respiration rate			0.005	0.005-0.5	1.047
BOD decay	8.5.1	k_d	0.0	0.0-10.0	1.047
Organic nitrogen decay	8.5.5+6	$k_{NO>NH4}$	0.0	0.0-10.0	1.047

Process	Equation number	Reaction rate name	Default reaction rate (day^{-1})	Max-min. reaction rate (day^{-1})	Temperature coefficient θ
Organic nitrogen settling	8.5.5	σ_4	0.0	0.0-10.0	1.024
Ammonia oxidation	8.5.6+7	$k_{NH4>NO2}$	0.0	0.0-10.0	1.083
Nitrite oxidation	8.5.7+8	$k_{NO2>NO3}$	2.0	0.0-10.0	1.047
Organic phosphorous decay	8.5.9+10	k_{op}	0.0	0.0-10.0	1.047

8.7 Phytoplankton

The most important types of plankton for water quality is free-flowing algae. Algae are plants with one or more cells, living in water. Two groups of algae exist:

- *periphyton*: algae attached to the river/lake bed
- *phytoplankton*: free flowing algae

The most common species of phytoplankton in freshwater can be classified in three main groups:

- *Cyanobacteria*
- *Flagellates*
- *Diatoms*

Cyanobacteria often have gas vesicles, variable in size. The buoyancy of the algae can thereby be changed and vertical movement take place. The main process in the algae is photosynthesis, and an appropriate amount of light is necessary. If too little light is present, the algae will move toward the water surface. And if the light is too strong the algae will want to move downwards, where the turbidity of the water cause decreased light intensity. The change in phytoplankton concentration may be due to the rise/fall velocity together with wind-induced currents and turbulence. Another process is algal growth and predation by zoo plankton.

Rise/sink velocity

Kromkamp and Walsby (1990) developed formulas for cyanobacteria buoyancy based on laboratory experiments:

The formula given by Kromkamp and Walsby was developed from data using an algae from the lake Gjersjøen in Norway

$$\rho_{a,1} = \rho_{a,0} + \Delta t\left(k_1 \frac{I}{I+K} - k_2 I_{24} - k_3\right) \qquad (8.7.1)$$

ρ_a is the algae density, Δt is the time step and k_1, k_2, k_3 and K are constants. I_{24} is the average irradiance over the last 24 hours. I is the irradiance, with maximum value at the water surface, and decreasing values downward in the water body, as shading occur. Bindloss (1976) investigated the damping of the irradiance for lakes in the UK, and found the following relationship to compute the specific light transmission coefficient, k_l:

$$k_l = 0.0086c + 0.69 \tag{8.7.2}$$

where c is the algal concentration. The irradiance is dampened by a factor *f*, given by the following formula:

$$f = \sum_y e^{k_l \Delta z} \tag{8.7.3}$$

The summation is over all layers with magnitude Δz from the surface down to the level *y*.

The fall/rise velocity, *w*, of the algae is calculated from Stoke's equation:

$$w = d^2 g \frac{\rho_w - \rho_a}{18 \rho_w \nu} \tag{8.7.4}$$

where ρ_a and ρ_w is the algal and water density, and ν is the kinematic water viscosity, evaluated as:

$$\nu = 10^{-6} e^{0.55234 - 0.026668T} \tag{8.7.5}$$

where *T* is the temperature in degrees Centigrade.

The flagellates also seek optimum light intensity. Instead of changing their buoyancy, the flagellates have flagelles, enabling movement. This is similar to fins on a fish, but much lower velocities are produced. The following formula is often used for flagellates:

$$w = w_{max}\left(\frac{I_{opt} - I}{I_{ref}}\right) \tag{8.7.6}$$

I is the actual irradiance, I_{opt} is the optimum irradiance, I_{ref} is a reference irradiance and w_{max} is the maximum rise/sink velocity for the flagellate.

The maximum rise/sink velocity of phytoplankton are in the order of one meter/hour.

The Diatoms have a specific weight slightly higher than water, giving a constant fall velocity. The density can not be changed, and the diatoms do not have flagelles. The only way to move diatoms upwards is by turbulence.

The size of the phytoplankton are often in the order of micrometer. A microscope is necessary to identify the different species. Certain types of cyanobacteria - *Microcystis* - form groups or colonies. The rise/sink velocity is a function of the algae buoyancy and the group diameter. A larger group will thereby get a much higher fall/rise velocity, giving increased efficiency in search for optimum light. Groups of up to 2 mm in size have been observed.

Growth

Time series of phytoplankton concentrations in a lake show variations over the year. Also, the type of algae changes. Diatoms may be dominant in the spring, followed by cyanobacteria in the summer. This all

depends on temperature, nutrients, shading, grazing by zoo plankton etc.

The algal growth can be computed by use of first-order kinetics:

$$c = c_0 e^{kt} \tag{8.7.7}$$

The growth rate coefficient, *k*, may be around 1.0/day for optimum conditions. The biomass will then increase by 200 % in one day, and by a factor 1000 in one week. Usually, optimum conditions do not exist, as the algae need several nutrients to achieve maximum growth. The limiting nutrient for Cyanobacteria and Flagellates in freshwater is most often phosphorous. Silica is often the limiting nutrient for Diatoms.

If sufficient amount of nutrients are present, the growth can be limited by light. Reynolds (1984) found the following formula to estimate the growth coefficient in lakes in the UK:

$$k = a\left(1 - e^{-\frac{f}{b}}\right) \tag{8.7.8}$$

The damping factor, *f*, is given by Eq. 8.4.3, and *a* and *b* are constants (0.4 and 9.0) as found by Reynolds (1984).

Modelling of phytoplankton

Phytoplankton can be computed in models having from zero to three spatial dimensions. A zero-dimensional model assumes complete mixing in the lake/reservoir, and predicts algae concentration over time. One-dimensional models are used for rivers and sometimes for lakes. Then horizontal layers are often used, and complete mixing within each layer is assumed. Three-dimensional CFD models have been used to predict spatial variation of algae in lakes (Hedger et. al. 2000) and reservoirs (Olsen et. al. 2000). The CFD model predicts velocities in all spatial directions on a three-dimensional grid. Wind-induced circulation can be modelled, together with effects of inflowing/outflowing water. The convection-diffusion equation for algae concentration can be solved including sink/source terms for algal growth and settling/rise velocities. Nutrients, light and temperature can be modelled simultaneously in time-dependent calculations, enabling modelling of most of the important processes affecting the algae.

8.8 Problems

Problem 1. Completely mixed lake:

A lake with volume 1 million m^3 has received phosphorous from a sewage plant for several years, with an amount of 2000 kg/day. Assume a loss rate of 0.1/day, and compute the average phosphorous concentration in the lake.

One day an improvement of the sewage treatment plant was made, causing the loading to decrease to 300 kg/day. How long time will it take before the phosphorus concentration is below 20 % of the original value?

Problem 2. The Streeter-Phelps equations

In 1925, a study of the water quality in the Ohio river in the USA was

published by H. W. Streeter and Earle B. Phelps. Their paper was a landmark for water quality modelling. Using first-order kinetics, they modelled BOD and the oxygen deficit (DO) in the water as a function of sewage released to the river. The following formulas were used:

$$\frac{dL}{dt} = -k_d L$$

$$\frac{dD}{dt} = -k_a D + r_{oc} k_d L$$

where D is the oxygen deficit: o_s-o. The concentration of BOD is denoted L, k_d is a reaction coefficient for consumption of oxygen and k_a is a reaeration coefficient. The parameter r_{oc} is the stochiometry coefficients for how much oxygen is consumed for each unit of BOD. Assume a value of 0.1 for the current problem.

Solve the equations using a spreadsheet for a 100 km long river with a water discharge of 100 m^3/s, where the upstream sewage outflow is 30 kg/s. Present longitudinal profiles of BOD and oxygen concentration for a steady situation. Assume k_d = 0.8 day^{-1}. The river is 2 meters deep and 200 meters wide.

Compare the results with the analytical solutions of the equations:

$$L = L_0 e^{-\frac{k_d}{U}x}$$

$$D = D_0 e^{-\frac{k_a}{U}x} + \frac{c_0 k_d}{k_a - k_d}\left(e^{-\frac{k_d}{U}x} - e^{-\frac{k_a}{U}x}\right)$$

Problem 3. The nitrogen cycle

Use a spreadsheet to compute the variation over time of various forms of nitrogen in a well-mixed lake, according to Eq. 8.5.5-8.5.8. Use the reaction rates and initial concentrations given in Table 8.8.1.

Table 8.8.1 Parameters for problem 3

Process	Reaction rate name	Reaction rate (day^{-1})	Variable	Initial conc.
Organic nitrogen decay	$k_{NO>NH4}$	0.15	Organic N	0.008
Ammonium oxidation	$k_{NH4>NO2}$	0.15	Nitrite	0.0
Nitrite oxidation	$k_{NO2>NO3}$	0.5	Nitrate	0.0
			Ammonium	0.008

Problem 4. Stratified lake

A 22 meter deep lake is thermally stratified, with a 1 meter thick thermo-

cline 7-8 meters below the water surface. It is assumed that the water on both sides of the thermocline is well-mixed, and the mixing through the thermocline is according to a diffusion coefficient, Γ, equal to 1.3×10^{-2} m^2/s.

Initially, the lake is fully saturated with oxygen. Assume an oxygen concentration of 9 mg/l. It is assumed that the wind mixes oxygen into the water, so the water above the thermocline stays saturated with oxygen. A the lake bottom, there is a sediment oxygen demand of 0.3 $(m^2 day)^{-1}$. What is the concentration of oxygen below the thermocline after a long time?

9. Sediment transport

9.1 Introduction

Sediments are small particles, like sand, gravel, clay and silt. The water in a river has a natural capacity of transporting sediments, given the velocity, depth, sediment characteristics etc. Man-made structures in a river may change the sediment transport capacity over a longer part of the river, or locally. Erosion may take place in connection with structures, such as bridges, flood protection works etc. The hydraulic engineer has to be able to assess potential scour problems. During a flood, the risk for erosion damages is at its highest.

Sediments cause many problems when constructing hydropower plants and irrigation projects in tropical countries. Deposition and filling of reservoirs is one problem, and the water intake has to be designed for handling the sediments. The sediments reaching the water turbine may cause wear on the components, as shown in the picture below.

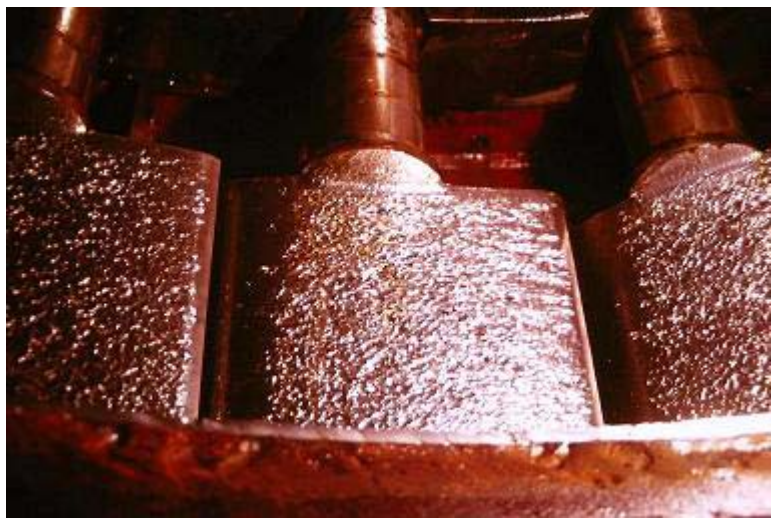

The picture shows erosion on hydraulic machinery: the blades leading the water towards the turbine. Photo: N. Olsen.

In recent years, the topic of polluted sediments has received increased interest. Organic and toxic substances may attach to inorganic sediment particles and affect the water quality. Erosion of old polluted sediments may create a hazard. Sediments also affects the natural biochemistry of shallow lakes.

The origin of sediments vary according to different climates. In tropical countries, rock decompose naturally. Water in form of rain and temperature fluctuations, together with chemical reactions cause cracks in the rock. The weathering cause a layer of particles to be formed above the solid rock. The particles close to the surface have the longest exposure to weathering, and have the smallest grain sizes. Larger stones are formed closer to the bedrock. Over time, the finer particles are removed by rain, causing erosion of the rock. The process is relatively slow, as vegetation cover prevents erosion from taking place. Where man removes the vegetation, there may be accelerated erosion.

The sediments are transported by the rivers and streams through the catchment. The annual sediment transport in a river, divided by its catchment area is called sediment yield. Typical numbers for tropical countries

The picture on the right is taken from a volcano in Costa Rica. The fine material of the volcano lies on steep slopes. It is relatively unprotected by vegetation. The rain fall then causes relatively extreme erosion rates. Such areas often have gullies, as shown on the picture. Photo: N. Olsen.

are around 100-2000 tons/km^2/year.

Sediment yield

In some countries, like Norway, the geology is very much influenced by the ice-age. The glaciers removed the upper layer with soil, leaving solid bedrock for a large part of many catchments. The sediment yield is therefore much lower, almost zero many places. The main sediment source in Norway is from the glaciers.

9.2 Erosion

The initial step to the science of sediment transport in a river is looking at forces on a sediment particle resting on the bed. The purpose is to find a method for determining when the particle will be eroded. There are four forces influencing the stability of the particle (Fig. 9.2.1) resting on a bed where the water has a velocity *U*.

- Gravity: *G*
- Drag: *D*
- Lift: *L*
- Friction: *F*

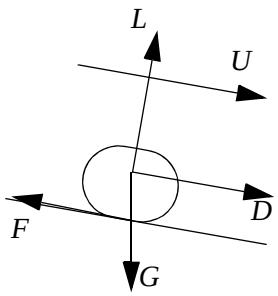

Fig. 9.2.1 Forces on a particle in a stream

Assuming the particle has diameter *d*, the forces can be written:

$$G = k_1(\rho_s - \rho_w)gd^3 \tag{9.2.1}$$

$$D = k_2 u^2 d^2 = k_2\left(IM^2 r^{\frac{4}{3}}\right)d^2 = k_2\frac{\tau}{\rho g r}M^2 r^{\frac{4}{3}}d^2 \approx k_3\tau d^2 \tag{9.2.2}$$

We have here assumed a wide channel, where the hydraulic radius is approximately equal to the water depth.

The density of a sediment particle is often set to 2.65 times the water density

$$L = \frac{1}{2}C_L\rho_w\frac{d^2}{4}\pi u^2 = \frac{1}{2}C_L\rho_w\frac{d^2}{4}\left(IM^2 r^{\frac{4}{3}}\right)\pi \approx k_4\tau d^2 \tag{9.2.3}$$

The friction force, *F*, is a function of the force pushing the particle downwards, multiplied with a friction coefficient. This friction coefficient is the same as tangens to the angle of repose of the material, α.

$$F = (G - L)\tan(\alpha) = \tan(\alpha)[k_1 g(\rho_s - \rho_w)d^3 - k_4\tau d^2] \tag{9.2.4}$$

Some constants are used: k_1 for the shape factor of the particle, k_2 is a drag coefficient and C_L is a lift coefficient. The critical shear stress on the bed for movement of a particle is denoted τ_c.

Equilibrium of forces along the direction of the bed gives:

$$F = D \tag{9.2.5}$$

Using Eq. 9.2.4 and 9.2.2, this gives

$$\tan(\alpha)[k_1 g(\rho_s - \rho_w)d^3 - k_4\tau d^2] = k_3\tau d^2 \tag{9.2.6}$$

The equation is solved with respect to the particle diameter:

$$d = \frac{\tau_c}{g(\rho_s - \rho_w)\left[\frac{k_1\tan(\alpha)}{k_3 + k_4\tan(\alpha)}\right]} = \frac{\tau_c}{g(\rho_s - \rho_w)\tau^*} \tag{9.2.7}$$

The parameter, τ^*, was found experimentally by Shields (1937), and can be taken from Fig. 9.2.2:

Fig. 9.2.2 Shields graph, giving the critical shear stress for movement of a sediment particle

$$\tau^* = \frac{\tau}{g(\rho_s - \rho_w)d}$$

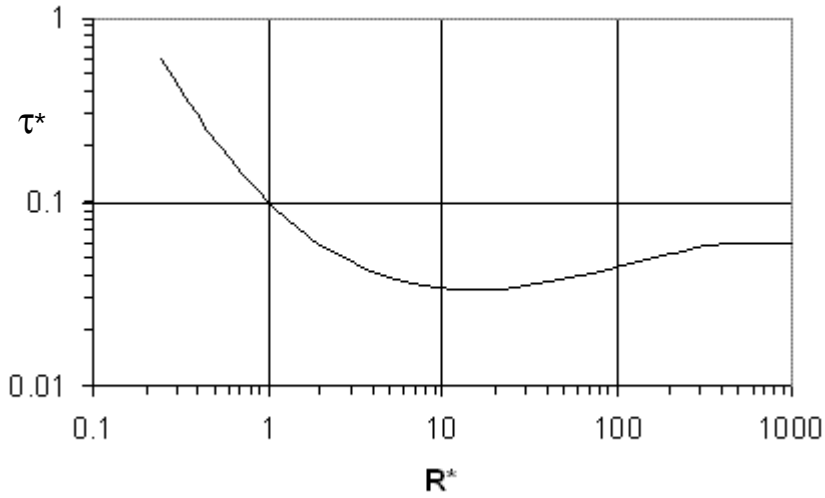

The value on the horizontal axis is the particle Reynolds number, given by:

$$R^* = \frac{u_* d}{\nu} = \frac{d\sqrt{\frac{\tau}{\rho}}}{\nu} \qquad (9.2.8)$$

The viscosity of water is denoted ν, d is the particle diameter, u_* is the shear velocity and τ is the shear stress on the bed.

Shields graph can be used in two ways: If the bed shear stress, τ, in a river is known, Eq. 9.2.7 can be used to determine the stone size that will not be eroded. Or if the particle size on the bed is known, Eq. 9.2.7 can be used to compute the critical shear stress for movement of this particle. In both cases, Eq. 9.2.7 is used, where the parameter τ^* is found by Fig. 9.2.2.

Cohesive sediments under 0.1 mm

If the particle is very small, under 0.1 mm, there are also electrochemical forces occurring. The sediments are then said to be cohesive. The critical shear stress then depend on the chemical composition of the sediments and the water.

Example: A channel with water depth 2 meters and a slope of 1/1000 is covered with stones of size 0.03 m. Will the stones be eroded or not?

First, the bed shear is computed:

$$\tau = \rho g h I = 1000x9.81x2x\frac{1}{1000} = 20Pa$$

Then the particle Reynolds number is computed.

$$R^* = \frac{u_* d}{\nu} = \frac{d\sqrt{\frac{\tau}{\rho}}}{\nu} = \frac{0.03\sqrt{\frac{20}{1000}}}{10^{-6}} = 4243$$

The Shields diagram gives the Shields coefficient as 0.06. The critical shear stress for the particle is then:

$$\tau_c = \tau^* g(\rho_s - \rho_w)d = 0.06x9.81x(2650 - 1000)x0.03 = 29Pa$$

We see that the critical shear stress for the particle is above the actual shear stress on the bed. The particle will therefore not be eroded.

Sloping bed

The decrease, *K*, in critical shear stress for the sediment particles as a function of the sloping bed was given by Brooks (1963):

Critical shear for sloping banks

$$K = -\frac{\sin\phi\sin\alpha}{\tan\theta} + \sqrt{\left(\frac{\sin\phi\sin\alpha}{\tan\theta}\right)^2 + cos^2\phi\left[1 - \left(\frac{\tan\phi}{\tan\theta}\right)^2\right]} \qquad (9.2.9)$$

The angle between the flow direction and the channel direction is denoted α. The slope angle is denoted ϕ and θ is a slope parameter. The factor *K* is calculated and multiplied with the critical shear stress for a horizontal surface to give the effective critical shear stress for a sediment particle.

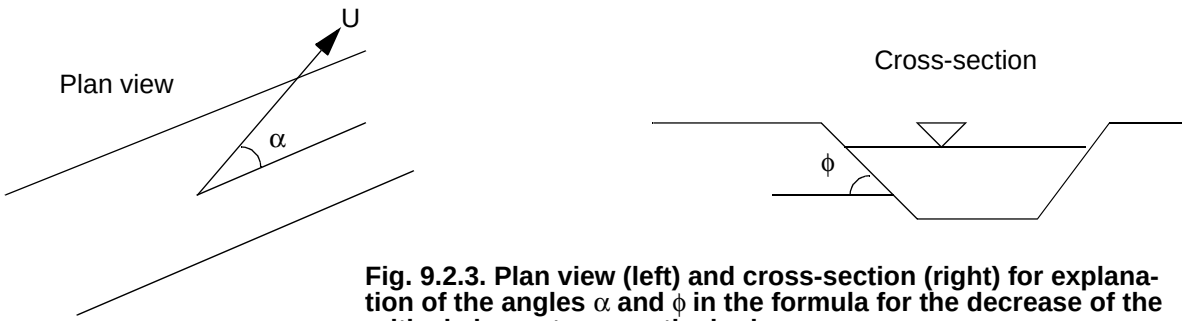

Fig. 9.2.3. Plan view (left) and cross-section (right) for explanation of the angles α and ϕ in the formula for the decrease of the critical shear stress on the bed.

Looking at the bank of a straight channel, where the water velocity is aligned with the channel direction, α is zero. Eq. 9.2.9 is then simplified to:

$$K = \cos\phi\sqrt{1 - \left(\frac{\tan\phi}{\tan\theta}\right)^2} \qquad (9.2.10)$$

The slope parameter, θ is slightly higher than the angle of repose for the material (Lysne, 1969). A value of 50 degrees was used by Olsen and Kjellesvig (1999) computing bed movements in a sand trap.

More recently, Dey (2003) developed another formula for K:

$$K = 0.954\left(1 - \frac{\phi}{\theta}\right)^{0.745}\left(1 - \frac{\alpha}{\theta}\right)^{0.372} \qquad (9.2.11)$$

A very good handbook for design of scour protection works in Norwegian is written by Fergus et. al. (2010).

The angles ϕ and α are here not defined in the same way as Brooks. The angle α is the bed slope normal to the direction of the velocity vector. While the angle ϕ is the bed slope in the direction of the velocity vector. Bihs and Olsen (2011) obtained fairly good results using this formula to compute local scour around an abutement in a channel.

9.3 Suspended sediments and bed load

When the bed shear stress exceeds the critical value for the bed particles, there will be a sediment transport in the river. The particles will roll along the bed or jump up into the flow. The latter process is called saltation. The length of the jump will depend on the fall velocity of the particles. Fig. 9.3.1 gives the fall velocity for quartz spheres at 20 ^{o}C.

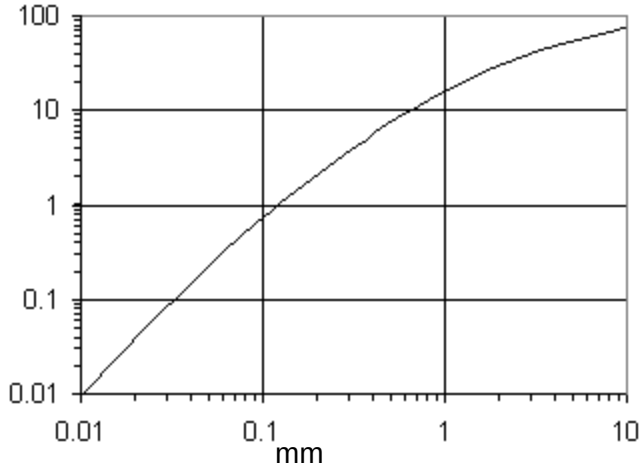

Fig. 9.3.1 Fall velocity of quartz spheres in water. The horizontal axis is the diameter of the spheres, and the vertical axis is the fall velocity

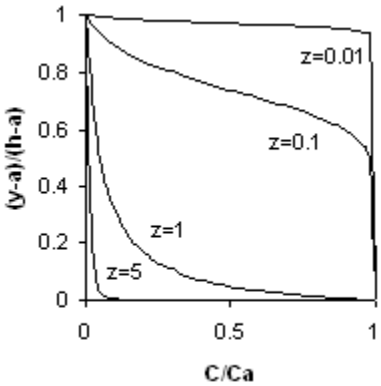

Figure 9.3.2. The vertical distribution of sediment concentration for some chosen values of *z*

The sediments will move close to the bed or in suspension, depending on the particle size and the turbulence in the water. The Hunter Rouse parameter (Eq. 9.3.1) is often used to determine the vertical distribution of the sediment concentration profile:

$$z = \frac{w}{\kappa u_*} \qquad (9.3.1)$$

The fall velocity of the particles is denoted w, κ is a constant equal to 0.4 and u_* is the shear velocity. High values of z indicates the fall velocity is high compared with the turbulence. The sediments will then move close to the bed. Low values of z indicates high amount of turbulence compared with the fall velocity, and the distribution becomes more uniform. Hunter Rouse also developed formulas for the vertical distribution of the concentration, $c(y)$:

$$\frac{c(y)}{c_a} = \left(\frac{h-y}{y}\frac{a}{h-a}\right)^z \qquad (9.3.2)$$

The water depth is denoted h, y is the distance from the bed and a is the distance from the bed where the reference concentration, c_a, is taken. Often a is set to $0.05h$. The vertical distribution of sediment concentration for some values of z is given in Fig. 9.3.2, by using Eq. 9.3.2.

Sediment transport capacity

The river will have a certain sediment transport capacity, given its hydraulic characteristics and the sediment particle size. Supplying more sediments than the transport capacity leads to sedimentation, even if the critical shear stress for the particles is exceeded. Less available sediment than the transport capacity leads to erosion.

Ralph A. Bagnold did most of his sediment research on sand transported by the wind. His initial field work was done in the desert of North-Africa. When the second world war broke out, his knowledge of the desert was used by a special regiment in the allied forces in Egypt, that he commanded (Bagnold, 1990).

Hans Albert Einstein was son of the famous Albert Einstein, the founder of the theory of relativity. One day while Hans Albert was at university, Einstein senior asked his son what he intended to choose as the topic for his research. He then answered the science of sediment transport. The father replied that he also thought of this when he was young, but he considered it to be too difficult.

Initial studies of sediment transport was done by Bagnold (1973), looking as sand transported by wind in the desert. Bagnold divided the transport into two modes: Bed load and suspended load. The bed load rolled along the ground, and the suspended load was transported in the air. For some reason, the same approach was used in water. The problem is that there is no clear definition of the difference between the two transport modes, agreed by most researchers. Some definitions are:

1. According to Einstein

Hans Albert Einstein, was a prominent researcher on sediment transport. According to him, the bed load is transported in a distance two particle diameters from the bed, as the transport mode was by sliding or rolling.

2. According to van Rijn

Van Rijn started from Bagnold's approach, and derived formulas for how far the bed load particles would jump up into the flow. This distance is far greater than predicted by Einstein's approach

3. According to measurements

Sediment transport in a river is often determined by measurements. A water bottle is lowered into the river, and water with sediments is extracted. The sediment concentration is determined in a laboratory. The water bottle is not able to reach all the way down to the bed, so there will be an unmeasured zone 2-10 cm from the bed. Often the measured sediment will be denoted suspended load, and the unmeasured load denoted bed load.

4. According to Hunter Rouse's example

Because Hunter Rouse showed an example where the reference level for the concentration was 5% of the water depth, some people assume the suspended load is above this level and the bed load is below.

As the definition of bed load and suspended load is not clear, it is necessary for the engineer to require further specification of the definition when using sediment transport data where the terms are used.

9.4 1D sediment transport formulas

There exist a large number of sediment transport formulas. Some of the formulas are developed for bed load, and some for total load. The total load is then the sum of the suspended load and bed load. All formulas contain empirical constants, so the quality of the formula depend on the data set used to calibrate the constants. In other words, some formulas work well for steep rivers, and some for rivers with smaller slopes, finer sediments etc. The formulas give very different result for the same case, and there is often an order of magnitude between lowest and highest value. It is therefore difficult to know which formula to use. Different researchers also have varying opinions and preferences as to what formula to use.

The formulas can be divided in two groups: Bedload formulas and total load formulas. The bedload formulas are developed for data sets where only bedload occur. When used in situations where the sediment transport is mainly suspended load, the formulas may give very inaccurate

Sediment transport formulas:

Engelund/Hansen
Danish researchers looking at rivers with relatively fine sediments and mild energy gradient.

Ackers&White
British researchers, using data from 925 individual sediment transport experiments to find the constants in their equation.

Mayer-Peter&Muller
Swiss researchers, working mostly on rivers with steep slopes, where most of the material moved close to the bed.

results. The total load formulas should work for both modes of transport. Note that a bed load formula will not predict the bed load in a situation where there is a combination of bed load and suspended load. It will predict the total load in a situation where most of the sediments move as bed load. Which is not the same.

Commonly used formulas for total load are:

Engelund/Hansen's (1967) formula:

$$q_s = 0.05\rho_s U^2 \sqrt{\frac{d_{50}}{g\left(\frac{\rho_s}{\rho_w}-1\right)}}\left[\frac{\tau}{g(\rho_s-\rho_w)d_{50}}\right]^{\frac{3}{2}} \qquad (9.4.1)$$

The sediment transport, q_s, is given in kg/s pr. m width. U is the velocity, ρ_s is the density of the sediments, ρ_w is the density of the water, τ is the shear stress on the bed, g is the acceleration of gravity and d_{50} is the average sediment diameter. This version of the formula works in the SI system of units.

Note that the shear stress term in the formula is divided by the critical shear stress. The critical shear stress is not subtracted from the actual shear stress. This means that the formula will give a sediment transport capacity also when the sher stress is lower than the critical shear stress for movement of a particle.

The **Ackers&White** (1973) formula requires five steps, given in the following. Note that the logarithm in the function has base 10, $\log_{10}$.

1. Compute a dimensionless particle size:

$$D_{gr} = d\left[\frac{g\left(\frac{\rho_s-\rho_w}{\rho_w}\right)}{\nu^2}\right]^{\frac{1}{3}} \qquad (9.4.2)$$

For uniform grain sizes, the mean particle diameter, d, is used. For graded sediments, the d_{35} value is used.

2. Compute four parameters, m, n, A and C, to be used later:

if $D_{gr} > 60$, the particle sizes are said to be coarse:

$$\begin{aligned} n &= 0.0 \\ A &= 0.17 \\ m &= 1.5 \\ C &= 0.025 \end{aligned} \qquad (9.4.3)$$

if D_{gr} is less than 60, but larger than 1, the sediments are medium sized:

$$n = 1.0 - 0.56 \log D_{gr}$$

$$A = \frac{0.23}{\sqrt{D_{gr}}} + 0.14$$

$$m = \frac{9.66}{D_{gr}} + 1.34 \qquad (9.4.4)$$

$$\log C = 2.86 \log D_{gr} - (\log D_{gr})^2 - 3.53$$

if D_{gr} is less than 1, the sediments are under 0.04 mm. It is assumed that cohesive forces may occur, making it difficult to predict the transport capacity. However, the transport capacity is then usually much larger than what is available for the river, so the sediment load is limited by the supply.

3. The mobility number is then computed (note simplification if n=0):

$$F_{gr} = \frac{u_*^n}{\sqrt{gd\left(\frac{\rho_s - \rho_w}{\rho_w}\right)}} \left[\frac{U}{\sqrt{32}\log\left(\frac{10h}{d}\right)} \right]^{1-n} \qquad (9.4.5)$$

The water depth is denoted h.

4. The sediment concentration, c, is then given in weight-ppm:

$$c = \frac{d\left(\frac{\rho_s - \rho_w}{\rho_w}\right)}{h} C \left(\frac{F_{gr}}{A} - 1\right)^m \left(\frac{U}{u_*}\right)^n \qquad (9.4.6)$$

5. The concentration is multiplied with the water discharge (in m^3/s) and divided by 10^3 to get the sediment load in kg/s.

Bed load formula

Mayer-Peter&Muller's formula for bed load

A formula for the total load in situations where there are dominantly bed load was given by **Mayer-Peter and Müller** (1948):

$$q_s = \frac{1}{g} \left[\frac{\rho_w g r I - 0.047 g(\rho_s - \rho_w) d_{50}}{0.25 \rho_w^{\frac{1}{3}} \left(\frac{\rho_s - \rho_w}{\rho_s}\right)^{\frac{2}{3}}} \right]^{\frac{3}{2}} \qquad (9.4.7)$$

The hydraulic radius is denoted r.

These are some of the most well-known formulas, together with Einstein's formula and Tofaletti's formula. The latter two are fairly involved, and are only used by some computer programs. There also exist a large number of other formulas giving more or less accurate answers.

Which formula to use?

The question remains on which formula to use. Three approaches exist:

1. Some formulas work better in particular situations, for example steep rivers etc. The problem with this approach is the difficult and inaccurate classification of the formulas.

2. Do a measurement in the river, and use the formula that best fits the result (Julien, 1989). The problem is the difficulty of obtaining a good measurement.

3. Use several formulas, and choose an estimate close to the average value.

Because of confusion on Imperial and metric units, and also because of misprinting, many textbooks do not give the correct sediment transport formulas

The final approach depend on the information available and the experience and knowledge of the engineer.

9.5 Bed forms

Sediment particles moving on an initially flat bed may generate bed forms. Sediments forms small bumps on the bed with regular shape and interval. The following classification system is used for different types of bed forms:

Four different bed forms:

1. Ripples
2. Dunes
3. Bars
4. Antidunes

The Norwegian words for ripples are “riller”. Dunes are called “dyner” or “sandbanker”. Bars are called “sandbanker” or “grusører”. Antidunes are called “motbanker” or “motdyner”.

The first three types of bed forms occur in subcritical flow. Sediments deposit on the down side of the bed form and erode from the upstream side. The ripples are fairly small, with a height under 3 cm, and occur only on sediment finer than 0.6 mm. The bars are much larger, with heights similar to the water flow depth. The dunes have a size between the bars and the ripples.

The antidunes are different in that they occur only in supercritical flow. A hydraulic jump is formed between the bedforms. Deposition takes place at the front of the dune, and the downstream side erodes. The bedform itself therefore may move upstream, even though the individual grain sizes move downstream. Antidunes may also move downstream or be stationary.

Figure 9.5.1 Antidunes at the Bodeneorf reservoir in Austria during flushing, 2006. Photo: N. Olsen.

There exist a large number of methods for prediction of bed forms, predicting both the type and size. Unfortunately, as for the sediment transport formulas, the various methods give highly different answers. An example of a bed form predictor is given by van Rijn (1984), estimating the bed form height, Δ of dunes:

$$\frac{\Delta}{h} = 0.11\left(\frac{D_{50}}{h}\right)^{0.3}\left(1 - e^{-\left[\frac{\tau - \tau_c}{2\tau_c}\right]}\right)\left(25 - \left[\frac{\tau - \tau_c}{\tau_c}\right]\right) \qquad (9.5.1)$$

where *h* is the water depth. This formula was developed based on curve-fitting with data from 88 laboratory experiments and 22 field observations. The particle sizes were between 0.19 and 2.3 mm for the lab experiments and 0.49-3.6 mm for the field observations. Van Rijn (1984) noted that the formula should only be applied to flows with relatively low Froude numbers. According to his observations, the dunes would vanish for Froude numbers above 0.6 in the laboratory and above 0.2-0.3 in natural rivers. They would also disappear if conditions were so that his formula would give negative dune heights. The formula only applies for normal dunes, not ripples or antidunes.

Karim (1999) developed a formua for the height of antidunes:

$$\frac{\Delta}{h} = \left[\frac{\left\{S - 0.0168\left(\frac{D_{50}}{h}\right)^{0.33} Fr^2\right\}\left(\frac{L}{h}\right)^{1.20}}{0.085 Fr^2}\right]^{0.73} \qquad (9.5.2)$$

L is the length of the antidune and Fr is the Froude number. Kennedy (1963) proposed the following formula for *L*:

$$L = 2\pi h Fr^2 \qquad (9.5.3)$$

The formula 9.5.2 gave very good results compared with both laboratory experiments and numerical modelling of antidunes (Olsen, 2016).

The bed form height can be used together with the bed sediment grain size distribution to compute an effective hydraulic roughness (van Rijn, 1987):

$$k_s = 3D_{90} + 1.1\Delta\left(1 - e^{-\frac{25\Delta}{\lambda}}\right) \qquad (9.5.4)$$

where λ is the bedform length, calculated as 7.3 times the water depth. The formula can be used to compute the velocities and the water surface elevation.

The resulting shear stress from the friction of the dunes is only partially used to move sediments. When computing the effective shear stress for the sediment transport, the shear due to the grain roughness only should be used. This can be computed by using partition coefficients. The partition of shear stress used to move the particles divided by the total shear stress is denoted:

$$p_\tau = \frac{\tau_s}{\tau} = \frac{\tau_s}{(\tau_d + \tau_s)} \qquad (9.5.5)$$

An alternative partitioning formula is

$$p_\tau = \frac{\tau_s - \tau_c}{\tau - \tau_c} = \frac{\tau_s - \tau_c}{(\tau_d + \tau_s) - \tau_c} \quad (9.5.6)$$

Here, τ_s denotes the shear stress due to the roughness of the sediment particles, and τ_d denotes the shear stress due to the roughness of the dunes.

Using several empirical formulas, the following equation can be derived to compute p_τ:

$$p_\tau = (p_r)^{0.25} \quad (9.5.7)$$

where p_r is the partition of the roughness, given as:

$$p_r = \frac{k_{s,\,particles}}{k_{s,\,total}} = \frac{3D_{90}}{3D_{90} + 1.1\Delta\left(1 - e^{-\frac{25\Delta}{\lambda}}\right)} \quad (9.5.8)$$

Many sediment discharge formulas are derived from laboratory experiments. It is very difficult, almost impossible, to scale the size of the bed forms in the laboratory to prototype conditions. This may be one of the reasons why the many sediment discharge formulas give different results.

In a laboratory experiment with movable sediments, the bed is often flattened before the experiment starts. The bedforms will grow over time, until they get the equilibrium size. The roughness will therefore also vary over time in this period.

9.6 CFD modelling of sediment transport

CFD modelling of sediment transport has currently been done by a number of researchers on many different cases: sand traps, reservoirs, local scour, intakes, bends, meandering channels etc.

The bed load can be computed with specific bed load formulas, for example (van Rijn, 1987):

$$\frac{q_b}{D_{50}^{1.5}\sqrt{\frac{(\rho_s - \rho_w)g}{\rho_w}}} = 0.053\frac{\left[\frac{\tau - \tau_c}{\tau_c}\right]^{2.1}}{\left\{D_{50}\left[\frac{(\rho_s - \rho_w)g}{\rho_w \nu^2}\right]^{\frac{1}{3}}\right\}^{0.3}} \quad (9.6.1)$$

The sediment particle diameter is denoted D_{50}, τ is the bed shear stress, τ_c is the critical bed shear stress for movement of sediment particles, ρ_w and ρ_s are the density of water and sediments, ν is the viscosity of the water and g is the acceleration of gravity.

Suspended load is computed using the algorithms given in Chapter 5. The convection-diffusion equation for suspended load is solved:

$$\frac{\partial c}{\partial t} + U_i\frac{\partial c}{\partial x_i} + w\frac{\partial c}{\partial z} = \frac{\partial}{\partial x_i}\left(\Gamma_T\frac{\partial c}{\partial x_i}\right) + S \quad (9.6.2)$$

The fall velocity for the particles is denoted *w*. This is a negative number if the *z* direction is positive upwards. *S* is a source term which can be used to prescribe a pick-up flux from the bed. An alternative method to model resuspension of sediments, is to give a a boundary condition near the bed. The most commonly used method is to use van Rijn's (1987) formula:

$$c_{bed} = 0.015 \frac{D_{50}}{a} \frac{\left[\frac{\tau - \tau_c}{\tau_c}\right]^{1.5}}{\left\{D_{50}\left[\frac{(\rho_s - \rho_w)g}{\rho_w \nu^2}\right]^{\frac{1}{3}}\right\}^{0.3}} \qquad (9.6.3)$$

The sediment particle diameter is denoted *d*, and *a* is a reference level set equal to the roughness height

It is also possible to adjust the roughness in the computation of the water velocities according to the computed grain size distribution at the bed and the bed forms (Eq. 9.5.2) (Olsen, 2000).

When the sediments are prescribed in the bed cell according to Eq. 9.6.3, sediment continuity is not satisfied for this cell. There may therefore be sediment deposition or erosion. The continuity defect can be used to change the bed. A time-dependent computation can compute how the geometry changes as a function of erosion and deposition of sediments.

Formulas for the correction of the critical shear stress as a function of the bed slope can be used. Also, formulas for the shear stress partition can be included in the numerical model. The formulas given earlier in this chapter can be used.

Non-uniform sediments

Many of the sediment transport formulas are developed for a uniform sediment distribution. All the sediment particles are then of similar size. In a natural river, this is often not the case. A mixture of coarse and fine particles are often found. The grain size distribution on the bed may look like the figure below:

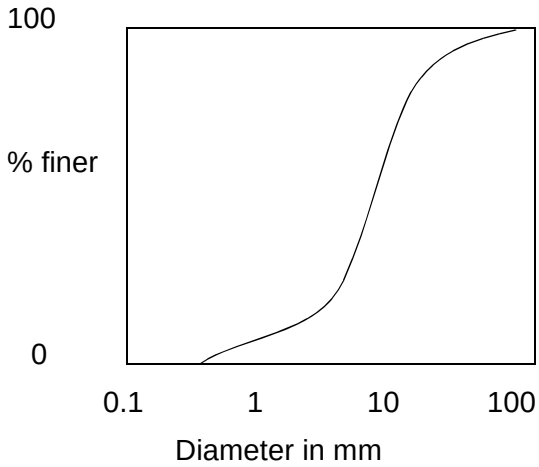

Figure 9.6.1. An example of the grain size distribution at the bed of a river.

A non-uniform sediment distribution is often modelled numerically by dividing the sediment into several sizes. Each size is then modelled with a separate sediment transport formula and convection-diffusion equation. There is some interaction at the bed that has to be taken into account. First, the sediment transport capacity is affected by the multiple sizes. This is usually taken into account by multiplying the transport capacity from the formula, q_{s0}, with the fraction, f, of each size on the bed:

$$q_s = q_{s0} f \tag{9.6.4}$$

There is also another process that can be important. Small particles may hide between larger ones, giving them more protection against erosion. The effect can be taken into account with a so-called hiding/exposure formula. The Shields factor is then modified by multiplying it with a parameter, ξ. One formula for the parameter for size fraction i is:

$$\xi_i = \left(\frac{d_i}{d_{50}} \right)^{-0.3} \tag{9.6.5}$$

The average sediment size is denoted d_{50}.

9.7 Reservoirs and sediments

A river entering a water reservoir will loose its capacity to transport sediments. The water velocity decreases, together with the shear stress on the bed. The sediments will therefore deposit in the reservoir and decrease its volume.

In the design of a dam, it is important to assess the magnitude of sediment deposition in the reservoir. The problem can be divided in two parts:

1. How much sediments enter the reservoir
2. What is the trap efficiency of the reservoir

In a detailed study, the sediment grain size distribution also have to be determined for question 1. Question 2 may also involve determining the

location of the deposits and the concentration and grain size distribution of the sediments entering the water intakes.

In general, there are two approaches to the sedimentation problem:

1. The reservoir is constructed so large that it will take a very long time to fill. The economical value of the project will thereby be maintained.

2. The reservoir is designed relatively small and the dam gates are constructed relatively large, so that it is possible to remove the sediments regularly by flushing. The gates are opened, lowering the water level in the reservoir, which increases the water velocity. The sediment transport capacity is increased, causing erosion of the deposits.

A medium sized reservoir will be the least beneficial. Then it will take relatively short time to fill the reservoir, and the size is so large that only a small part of the sediments are removed by flushing.

The flushing has to be done while the water discharge into the reservoir is relatively high. The water will erode the deposits to a cross-stream magnitude similar to the normal width of the river. A long and narrow reservoir will therefore be more effectively flushed than a short and wide geometry. For the latter, the sediment deposits may remain on the sides.

The flushing of a reservoir may be investigated by physical model studies.

Another question is the location of the sediment deposits. Fig. 9.7.1 shows a longitudinal profile of a reservoir. There is a dead storage below the lowest level the water can be withdrawn. This storage may be filled with sediments without affecting the operation of the reservoir.

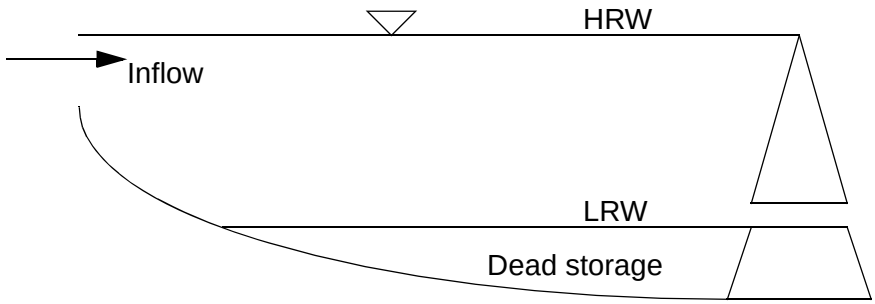

Figure 9.7.1 Longitudinal profile of a reservoir. HRW is the highest regulated water level. LRW is the lowest regulated water level. The reservoir volume below LRW is called the dead storage, as this can not be used.

Sediment load predicion

Rough estimates of sediment load may be taken from regional data. Often the sediment yield in the area is known from neighbouring catchments. It is then possible to assess the seriousness of the erosion in the present catchment and estimate rough figures of sediment yield. The land use, slope and size of the catchment are important factors.

For a more detailed assessment, measurements of the sediment concentration in the river have to be used. Sediment concentrations are measured using standard sampling techniques, and water discharges are recorded simultaneously. The measurements are taken at varying water discharges. The values of water discharge and sediment consternations are plotted on a graph, and a rating curve is made. This is often on the form:

$$Q_s = aQ_w^b \qquad (9.7.1)$$

Q_S is the sediment load, Q_W is the water discharge and *a* and *b* are constants, obtained by curve-fitting.

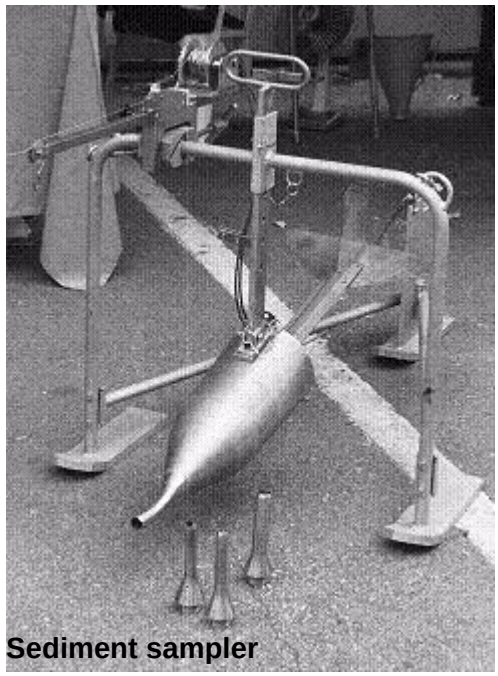
Sediment sampler

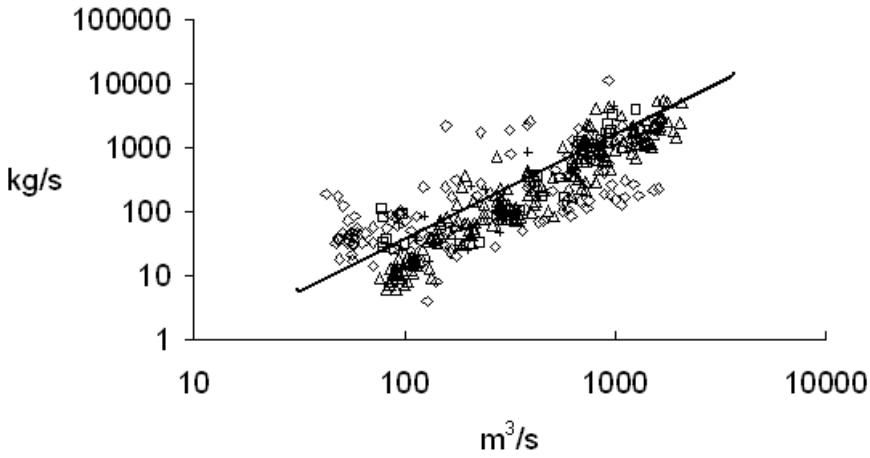

Fig. 9.7.2 Example of sediment rating curve. The sediment load is on the vertical axis, and the water discharge on the horizontal axis. The points are measured values, and the line is Eq. 9.7.1

Note: Often, most of the sediments are transported during the larger floods

The annual average sediment transport is obtained by using a time-series of the water discharge over the year together with Eq. 9.7.1.

9.8 Fluvial geomorphology

The river plays an essential role in shaping the landscape, in the process of transporting eroded sediments to the sea. The transport mechanisms are described differently depending on the river characteristics. In the upper part of the catchment, the creeks will have relatively large slopes. The transport capacity will often exceed the amount of available material, leaving bedrock or larger stones on the river bed. Closer to the sea, the river gradient will be lower, and the river will not be able to transport large-sized material.

Alluvial river

An **alluvial river** is formed where the bed material have sufficient magnitude to enable free vertical bed fluctuations. Also, the bed material has a lower size than what is given by Shields curve, so there is continuous

The **regime theory** was developed by British water engineers in India at the end of the 19th century.

sediment transport. The bed fluctuates depending on the sediment concentraion. If the supply of sediment is larger than the capacity, the bed rises. If the supply is lower then the capacity, the bed is lowered. If the bed is in equilibrium, the river is said to be **in regime**. There exist theory for the relationship should be between different parameters for the channel. This is called regime theory (Blench, 1970). An example is a relationship between the water velocity, U, and the water depth, d:

$$U = 0.84 d^{0.64} \tag{9.8.1}$$

The formula is given in British Imperial units, where the velocity is in feet pr. seconds and the water depth is in feet. Also formulas exist where the river width and slope can be computed.

Paving is called “dekklag” in Norwegian. Meander is called “elveslyng”.

Many steeper rivers are not in regime. Very little sediments may be transported during normal and low flow. Only during large floods, the bed material moves. These rivers often have large stones at the bed. They are said to be **paved**. The paving protects the underlaying sediments. Only during very large floods the paving will be removed, and then large changes in the bed geometry may occur. In general, the bed changes and shape of a river usually change mostly during large floods.

Meandering rivers

The river may also move sideways (laterally), as the classical meandering pattern evolves. As the water velocity is higher closer to the water surface, than at the bed, a vertical pressure gradient will be formed when the water meets an obstacle or a river bank in a bend. The result is a downwards velocity component, causing a secondary current. (Fig. 9.8.1)

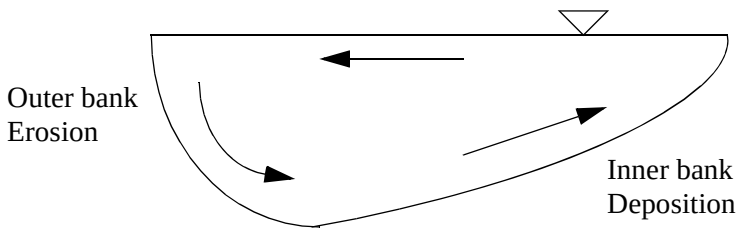

Figure 9.8.1 Cross-sectional view of a river bend, where the arrows indicate the secondary current

The flow pattern causes the sediment transported on the bed to move to the inside of the curve. The shape of the resulting cross-section is given in Fig. 9.8.1, with the deeper part on the outside of the curve. Over time, sediments deposit on the inside of the curve and erosion will take place on the outside. Looking at a plan of the river, the meanders will move outwards and downstream. There exist different classification systems for the plan form (Schumm et. al., 1987).

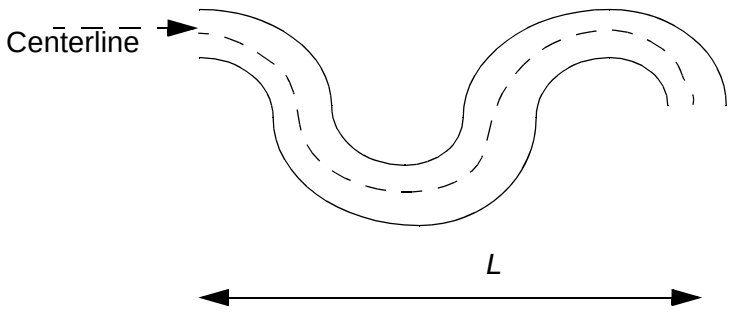

Figure 9.8.1. Definition of sinuosity of a river. The figure shows a plan view of the river. The length of the centerline is denoted *C*, and the length along the valley is denoted *L*. The sinuosity is then the ratio between these numbers: *C*/*L*.

A river can be classified according to its sinuosity (Fig. 9.8.2). If the sinuosity is below 1.05, the river is straight. Some researchers classify a meandering river by a sinuosity above 1.25.

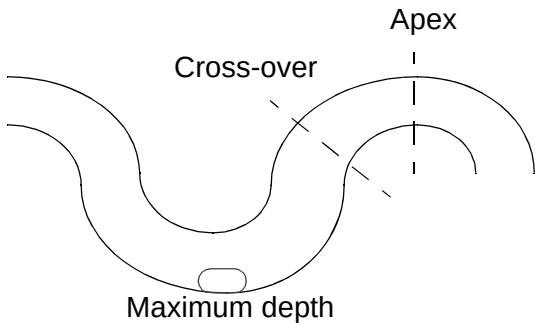

Figure 9.8.3. Plan view of a meandering river. The location of the **apex** and **cross-over** is shown. The maximum depth is at the outer side of the bend at the apex.

Cross-over is called “brekk” in Norwegian. The area at the apex with the scour is called “kulp”.

Useful terminology on meandering rivers is given in Fig. 9.8.3, giving the location of the apex and the cross-over. The secondary currents will have maximum strength at the apex, giving the largest scouring and maximum depth at this location, on the outside of the bend. This is also shown in Fig. 9.8.4, giving a longitudinal profile of a meandering river and explaining the word **thalweg**.

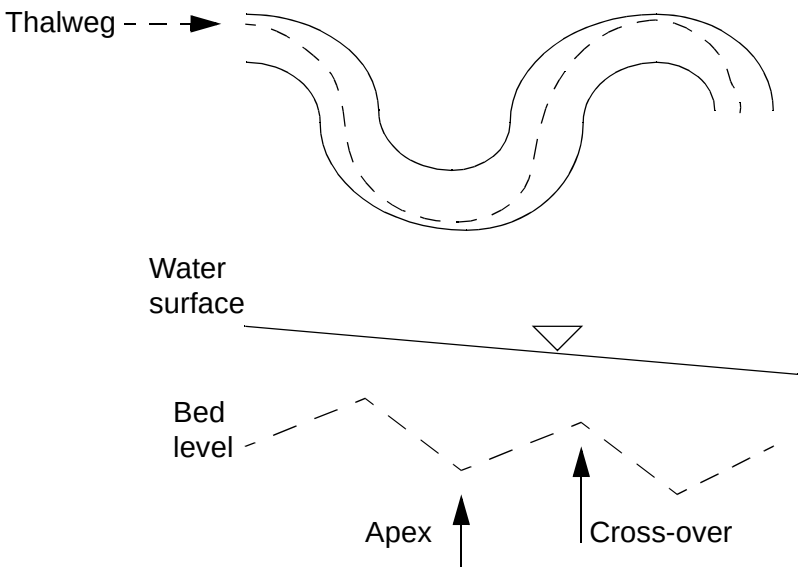

Figure 9.8.4.

The upper figure shows a plan view of the meandering river. The broken line shows the location of the maximum depth of the river. This is also called the **thalweg**.

The lower figure shows a longitudinal profile of the river, with the water surface and the bed level at the thalweg. The thalweg level shows a pattern with highest value at the cross-over and lowest level at the apex.

There are many factors affecting the meander formation, magnitude of the sinuosity etc. for a river: Valley slope, size of sediments, sediment discharge and water discharge. Cohesion of the bank material also seems to be important, as it affects the bank stability. Vegetation along the river is then also important.

Experiments on meandering channels

A natural meandering channel often do not show regular patterns. This is due to inhomogenities in bed material, local geology, vegetation, man-made scour protection etc. To study the meander formation, flume studies in the laboratory have been carried out. An example is large flume studies at Colorado State University in the 1970's. (Schumm et. al., 1987). The flume was 28 meters long, and was initially filled with sand. A straight channel was moulded in the sand, and a water was then run through it. After some time, a meandering pattern emerged. This case was later computed using a CFD model (Olsen, 2003). The results are shown in Fig. 9.8.5, 9.8.6 and 9.8.7.

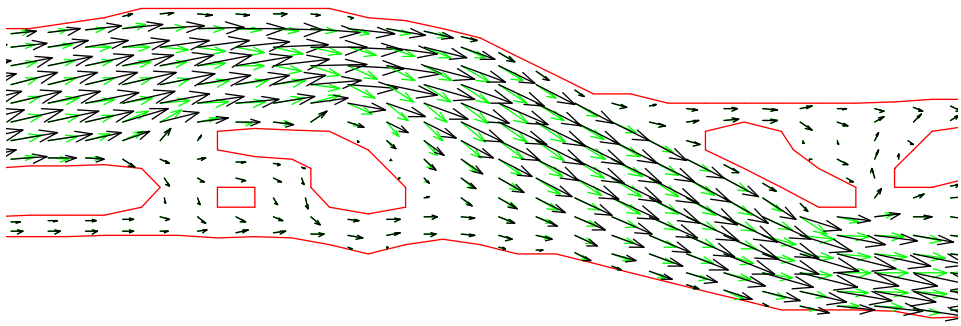

Figure 9.8.5 Plan view of velocity vectors in a meandering river, modelled with CFD. The black arrows shows the vectors at the water surface, and grey arrows close to the bed.

Note the velocity vectors close to the bed points more towards the inside of the curve than the vectors at the surface. This corresponds with Fig. 9.8.1.

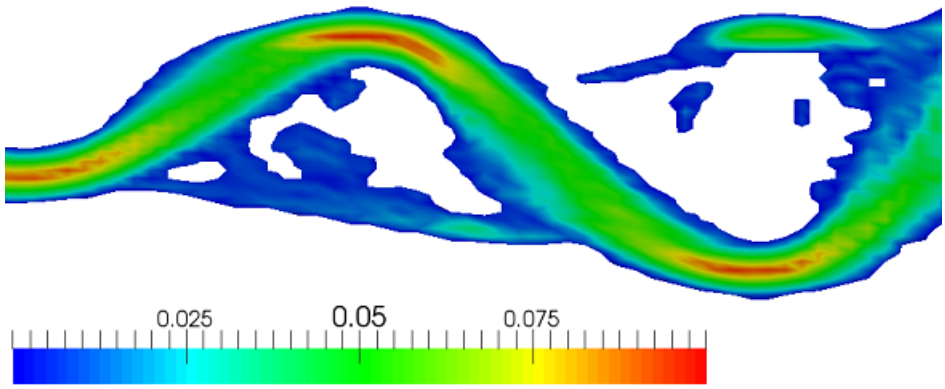

Figure 9.8.6 Plan view of water depths in a meandering river, modelled with CFD. The values are given in cm.

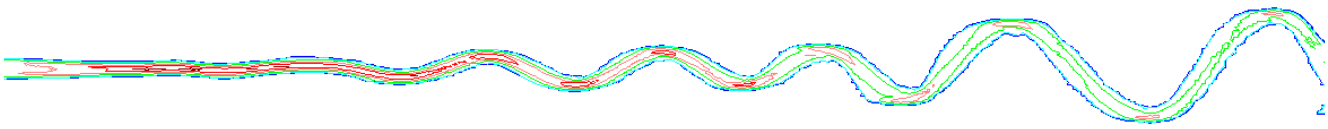

Figure 9.8.7 Plan view of the meandering pattern in a channel computed with a CFD model. The case is a replication of a physical model study by Zimpfer (1975).

If a meander short-cuts like shown in Fig. 9.8.8, this is often called a **chute**. Chutes can also be seen in Fig. 9.8.5 and Fig. 9.8.6 by close examination.

Figure 9.8.8. Plan view of the meandering river, where a chute has formed.

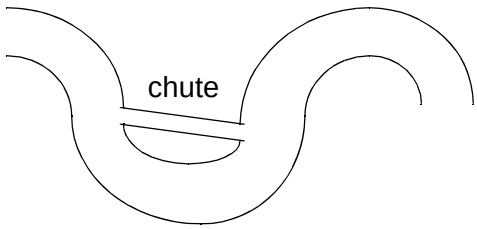

Braided rivers

Beside being straight or meandering, the river may have a third plan form: **braided**. This usually takes place at a steeper valley slope than the meandering plan form. Also, braided river systems often occur in reaches where the sediment transport capacity is lower than the sediment inflow, so that a net deposition occurs.

A river can evolve from a meandering planform to braided. Then chutes form first and grow larger. The braided river does not follow a regular pattern, but consists of several parallel channels, separating and joining each other.

The flume study described in the figures above also evolved into a braiding pattern. After the meandering channel had evolved, the meander bends became very large and channel cutoffs emerged. When several cutoffs had formed, the resulting plan form was braided (Zimpfer, 1975). CFD modelling of a braided system is shown in Fig. 9.8.9.

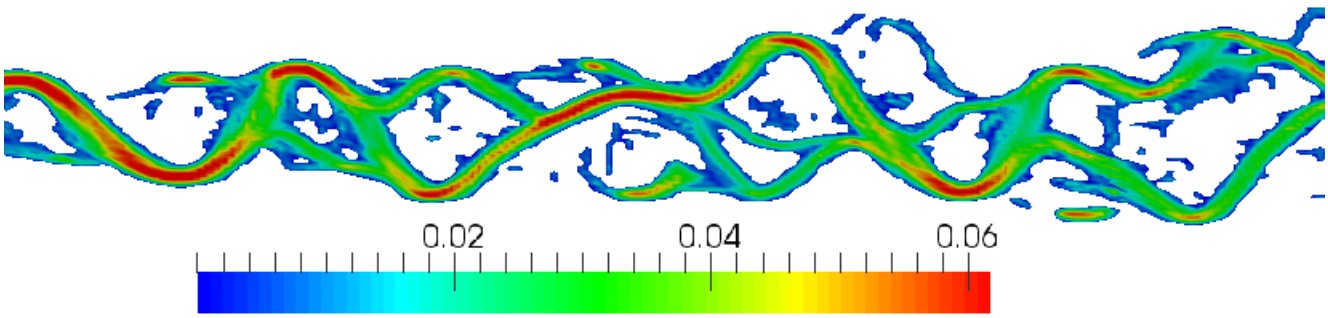

Figure 9.8.9 Plan view of the water depths in a meandering river, where cutoffs have started to make a braided plan form.

Smaller islands in the river are often called **bars**.

A parameter describing the intensity of the braiding is the Braiding Index (BI). This index tells how many channels there is in a river on average. With no braiding and a single channel, the BI becomes 1.

The method to compute the BI is to analyze photographs of the braided-channel, where a number of cross-sections are made. For each cross-secions, the number of channels are counted. The average number for all cross-sections becomes the BI.

A question is then what is a channel? Looking at Fig. 9.8.9, some channels have dead ends and no water velocities. Should these channels be taken into account when computing the BI? Egozi and Ashmore (2009) worked on braiding studies using physical models. They defined two braiding indexes: One active BI, which only counted the channels where there were sediment transport. In these channels, the bed shear stress was larger than the critical shear stress for the particles. The other index was a total BI, which counted all channels, both active and inactive.

9.9 Physical model studies

A physical model is an important tool to estimate effects of sediment transport for engineering purposes. There exist a large number of scaling laws that has to be used according to the purpose of the study. A detailed description of the different methods are given by Kobus (1980).

Water flow

The water discharge in the physical model is usually determined by the the Froude law, based on the similarity between momentum and gravitational forces. The Froude number should be the same in the model as in the river:

Scaling the water discharge in the physical model

$$Fr = \frac{U}{\sqrt{gh}} \tag{9.9.1}$$

Given the geometrical scale,s_g, the Froude number determines the water discharge in the model. The next problem is to determine the correct roughness in the physical model The roughness will affect the shear forces on the bed and thereby the energy slope in the model. The shear force is affected by viscosity and the Reynolds number. The Darcy-Weissbach's diagram for the friction coefficients can be used to compute the physical model friction factors. This friction factor should be the same in the physical model as in the prototype. Given the two Reynolds numbers in the physical model and the prototype, the diagram can be used to compute the relative roughness (k_s/r_h roughness to hydraulic radius) of the physical model, given the similar parameter for the prototype.

The scaling of the sediments is more difficult.

Erosion

If the main topic of the investigation is the computation of maximum scour or erosion, Shield's graph may be used.

$$\tau^* = \frac{\tau}{g(\rho_s - \rho_w)d}. \tag{9.9.2}$$

Scaling sediments for erosion studies

A simplified approach is to say that τ* should be the same in the prototype as in the physical model. Eq. 9.9.2 is then solved with respect to the particle diameter, giving the following equation:

$$\frac{d_m}{d_p} = \frac{\tau_m(\rho_{s,p} - \rho_w)}{\tau_p(\rho_{s,m} - \rho_w)} = \frac{\rho g h_m I(\rho_{s,p} - \rho_w)}{\rho g h_p I(\rho_{s,m} - \rho_w)} = s_g \frac{(\rho_{s,p} - \rho_w)}{(\rho_{s,m} - \rho_w)} \tag{9.9.3}$$

The density of the sediments in the prototype is denoted $\rho_{s,p}$, and $\rho_{s,m}$ is the density of the sediments in the model. The computation involves the shear stress and particle diameter in the prototype and in the model. Subscripts *m* and *p* are used for model and prototype, respectively. It is assumed that the particle Reynolds numbers are so large that the τ* value is the same in prototype and model. The equation is also only valid for particle sizes and bed shear stresses close to erosion. For finer particles, a more involved approach must be used.

Suspended sediments

Scaling sediments for suspended load

If the main topic of the investigation is suspended sediments, the Hunter Rouse number, *z*, is usually used:

$$z = \frac{w}{\kappa u_*} \tag{9.9.4}$$

If the Hunter-Rouse number is the same in the prototype and the model, then this gives the fall velocity of the particles in the physical model. The sediment diameter and density then have to be chosen accordingly.

Scaling time

To model the time for the movement of the sediments, the ratio of sediment transport to volume of sediments is used:

$$\frac{TQ_s}{V} \tag{9.9.5}$$

T is the time, Q_S is the sediment load and *V* is the volume of the material being transported. The scaling factor for time, s_t, is given as

$$s_t = \frac{T_{model}}{T_{prototype}} \tag{9.9.6}$$

A sediment transport formula can then be used to give the sediment discharge pr. unit width, q_S. If *s* is the geometric scale (for example 1:20), then Eq. 9.9.5 and 9.9.6 can be combined to:

$$s_t = \left(\frac{q_{s,prototype}}{q_{s,model}}\right) s_g^{\,2} \tag{9.9.7}$$

Example: *Find the scaling time for a physical model with sediments of size 4 mm in the prototype and 2.5 mm in the physical model. The water velocity is 0.2 m/s in the model, and the water depth is 0.2 m. The proto-*

type sediments have a density of 2.65 kg/dm3, and the model sediments have a density of 1.05 kg/dm3. Manning-Stricklers friction factor is 40, and the model scale is s=0.015 (1:66.67).

Solution: First, the sediment discharge is computed in both the prototype and the model, using Engelund-Hansens formula. This gives:

q_s *= 0.030 kg/s/m (model)*
q_s *= 0.191 kg/s/m (prototype)*

The time scale becomes:

$$s_t = \left(\frac{0.191}{0.030}\right)(0.015)^2 = 0.001435 = \frac{1}{697}$$

A simulation time of 1 hour in the lab will be similar to 697 hours in the prototype.

The accuracy of the scaling of the time will not be better than the accuracy of the sediment transport formula used.

Multiple sediment processes

If the topic of the investigation involves both suspended sediments, erosion and sediment transport, then the different methods of scaling the sediments may give different model sediment characteristics. It may therefore not be possible to model all transport modes and processes. This has been one of the motivations for developing CFD models with sediment transport processes.

Fig. 9.9.1 Photo of the physical model made at SINTEF, Norway, for the **Kali Gandaki** hydropower plant in Nepal. The model was used to investigate sediment flushing from the hydropower reservoir. The dams are shown in the lower left corner. The water is fed into the model at the upper left part of the picture. The model is approximately ten meters long from the dam to the end shown on the right. The model was built of concrete according to the prototype bed, and filled with sand to the level of the spillway crest. The model was then carefully filled with water, and then the flushing started by opening the dam gates. As the run-of-the-river reservoir is fairly narrow, much of the sediments was removed by the flushing

Other problems

Scaling down finer sediments can result in particles with cohesive forces. This would be the case for particles under 0.1 mm. To avoid this, it is possible to use a distorted physical model. Then the vertical scale is larger than the horizontal scale. However, this will also distort all secondary currents, which will not be correctly modelled.

Another problem is to scale bedforms. Dunes and ripples occur at different hydraulic conditions, and it is almost impossible to get for example

the ratio bedform height to water depth to be the same in the physical model and the prototype. Also, bedforms may occur only in the physical model and not in the prototype. The bedforms will then cause different effects for energy loss and sediment transport capacity in the physical model and the prototype.

9.10 Problems

Problem 1. Channel design

A discharge channel from a power station is 30 m wide and has a rectangular cross-section. The bed slope is 1:200 and the maximum water discharge from the power station is 100 m^3/s. To prevent erosion of the channel, stones are used at the bed of the channel. How large must the stones be? Assume uniform grain size distribution for the stones.

Problem 2. Sediment transport

Problem 2 is taken from the Iffezheim dam in the River Rhine in Germany (Kuhl, 1992), where this solution was chosen.

The construction of a dam in a river caused erosion downstream. What would be the reason?

The river authorities solved the problem by adding gravel to the river, downstream of the dam. What would be the required amount of gravel, when the water discharge was assumed to be 1500 m^3/s, the water depth 3.5 meters, the width 100 meters and the slope 1:1600 The gravel size was identical to the sediment size at the bed: a diameter of 20 mm.

Can you think of an alternative solution to the problem?

Problem 3. Sediment load estimation

Estimate the annual sediment load in a river, given the flow duration curve below, and the rating curve in Fig. 9.7.1. How much of the sediments are transported by the highest floods, occurring under 5 % of the time?

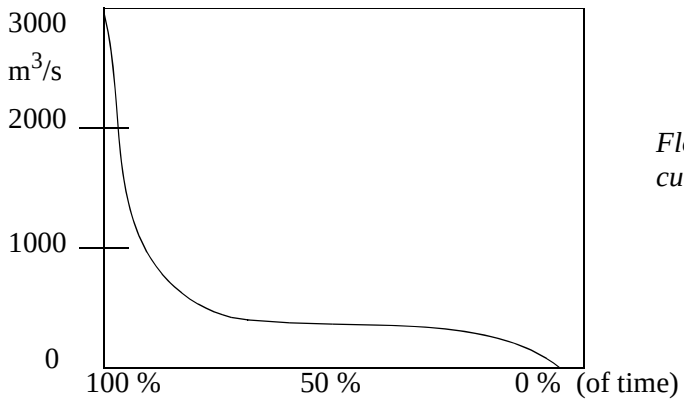

Flow duration curve

Problem 4. Physical model study

A physical model study of a reservoir is conducted. The scale is 1:30. The water discharge in the prototype is 300 m^3/s. What is the discharge in the model?

The average dimensions of the physical model is 10 m long, 5 m wide,

and 10 cm deep. Suggest a sediment type and size for the physical model, when investigating sedimentation of prototype silt particles of 0.3 mm.

Suggest a sediment type for modelling flushing of the same silt.

If a water discharge over time were to be modelled, including both sedimentation and erosion, what kind of sediment should be chosen?

Problem 5. HEC-6

Compute the trap efficiency over time in a water reservoir built in a river with slope 1:200. The water discharge is 100 m^3/s, the river width is 30 meters, the dam height is 30 meters. Assume a constant reservoir width of 200 meters. The inflow sediment is silt with particle diameter 0.3 mm, and the concentration is 2000 ppm.

Problem 6. Sediment load formulas

Compute the sediment transport capacity pr. m. width in an alluvial channel, with the following data:

U=2.5 m/s
Depth, y = 1.5 m
Manning-Strickler coefficient: 50
Sediment size: 1 mm

Use both Engelund-Hansen's and van Rijn's formulas.

10. River habitat modelling

10.1 Introduction

Earlier methods of evaluating impacts of river regulations on fish was dubbed **BOGSAT**: **B**unch **O**f **G**uys **S**itting **A**round a **T**able, discussing the effects of the regulation. The purpose of River Habitat Modelling is to improve the scientific background for the evaluation.

The science has also lead to increased cooperation and understanding between biologists and engineers working in rivers.

The science of River Habitat Modelling has evolved over the last ten years. The main purpose is to assess the effect of habitat for fish, mostly salmon, in relation to river regulations. Hydropower production has often been the cause of changes in the water discharge. River Habitat Modelling aims to quantify the effects of changes in the river flow conditions and geometry, to assess the impact of regulations on the fish production. In Norway, this has been used to determine minimum flow regulations in rivers. Also, it is used for assessing environmental effects from hydropeaking.

10.2 Fish habitat analysis

The basis of the currently used method is that fish will seek an optimum condition with respect to:

- Feeding
- Energy to stay in the river
- Spawning
- Protection from predation

The factors vary depending on the age of the fish. Often, the critical age for salmon will be the juvenile stage. The studies often look at the rearing and growing areas of the fish.

Looking at river regulations, the main changes in the river will be the physical habitat. The main factors often used are:

Main factors affecting the fish:

- Water depth
- Water velocity
- Substrate/cover

Substrate is usually determined by a characteristic size of the stones on the river bed. The stones provide cover/hiding places for the fish. However, plants with leaves extending out over the river will also provide cover.

The effect of feeding is neglected in simpler models. Then, it is assumed the fish prefers optimum values of the parameters given above.

The currently most used methodology for fish habitat analysis is called the Instream Flow Incremental Methodology (IFIM). It can be divided in the following stages:

Instream Flow Incremental Methodology (IFIM):

1. Selection of representative reach of the river
2. Counting the fish at different locations, recording habitat parameters
3. Generating habitat preference functions
4. Measuring habitat parameters at different discharges
5. Generating spatially distributed habitat as a function of discharge
6. Computing the habitat as a function of a time series of discharge

The selection of representative reach of the river has to be done with respect to typical values of depth, velocity and substrate. Often, fish biologists provide input for the selection.

The preferred method for counting the fish is by diving. The diver covers the whole area of the selected reach, and put a marker on the river bed for each fish observation. Afterwards, the depth, velocity and substrate is recorded for each marker. It is also possible to identify fish locations from the surface, but then it is often more difficult to spot the fish. Then the velocity, depth and substrate is divided into groups, and it is counted how many fish there is in each group. This is shown in Fig. 10.2.1:

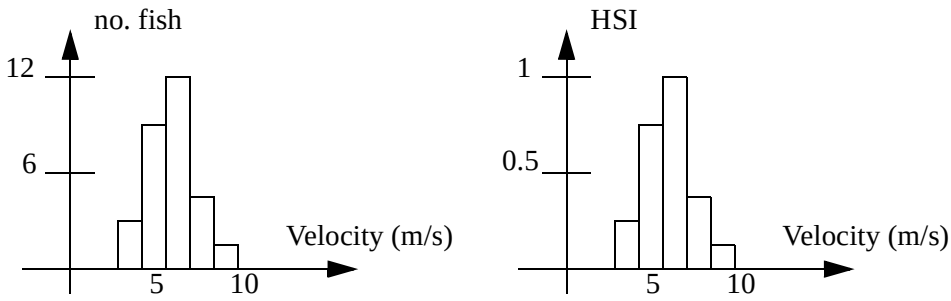

Figure 10.2.1. Generation of HSI index for velocity. The number of fish in each velocity group is counted (left figure), and scaled to max value of unity to become the HSI index (right)

The HSI index indicates the preferred velocity for the fish. Another question is how much area of a preferred velocity there is in the river. This is called availability of velocity. The availability is computed the same way as the HSI index, but on the vertical axis is the area of a given velocity interval. This can also be scaled to unity as the maximum area.

A preference index, *D*, is made from the HSI index and the availability function, by using the following formula:

$$D = \frac{r - p}{(r + p) - 2rp} \qquad (10.2.1)$$

where *p* is the available habitat of a defined velocity range, and *r* is the HSI index. Both *p* and *r* are scaled so their values range between zero and 1.

Three regions are made:

- Preferred habitat, where most of the fish observations are
- Avoided habitat, where there are no observations
- Indifferent, the region between

Preferred habitat is if *D* is above 0.2. If *D* is below -0.2, this is avoided habitat. The area between -0.2 and 0.2 is indifferent. An example is given in Fig. 10.2.2.

It is also possible to make an index by combining the curves for velocity, depth and substrate.

Given the indexing system, a map of preferred, indifferent and avoided habitat is made. This is called a habitat map, and an example is given in Fig. 10.2.3. The habitat will vary according to the water discharge. Summing up the preferred area in a time series of water discharge, a measure of fish habitat for a given river regulation is made. Effects of changes in the regulations can thereby be computed, but using different regulated discharges over the year.

Figure 10.2.2 Generation of preference curve as a function of velocity

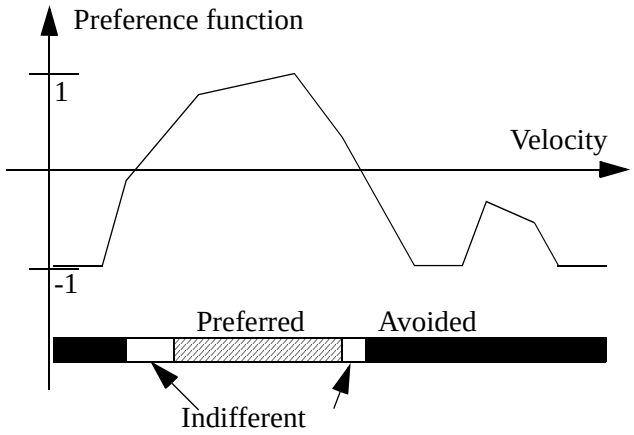

The preference curve is a **biological model** for the fish habitat. There also exist other biological models, based on different approaches.

The method will, however, only work if it is possible to estimate the velocity and depth as a function of the water discharge. This has to be made in preferably three dimensions, as the spatial variation of velocity near the bed is required. The fish is often found near the bed. The following two chapters shows the two main methods:

- Measurements and zero/one-dimensional models
- Multidimensional numerical models

This is described in the following chapters.

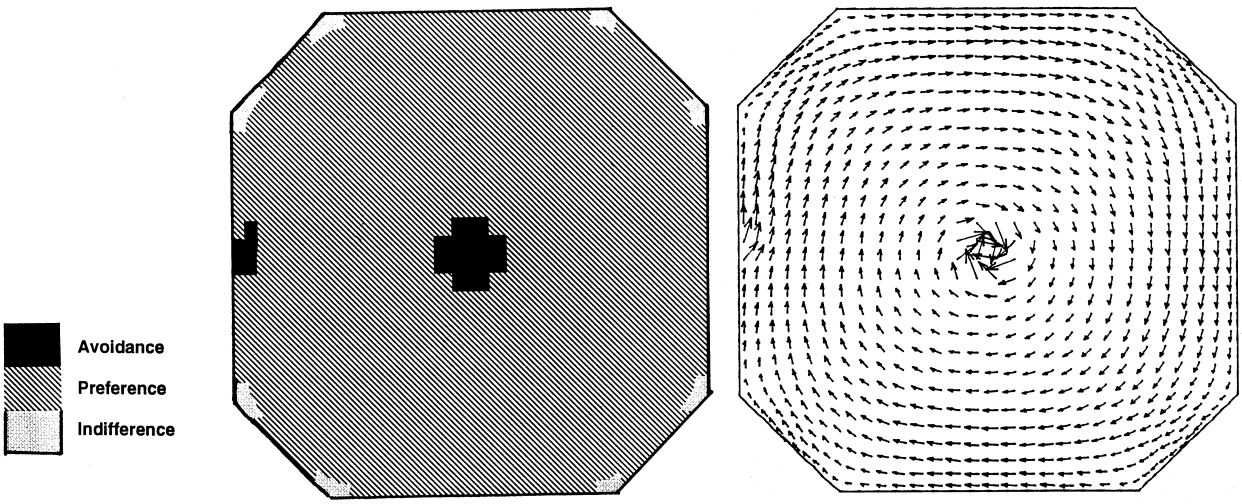

Figure 10.2.2 Velocity vector map (right) and computed habitat (left) near the bed for juvenile salmon in a fish farm tank, seen from above. The water is entering on the left side, creating the current shown. The outlet is in the center of the tank, at the bottom. The fish farm tank is 1.5 meters deep and 2.7 meters wide (Olsen and Alfredsen, 1994). Most of the area has preferred velocity, except for the entrance and exit region where the velocity is too high, and the corners where the velocity is lower than preferred.

10.3 Zero and one-dimensional hydraulic models

Initial work on habitat hydraulics started with measuring the water velocities in the characteristic reach of the river. Measurements were made in multiple cross-sections, or transects. A two-dimensional map of the velocities and depths were then obtained for a given discharge. This was repeated for several water discharges. An interpolation function was used for discharges between the measured ones.

The interpolation function could be fairly involved, and often a one-dimensional backwater program was used. Various weighing functions were calibrated for the velocity distribution in the lateral direction. Examples of computer programs using this procedure is RIMOS and PHABSIM.

There were two problems with this procedure:

1. A large number of field measurements had to be carried out
2. The calibration of the interpolation functions were only valid for the geometry where the measurements were taken. In other words, it was not possible to estimate the effects of changes in the geometry.

To solve this problem, multi-dimensional models have to be used.

10.4 Multidimensional hydraulic models

The multidimensional numerical models are two-dimensional depth-averaged or three dimensional. The models solve the Navier-Stokes equations using for example the methods given in Chapter 6. The models can compute the effect of changes in the bed geometry, as the geometry is given as input for the grid. This is very useful for assessment of fish habitat studies for river regulations, as a mean of improving the habitat is often to create small dams or obstacles in the flow. The water depth is thereby increased, and also the variation in water velocity.

10.5 Bioenergetic models

At the time this book was made, the bioenergetic models were still on the research stage.

Bioenergetic models are the latest in a succession of habitat assessment methodologies. The theory is to compute how much energy the fish uses in different locations of the flow, as a function of water velocity and possibly turbulence. As opposed to earlier studies, the food intake is also taken into account. The fish feed on small organisms, which have different concentrations in various locations of the river. This means the fish will receive more food/energy in some locations than in others. The models also assess how much energy is consumed by the fish. This is a function of the velocity in the river. Using three-dimensional numerical models, it is possible to compute the food concentration, water velocity and turbulence over the whole three-dimensional river body. The optimum location for the fish can then be estimated, with the assumption that the fish will seek a maximum possible difference between the energy intake and consumption.

10.6 Problems

Problem 1. Preference curves

The figures below give depth and velocity in a representative reach of Sokna River in Norway, at a discharge of 10 m^3/s. The figure with the dots provide locations of fish observations. Make preference curves for the fish, for both depth and velocity.

Velocity (cm/s) near the bed for a discharge of 10 m^3/s.

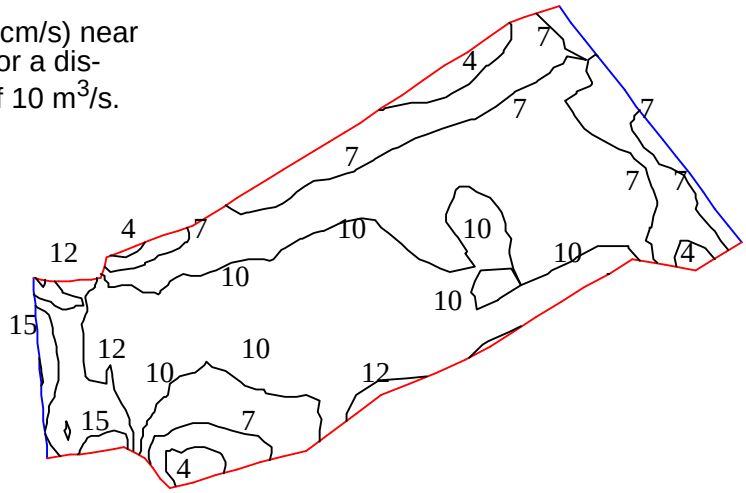

Fish observations

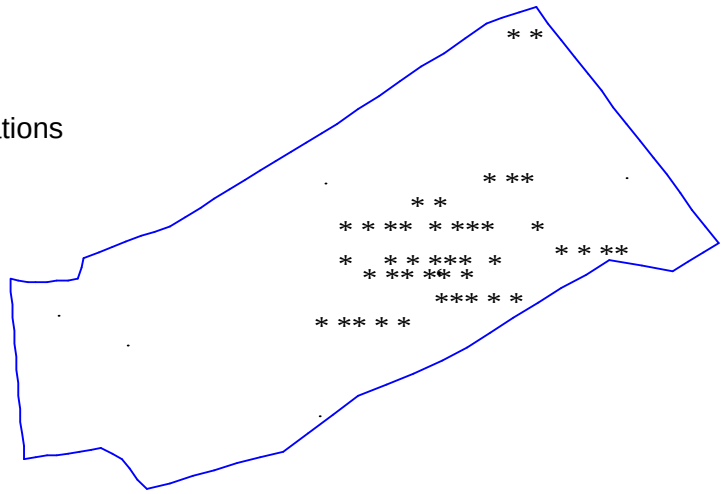

Depth in meters, for 10 m^3/s

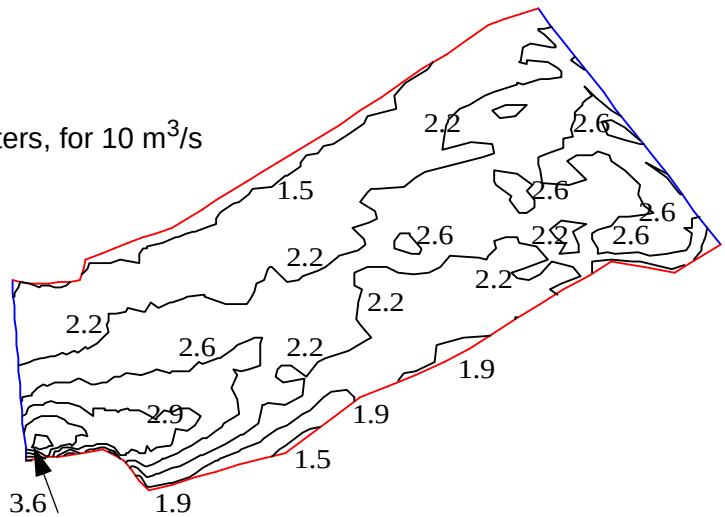

Problem 2. Habitat map

Make habitat maps for Sokna River, for 10 m^3/s, for both water depth and velocity.

Problem 3. Habitat map for changed velocity

Compute the habitat maps when the discharge is lowered to 3 m^3/s. The velocity and depth is given below. Is the habitat improved or has it deteriorated?

Water depth in meters for 3 m^3/s

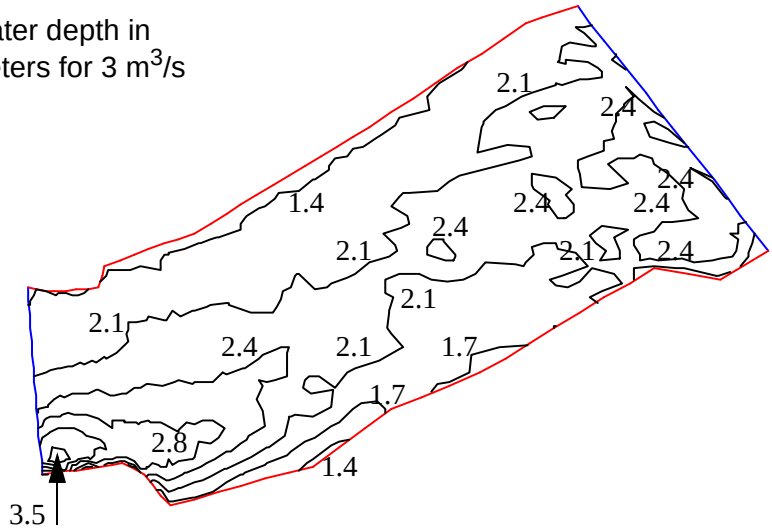

Velocity in cm/s near the bed at 3 m^3/s.

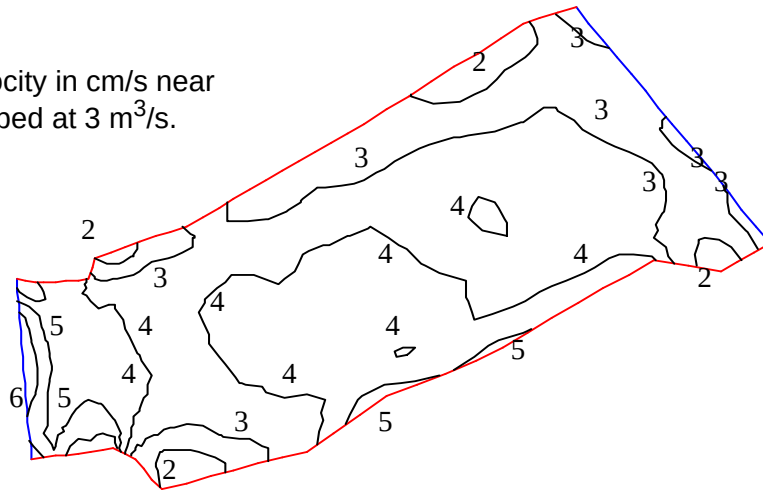

Problem 4. Habitat improvement

Suggest measures to improve the habitat in the river, and methods to document the improvements before they are carried out.

Literature

Ackers, P. and White, R. W. (1973) "Sediment Transport: New Approach and Analysis", ASCE Journal of Hydraulic Engineering, Vol. 99, No. HY11.

Ahmad, Z., Kothyari, U. C. and Ranga Raju, K. G. (1999) “Longitudinal dispersion in open channel flows”. Journal of Hydraulic Engineering 5 (2), pp 1-21.

Bagnold, R. A. (1973) “The nature of saltation and of ‘bed-load’ transport in water”, Proceedings of the Royal Society of London, A332. pp473-504.

Bagnold, R. A. (1988) “The physics of sediment transport by wind and water”, A collection of hallmark papers, ASCE Publications.

Bagnold, R. A. (1990) “Sand, wind, and war: memoirs of a desert explorer“, Tucson : University of Arizona Press.

Bakhmeteff (1932) “Hydraulics of open channels”, McGraw-Hill Book Company, New York.

Baranya, S., Olsen, N. R. B., Stoesser, T. and Sturm, T. (2014) “A nested grid based computational fluid dynamics model to predict bridge pier scour”, Water Management, Vol. 167, Issue 5, pp 259–268.

Bengtsson, L. (1973) "Wind Stress on Small Lakes", Tekniska Høgskolan, Lund, Sweden.

Bihs, H. and Olsen, N. R. B. (2011) “Numerical Modeling of Abutment Scour with the Focus on the Incipient Motion on Sloping Beds“, Journal of Hydraulic Engineering.

Bindloss, M. (1976) "The light-climate of Loch Leven, a shallow Scottish lake, in relation to primary production of phytoplankton", Freshwater Biology, No. 6.

Blench, T. (1970) “Regime theory design of canals with sand beds”, ASCE Journal of Irrigation and Drainage Engineering, Vol. 96, No. IR2, Proc. Paper 7381, June, pp. 205-213.

Bowles, C., Daffern, C. D. and Ashforth-Frost, S. (1998) "The Independent Validation of SSIIM - a 3D Numerical Model", HYDROINFORMATICS '98, Copenhagen, Denmark.

Brooks, H. N. (1963), discussion of "Boundary Shear Stresses in Curved Trapezoidal Channels", by A. T. Ippen and P. A. Drinker, ASCE Journal of Hydraulic Engineering, Vol. 89, No. HY3.

Brethour, J. M. (2002) “Transient 3-D model for lifting, transporting and depositing solid material”, Proceedings from the Fifth International Conference on Hydroinformatics, Cardiff, UK.

Brunner, G. W. (2010) “HEC-RAS, River Analysis System Hydraulic Reference Manual, Report no. CPD-69, US Army Corps of Engineers, Hydrologic Engineering Center, USA.

Carstens, T. J. (1997) “Class notes in fluvial hydraulics - hydraulics of receiving waters”, Department of Hydraulic and Environmental Engineer-

ing, The Norwegian University of Science and Technology. (In Norwegian)

Celik, I. B., Ghia, U., Roache, P. J., Freitas, C. J., Coleman, H. and Raad, P. E. (2008) “Procedure for Estimation and Reporting of Uncertainty Due to Discretization in CFD Applications”, Transactions of the ASME, Vol. 130, pp 078001-1 - 078001-4.

Chapra, S. C. (1997) "Surface water-quality modelling", McGraw-Hill, ISBN 0-07-115242-3.

Demuren, A. O. and Rodi, W. (1984) “Calculation of turbulence-driven secondary motion in non-circular ducts”, Journal of Fluid Mechanics, vol. 140, pp. 189-222.

Dey, S. (2003) “Threshold of sediment motion on combinded transverse and longitudinal sloping beds”, Journal of Hydraulic Research, Vol. 41 (4), pp. 405-415.

van Dorn, W. (1953) "Wind stress on an artificial pond", Journal of Marine Research, No. 12, pp. 249-276.

Egozi, R. and Ashmore, P. (2009) “Experimental analysis of braided channel pattern response to increased discharge, Journal of Geophysical Research, Vol. 114. F02012.

Einstein, H. A., Anderson, A. G. and Johnson, J. W. (1940) “A distinction between bed-load and suspended load in natural streams”, Transactions of the American Geophysical Union’s annual meeting, pp. 628-633.

Einstein, H. A. and Ning Chien (1955) "Effects of heavy sediment concentration near the bed on velocity and sediment distribution", UCLA - Berkeley, Institute of Engineering Research.

Engelund, F. (1953) "On the Laminar and Turbulent Flows of Ground Water through Homogeneous Sand", Transactions of the Danish Academy of Technical Sciences, No. 3.

Engelund, F. and Hansen, E. (1967) "A monograph on sediment transport in alluvial streams", Teknisk Forlag, Copenhagen, Denmark.

Fergus, T., Hoseth, K. A. and Sæterbø, E. (2010) “Handbook of rivers” (Vassdragshåndboka), Tapir forlag, Norway, ISBN 978-82-519-2425-2 (in Norwegian).

Fisher, H. B., List, E. J., Koh, R. C. Y., Imberger, J. and Brooks, N. H. (1979) “Mixing in Inland and Coastal Waters”, Academic Press.

Fischer-Antze, T., Stösser, T., Bates, P. and Olsen, N. R. B. (2001) "3D numerical modelling of open-channel flow with submerged vegetation", IAHR Journal of Hydraulic Research, No. 3.

Fisher, H. B., List, E. J., Koh, R. C. Y., Imberger, J. and Brooks, N. H. (1979) “Mixing in inland and costal waters”, Academic press, New York.

French, R. H. (1994) “Open-channel hydraulics”, McGraw-Hill.

Graf, W. H. and Altinakar, M. S. (1996) “Fluvial hydraulics, Vol. 2, Flow and transport processes in channels of simple geometry”, Wiley Publishers.

Hedger, R. D., Olsen, N. R. B., Malthus, T. J. and Atkinson, P. M. (2002)

"Coupling remote sensing with computational fluid dynamics modelling to estimate lake chlorophyll-a concentration", Remote Sensing of Environment, Vol. 79, No. 1, pp. 116-122.

Henderson-Sellers, B. (1984) “Engineering Limnology”, Pitman Publishing Limited, ISBN 0-273-08539-5.

Hervouet, J-M. and Petitjean, A. (1999) “Malpasset dam-break revisited with two-dimensional computations”, IAHR Journal of Hydraulic Research, Vol. 37, No. 6.

Hey, R. D. (1979) “Flow resistance in gravel-bed rivers”, ASCE Journal of Hydraulic Engineering, Vol. 105, No. 4, April.

Jones, W. P. and Launder, B. E. (1972) “The prediction of Laminarization with a Two-Equation Model of Turbulence”, International Journal of Heat and Mass Transfer, Vol. 15, pp.

Kamphuis, J. W. (1974) “Determination of sand roughness for fixed beds“, Journal of Hydraulic Research, Vol. 12, No. 2.

Karim, F. (1999), Bed-form geometry in sand-bed flows, J. of Hydraulic Eng., Vol. 127, No. 12, pp 1253-1263

Kawai, S. and Julien, P. Y. (1996) “Point bar deposits in narrow sharp bends”, IAHR Journal of Hydraulic Research, No. 2.

Kennedy, J. F. (1963) “The mechanics of dunes and antidunes in erodible-bed channels”, Journal of Fluid Mechanics, Vol. 16, No. 4, pp 597-604.

Kobus, H. (1980) “Hydraulic modelling”, German Association for Water Resources and Land Improvement, Hamburg, Germany.

Kreyszig, E. (1983) “Advanced Engineering Mathematics”, John Wiley & Sons Publishers.

Kuhl, D. (1992) “14 years artificial grain feeding in the Rhein, downstream the barrage Iffezheim”, 5th Int. Symp. on River Sedimentation, Karlsruhe, Germany.

Launder, B. E. and D. B. Spalding (1974) “The numerical computation of turbulent flows”, Comput. Meths. Appl. Mech. Eng., Vol. 3, No. 2, pp 269-289.

Lysne, D. K. (1969) “Movement of sand in tunnels”, ASCE Journal of Hydraulic Engineering, Vol. 95, No. 6, November.

Mayer-Peter, E. and Mueller, R. (1948) "Formulas for bed load transport", Proceedings from the Second Meeting of the International Association for Hydraulic Structures Research, Stockholm, Sweden.

McQuivey, R. S. and Keefer, T. N. (1974) “Simple method for predicting dispersion in streams”, ASCE Journal of Environmental Engineering, pp. 997-1011.

Melaaen, M. C. (1992) "Calculation of fluid flows with staggered and nonstaggered curvilinear nonorthogonal grids - the theory", Numerical Heat Transfer, Part B, vol. 21, pp 1- 19.

Munk, W. H. and Anderson, E. R. (1948) “Notes on the theory of the thermocline”, Journal of Marine Research, Vol. 1.

Naot, D. and Rodi, W. (1982) “Calculation of secondary currents in channel flow”, ASCE Journal of Hydraulic Engineering, No. 8, pp. 948-968.

Nikuradse, J. (1933) “Flow in rough pipes”, ?? Report no. 361.

O’Connor, D. J. and Dobbins, W. E. (1958) “Mechanisms of reaeration in natural streams”, Trans. ASCE, no. 123, pp. 641-684.

Olsen, N. R. B. and Melaaen, M. C. (1993) "Three-dimensional numerical modelling of scour around cylinders", ASCE Journal of Hydraulic Engineering, Vol. 119, No. 9, September.

Olsen, N. R. B., Jimenez, O., Lovoll, A. and Abrahamsen, L. (1994) "Calculation of water and sediment flow in hydropower reservoirs", 1st. International Conference on Modelling, Testing and Monitoring of Hydropower Plants, Hungary.

Olsen, N. R. B. and Alfredsen, K. (1994) "A three-dimensional model for calculation of hydraulic parameters for fish habitat", IAHR Conference on Habitat Hydraulics, Trondheim, Norway.

Olsen, N. R. B. and Skoglund, M. (1994) "Three-dimensional numerical modelling of water and sediment flow in a sand trap", IAHR Journal of Hydraulic Research, No. 6.

Olsen, N. R. B. and Stokseth, S. (1995) "Three-dimensional numerical modelling of water flow in a river with large bed roughness", IAHR Journal of Hydraulic Research, Vol. 33, No. 4.

Olsen, N. R. B. (1999) "Computational Fluid Dynamics in Hydraulic and Sedimentation Engineering", Class notes, Department of Hydraulic and Environmental Engineering, The Norwegian University of Science and Technology.

Olsen, N. R. B. and Kjellesvig, H. M. (1998) "Three-dimensional numerical flow modelling for estimation of maximum local scour depth", IAHR Journal of Hydraulic Research, No. 4.

Olsen, N. R. B. and Kjellesvig, H. M. (1998) "Three-dimensional numerical flow modelling for estimation of spillway capacity", IAHR Journal of Hydraulic Research, No. 5.

Olsen, N. R. B. (1999) "Two-dimensional numerical modelling of flushing processes in water reservoirs", IAHR Journal of Hydraulic Research, Vol. 1.

Olsen, N. R. B. and Kjellesvig, H. M. (1999) "Three-dimensional numerical modelling of bed changes in a sand trap", IAHR Journal of Hydraulic Research, Vol. 37, No. 2. abstract

Olsen, N. R. B. and Lysne, D. K. (2000) "Numerical modelling of circulation in Lake Sperillen, Norway", Nordic Hydrology, Vol. 31, No. 1.

Olsen, N. R. B., Hedger, R. D. and George, D. G. (2000) "3D Numerical Modelling of Microcystis Distribution in a Water Reservoir", ASCE Journal of Environmental Engineering, Vol. 126, No. 10, October.

Olsen, N. R. B. (2003) "3D CFD Modeling of a Self-Forming Meandering Channel", ASCE Journal of Hydraulic Engineering, No. 5, May.

Olsen, N. R. B. (2013), Numerical Algorithms for Predicting Sediment

Slides in Water Reservoirs, Electronic Journal of Geotechnical Engineering, Vol. 18, Bund.Y, Paper 2013.496.

Olsen, N. R. B. (2015), Four free surface algorithms for the 3D Navier-Stokes equations, Journal of Hydroinformatics, Vol. 17, Issue 6, pp 845-856.

Patankar, S. V. (1980) "Numerical Heat Transfer and Fluid Flow", McGraw-Hill Book Company, New York.

Reynolds, C. S. (1984) "The ecology of freshwater phytoplankton", Cambridge University Press, Cambridge, UK.

Rhie, C.-M, and Chow, W. L. (1983) "Numerical study of the turbulent flow past an airfoil with trailing edge separation", AIAA Journal, Vol. 21, No. 11.

van Rijn, L. C. (1982) “Equivalent roughness of alluvial bed”, Journal of Hydraulic Engineering, Vol. 108, No. 10.

van Rijn, L. C. (1984) “Sediment Transport, Part III: Bed Forms and Alluvial Roughness”, Journal of Hydraulic Engineering, Vol. 110, No. 12, pp. 1733-1754.

van Rijn, L. C. (1987) "Mathematical modelling of morphological processes in the case of suspended sediment transport", Ph.D Thesis, Delft University of Technology.

Rodi, W. (1980) "Turbulence models and their application in hydraulics", IAHR State-of- the-art paper.

Rouse, H. (1937) "Modern Conceptions of the Mechanics of Fluid Turbulence", Transactions, ASCE, Vol. 102, Paper No. 1965.

Rouse, H., Yih, C. S. and Humphreys, H. W. (1952) “Gravitational convection from a boundary source”, Tellus, pp. 201-210.

Schall, J. D. (1983) “Two-dimensional investigation of shear flow turbulence in open-channel flow”, PhD dissertation, Colorado State University, USA.

Schlichting, H. (1936) “Experimental Investigations of Roughness”, Proc. Soc. Mech. Eng., USA.

Schlichting, H. (1979) "Boundary layer theory", McGraw-Hill.

Schumm, S. A., Mosley, M. P. and Weaver, W. E. (1987) “Experimental fluvial geomorphology”, John Wiley & Sons Publishers.

Shields, A. (1936) “Use of dimensional analysis and turbulence research for sediment transport”, Preussen Research Laboratory for Water and Marine Constructions, publication no. 26, Berlin (in German).

Seed, D. (1997) "River training and channel protection - Validation of a 3D numerical model", Report SR 480, HR Wallingford, UK.

Spallart and Allmaras (1994) “A one-equation turbulence model for aerodynamic flows”, La Recherche Aerospatiale, no 1. pp 5-21.

Speziale, C. G. (1987) “On nonlinear K-l and k-e models of turbulence”, Journal of Fluid Mechanics, vol. 178, pp. 459-475.

Stigebrandt, A., (1978) “Three-dimensional selective withdrawal”, Report No. STF60 A78036, The Norwegian River and Harbour Laboratory, Trondheim, Norway.

Steen, J-E. and Stigebrandt, A. (1980) “Topological control of three-dimensional selective withdrawal”, Second Int. Symp. on Stratified Flows, Trondheim, Norway, pp.447-455.

Streeter, H. W. and Phelps, E- B. (1925) "A study of the pollution and natural purification of the Ohio River", US Public Health Service, Washington DC, Bulletin 146.

Vanoni, V., et al (1975) "Sedimentation Engineering", ASCE Manuals and reports on engineering practice - No54.

Wu, J. (1969) "Wind Shear Stress and Surface Roughness at Air-Sea Interface", Journal of Geophysical Research, No. 74, pp. 444-455.

Yang, T. C. (1973) "Incipient Motion and Sediment Transport", ASCE Journal of Hydraulic Engineering, Vol. 99, No HY10.

Zimpfer, G. L. (1975) “Development of laboratory river channels”, PhD Thesis, Department of Earth Resources, Colorado State University.

Appendix I. Source code for explicit solution of Saint-Venant equations

```
#include "stdio.h"
#include "math.h"


main()
{

FILE *in;
FILE *out;

int i,j,k,n;
double timein[100];
double qinn[100];
double depth[200][2];
double velocity[200][2];
double time, y, u, alpha, beta, q, dummy;
double timestep = 3.0;
double deltax = 50.0;
double slope = 0.005;
double manning = 30.0;
int sections = 99;

in = fopen("inflow","r");
out = fopen("outflow","w");
fclose(out);

/* reading time series */

n=0;
for(j=0;j<100;j++) {
  if(fscanf(in,"%lf %lf",&timein[j], &qinn[j]) != 2) break;
  n++;
  }

fclose(in);

/* initialization */

y = pow (qinn[0]/(manning*sqrt(slope)),0.6);
u = qinn[0] / y;
for(i=0;i<sections+1;i++) {
        depth[i][0] = y;
        depth[i][1] = y;
        velocity[i][0] = u;
        velocity[i][1] = u;
        }

/* main loop */

time = timein[0];
for(j=0;j<=1000;j++) {
```

```
/* boundary conditions */

        for(k=0;k<n;k++) if(timein[k]>time) break;
        beta = (timein[k] - time) / (timein[k] - timein[k-1]);

        q = qinn[k-1] * beta + qinn[k] * (1.0-beta);
        y = pow (q/(manning*sqrt(slope)),0.6);
        u = q / y;

        velocity[0][0] = u;
        velocity[0][1] = u;
        depth[0][0] = y;
        depth[0][1] = y;

        velocity[sections][0] = velocity[sections-1][1];
        depth[sections][0] = depth[sections-1][1];

/* first computation of the water depth, according to Eq. 3.4.5 */

        for(i=1;i<sections;i++) {
          depth[i][1] = depth[i][0] - timestep / (2.0 * deltax) * (velocity[i][0] *
                (depth[i+1][0] - depth[i-1][0]) + depth[i][0] *
                (velocity[i+1][0] - velocity[i-1][0]));
          }

/* compute the water velocity */

        for(i=1;i<sections;i++) {
          dummy = - velocity[i][0] * timestep * 0.5 / deltax
                    * (velocity[i+1][0] - velocity[i-1][0]);
          dummy += - 9.81 * (timestep * 0.5 / deltax) * (depth[i+1][0] -
                depth[i-1][0]);
          dummy += 9.81 * slope * timestep;
          dummy += - velocity[i][0] * velocity[i][0] * timestep * 9.81
                / (pow(depth[i][0],1.3333) * manning * manning);
          velocity[i][1] = velocity[i][0] + dummy;
          }

/* depth according to continuity - control volume approach*/

        for(i=1;i<sections;i++) {
          u = 0.5 * (velocity[i][0] + velocity[i][1]);
          depth[i][1] =
                (0.25 * (velocity[i-1][1] + velocity[i-1][0]) *
                (depth[i-1][1]+depth[i-1][0])
                + depth[i][0] * (deltax / timestep - 0.5 * u ))
                / (deltax / timestep + 0.5 * u );
          }

/* updating variables */

        for(i=1;i<sections;i++) {
          velocity[i][0] = velocity[i][1];
          depth[i][0] = depth[i][1];
          }
```

```
/* printing */

        time = time+timestep;
        out = fopen("outflow","a");
        fprintf(out,"%lf ", time);
        fprintf(out,"%lf ",velocity[0][1]*depth[0][1]);
        fprintf(out,"%lf ",velocity[1][1]*depth[1][1]);
        fprintf(out,"%lf ",velocity[sections/4][1]*depth[sections/4][1]);
        fprintf(out,"%lf ",velocity[sections/2][1]*depth[sections/2][1]);
        fprintf(out,"%lf ",velocity[sections-1][1]*depth[sections-1][1]);
        fprintf(out,"\n");
        fclose(out);

        }

}
```

INFLOW FILE:

0.0 10.0
100.0 15.0
200.0 20.0
300.0 15.0
400.0 10.0
10000.0 10.0

Appendix II List of symbols and units

The units are in brackets []

Latin

A	area [m^2]
B	width of a river/channel [m]
c,C	constants in k-ε turbulence model [dimensionless]
c	concentration [ppm, kg/m^3, dimensionless]
d	sediment particle diameter [m]
D	habitat preference index
E	specific energy height [m]
F	flux [kg/s]
g	acceleration of gravity [m/s^2]
h	water depth [m]
I	slope [dimensionless]
I_b, I_0	bed slope [dimensionless]
$I_f, I_e,$	friction or energy slope [dimensionless]
I	heat flux
k	friction loss coefficient [dimensionless]
k	turbulent kinetic energy [m^2/s^2]
k	coefficient for biological reactions [1/day]
K	coefficient in hydrologic routing method [s]
M	Manning-Stricklers friction coefficient [$m^{1/3}$/s]
n	Mannings friction coefficient [s/$m^{1/3}$]
N	Brunt-Väisälä frequency [1/s]
p	habitat availability index
P	pressure [N/m^2]
P	wetted perimeter [m]
q	water discharge/width [m^2/s]
q_s	sediment discharge/width [kg/s/m]
Q	water discharge [m^3/s]
r	hydraulic radius [m]
r	distance from centerline of plume [m]
r	HSI index (habitat hydraulics)
t	time [sec.,days]
T	temperature [^0C, ^0K]
U	average velocity [m/s]
u	fluctuating velocity [m/s]
u_*	shear velocity [m/s]
V	average velocity in direction 2 [m/s]
V	volume [m^3]
v	fluctuating velocity [m/s]
W	average velocity in vertical direction [m/s]
w	fluctuating velocity in vertical direction [m/s]
x	spatial variable [m]
X	coefficient in hydrologic routing method [dimensionless]
y	spatial variable [m]
y	water depth [m]
z	spatial variable - vertical distance [m]

Greek

ε	dissipation of turbulent kinetic energy [m^2/s^2]
γ	specific density for water [N/m^3]

κ	constant in velocity wall law (0.4) [dimensionless]
μ	dynamic viscosity of water [Ns/m^2] ($1.3x10^{-3}$ at 20 ^0C)
ν	kinematic viscosity of water [m^2/s] ($1.3x10^{-6}$ at 20 ^0C)
ν_T	turbulent eddy-viscosity [m^2/s]
ρ	density of water [kg/m^3]
ρ_w	density of water [kg/m^3]
ρ_s	density of sediments [kg/m^3] (often set to 2.65 kg/dm^3)
τ	shear stress [N/m^2]
$\tau*$	dimensionless shear stress [dimensionless]
ξ	coordinate system direction 1 [dimensionless]
ψ	coordinate system direction 2 [dimensionless]
ζ	coordinate system direction 3 [dimensionless]
Γ	diffusion coefficient [m^2/s]

Appendix III Solutions to selected problems

Chapter 2, Problem 2

First, compute the cross-sectional area:

A = 8x2+10x+15x2 = 96 m^2

The wetted perimeter is:

P = 2+15+3+10+3+8+2 = 43 m

The hydraulic radius is:

$$r = \frac{A}{P} = \frac{96}{43} = 2.23m$$

Mannings formula gives the water velocity:

$$U = MI^{\frac{1}{2}}r^{\frac{2}{3}} = 60\sqrt{\frac{1}{500}}2.23^{\frac{2}{3}} = 4.5 \text{ m/s}$$

The water discharge is:

$Q = UA$ = 4.5x96 = 440 m^3/s

When the Manning-Strickler friction coefficient varies, the same procedure and formulas have to be used for each part of the cross-section. The following table gives the results:

	Section A	Section B	Section C
Area	30	50	16
Wetter perimeter	17	16	10
Hydraulic radius	1.76	3.12	1.6
Velocity	2.6	5.73	2.44
Discharge	78	286	39

The total discharge is the sum of the discharges in the three parts.

Q = 78+286+39=403 m^3/s.

Chapter 2, Problem 3

First, find the water level at *B*, from the equation for the hydraulic jump:

$$\frac{h_B}{h_C} = \frac{1}{2}(\sqrt{1 + 8Fr_C^2} - 1)$$

The velocity at *C*:

$$U_C = \frac{Q}{y_C} = \frac{6}{3} = 2 \text{ m/s}$$

The Froude number at *C* is:

$$Fr_C^2 = \frac{U_C^2}{gy_C} = \frac{2^2}{9.81x3} = 0.136$$

The depth is then given by:

$$\frac{h_B}{h_C} = \frac{1}{2}(\sqrt{1 + 8Fr_C^2} - 1) = \frac{1}{2}(\sqrt{1 + 8x0.136^2} - 1) = 0.222$$

and

$$h_B = 0.222h_C = 0.222x3 = 0.667m$$

The main method to compute the distance from A to B is to start at A and compute the water surface profile. When it reaches 0.667m, this will be the location of the jump.

The following formula is used:

$$\frac{dy}{dx} = \frac{I_f - I_0}{1 - Fr^2}$$

It is converted to:

$$\Delta x = \Delta y \frac{(1 - Fr^2)}{I_f}$$

This has to be solved in a table, where I_f and *Fr* are computed. I_f is computed by Manning's formula:

$$I_f = \frac{U^2}{M^2 y^{\frac{4}{3}}}$$

Table 1:

Δy	y	U	I_f	Fr^2	Δx	x
-	0.4	-	-	-	-	0
0.05	0.425	14.11	0.25	47.8	9.4	9.4
0.05	0.475	12.63	0.172	34.24	9.7	19.1
0.05	0.525	11.43	0.123	25.36	9.9	29.0
0.05	0.575	10.43	0.0910	19.28	10.0	39.0
0.037	0.6185	9.70	0.0714	15.51	7.5	46.5
0.03	0.652	9.2	0.0599	13.24	6.13	52.6

The distance from A to B is 53 meters.

Chapter 2, problem 5

The integral of the concentration over time becomes:

$$I = \int c dt = \bar{c}\Delta t = 500x1 ppm minutes$$

The discharge is:

$$Q = \frac{m}{\int c dt} = \frac{m}{I} = \frac{2kg}{\frac{500min}{10^6}} = 4000\frac{kg}{min} = 4\frac{m^3}{min} = 0.067\frac{m^3}{s} = \underline{67\frac{l}{s}}$$

Chapter 4, Problem 1

The continuity equation gives the water velocity as:

$$U = \frac{Q}{By} = \frac{20}{2x30} = 0.33\frac{m}{s}$$

The shear stress is:

$$\tau = \rho g y I = 1000x9.81x2x\frac{1}{63} = 313 Pa$$

The shear velocity is:

$$u_* = \sqrt{\frac{\tau}{\rho}} = \sqrt{\frac{313}{1000}} = 0.56\frac{m}{s}$$

Computing the diffusion coefficient. Using Fischer et al. (1979): (Eq. 4.3.3)

$$\Gamma = 0.011\frac{(UB)^2}{Hu_*} = 0.011\frac{(0.33x30)^2}{2x0.56} = 0.96$$

The initial concentration is equal to the mass divided by the volume of water in the river in the time period:

$$c_0 = \frac{m}{\rho Qt} = \frac{2000}{1000x(20x10x60)} = 0.000167 = 167ppm$$

These numbers we use in the general equation for the concentration downstream of a spill: (Eq. 4.3.4)

$$c(t) = \frac{c_0 L}{2\sqrt{\pi\Gamma t}} e^{-\frac{(x-Ut)^2}{4\Gamma t}} = \frac{167x200}{2\sqrt{0.96\pi t}} e^{-\frac{(10000-0.33t)^2}{3.84t}}$$

This equation is plotted below:

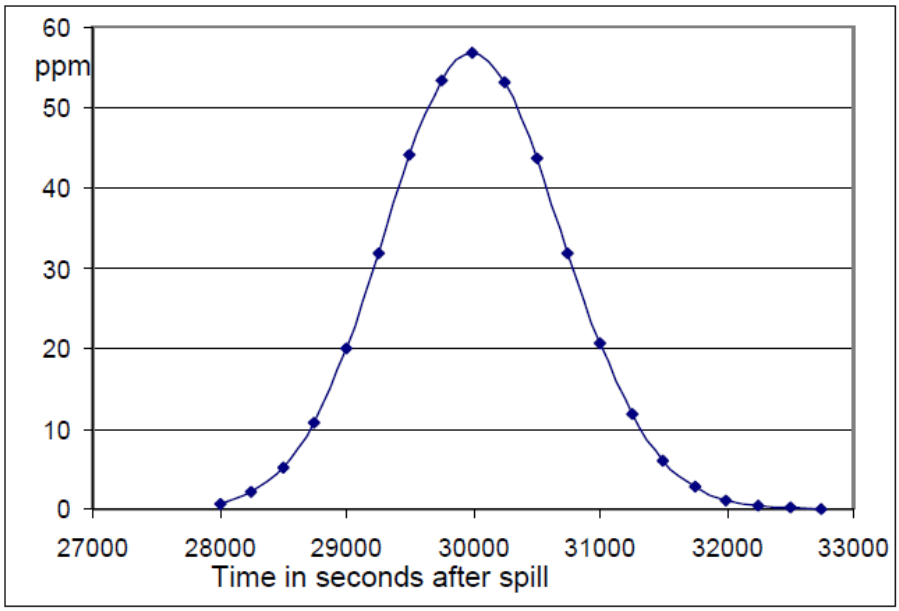

Chapter 4, Problem 2

The densimetric Froude number is:

$$Fr' = \frac{u_0}{\sqrt{\left(\frac{\rho_{res}-\rho_0}{\rho_{res}}\right)gd_0}} = \frac{\frac{50}{(3.14x1.5x1.5)}}{\sqrt{\left(\frac{1023-1000}{1023}\right)9.81x3}} = 8.7$$

The velocity is computed from:

$$\frac{u}{u_0} = 4.3(8.7)^{-\frac{2}{3}}\left(\frac{20}{3}\right)^{-\frac{1}{3}} e^{\left[-96\frac{0^2}{20^2}\right]} = 0.56$$

The velocity is 0.56 * 7 m/s = 3.8 m/s.

Chapter 5, Problem 5

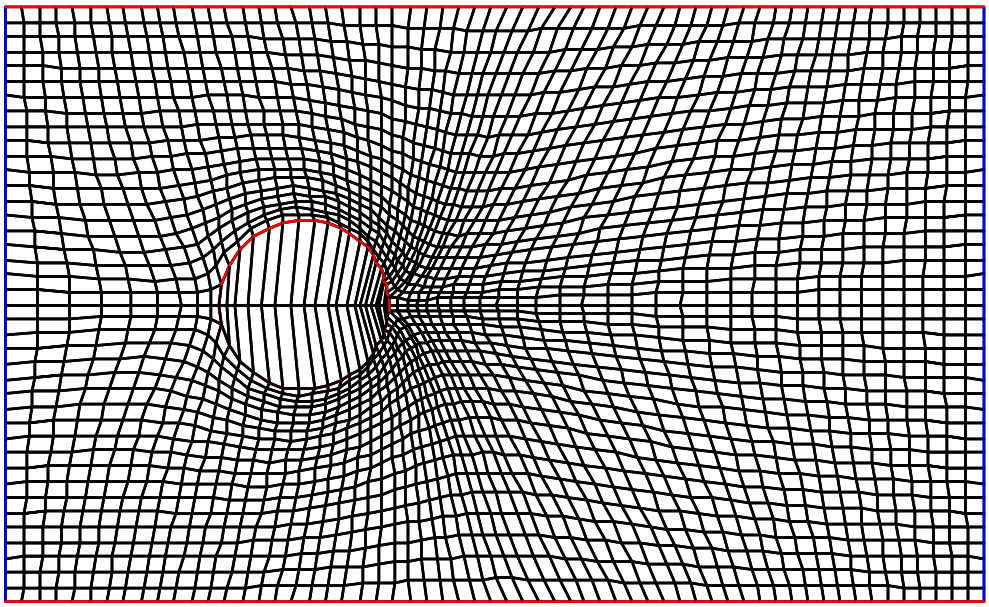

Chapter 7, Problem 1

The shear stress on the lake is computed from Eq. 7.2.1 as

$$\tau = c_{10}\rho_a U_a^2 = 1.1x10^{-3}x1.2x15^2 = 0.3Pa$$

The slope of the water surface is given by Eq. 7.2.3:

$$I = \frac{\tau}{\rho g h} = \frac{0.3}{1000x9.81x100} = 3x10^{-7}$$

The density at 15 ^{o}C is approximately 999.12 kg/m^3 according to the table in Chapter 7.4, and the density for 5 ^{o}C is 999.99 kg/m^3.

The slope of the thermocline is given by Eq. 7.4.10:

$$I' = -I\frac{\rho_1}{\rho'} = -3x10^{-7}x\frac{1000}{999.99 - 999.12} = 3.5x10^{-4}$$

The thermocline will tilt around an axis in the middle of the lake. The distance from the middle of the lake to the far ends is half the length of the

lake. The rise/fall in the thermocline at these locations will be:

$$\Delta h = \frac{L}{2}\Gamma = \frac{5000}{2} x 3.5 x 10^{-4} = \underline{0.87m}$$

Chapter 7, Problem 2

We start by computing the density gradient from the temperature gradient. The temperature gradient at 10 meter is 0.5 degrees/meter. There will therefore be 4 meters between 10 and 12 degrees. The table in Chapter 7.3 gives the densities at these temperatures as 999.73 and 999.52. The density gradient becomes:

$$\frac{d\rho}{dz} = \frac{999.52\frac{kg}{m^3} - 999.73\frac{kg}{m^3}}{4m} = -0.0525\frac{kg}{m^3}$$

The Brunt-Väisälä frequency is given as:

$$N^2 = -\frac{g}{\rho}\frac{d\rho}{dz} = -\frac{9.81}{1000}(-0.0525) = 0.000515Hz \qquad (7.8.2)$$

This is inserted into the formula for the thickness of the abstraction layer:

$$d = k_3\left(\frac{Q^2}{B^2 h N^2}\right)^{\frac{1}{3}} = 1.2\left(\frac{\left(2\frac{m^3}{s}\right)^2}{(2m)^2 x 1m(0.000515Hz)}\right)^{\frac{1}{3}} = 15m$$

(7.8.4)

The thickness of the abstraction layer is both above and below the intake. Therefore, it will only reach half the thickness above the intake, or 7.5 m. This is below 9 meters, which means the intake will not take water from the upper 1 meter layer.

Chapter 8, Problem 1

A stable condition means that the loss is equal to the inflow: 2000 kg/day. The loss rate is 0.1, meaning 2000 kg/day is 10 % of the total. The total phosphorous is therefore 2000/0.1 = 20 000 kg. The concentration is:

$$c = \frac{20000kg}{10^6 x 10^3 kg} = 2x10^{-5} = 20ppm$$

The steady state concentration for an inflow of 300 kg/day is similarly 3 ppm. The reduction will therefore be 17 ppm. 20 % of the original value is 4 ppm. After time *t*, there will be 4-3=1 ppm left of the reduction. The time is described by the following equation:

$$c = c_0 e^{-kt} \Rightarrow 1 = 17e^{-0.1t} \Rightarrow t = 10\ln\left(\frac{17}{1}\right) = \underline{28days}$$

Chapter 9, problem 1

Assume uniform flow and that the bed shear stress is equal to the critical shear stress given by Shields graph. Also, assume the channel is wide, so that the hydraulic radius is equal to the water depth. This gives six unknown and six equations. The unknown are:

- water depth *h*
- water velocity *U*
- particle diameter *d*
- bed roughness k_s
- Manning-Stricklers friction factor *M*
- bed shear stress τ

The six equations are:

- Water continuity: *Q=BhU*

$$\tau = \rho g h I \qquad (2.1.1)$$

$$k_s = 3d_{90} \qquad (2.1.4)$$

$$U = M\, r_h^{\frac{2}{3}} I^{\frac{1}{2}} \qquad (2.2.4)$$

$$M = \frac{26}{k_s^{\frac{1}{6}}} \qquad (2.2.5)$$

$$\tau^* = \frac{\tau_c}{g(\rho_s - \rho_w)d}$$ From Shields graph

The equations are best solved in the following manner:

1. Guess a Manning's coefficient, *M*.
2. Computer the water velocity using Eq. 2.2.4
3. Compute the water depth using the continuity equation
4. Compute the shear stress using Eq. 2.2.1.
5. Compute R* in Shields diagram
6. Find $\tau*$ from Shields diagram
7. Compute *d* from the equation in Shields graph
8. Compute k_s using 2.1.4
9. Compute Mannings *M* value from Eq. 2.2.5.
10. Check if *M* is equal to what was assumed in point 1. If it is very different, do another iteration starting from point 1, with the *M* value from point 9.

Using this method we get:

1. *M*=30 (guess)
2. *U*=2.6 m/s
3. *y* = 1.3 m
4. τ = 60 N/m2
5. *R** = 18 000
6. $\tau* = 0.06$
7. *d* = 0.06 m
8. k_s = 0.18 m
9. *M* = 34
10. Iteration with M=34 gives *d*=0.06 m.

Chapter 9, problem 6

First, the particle fall velocity is obtained from Fig. 9.3.1 to be 0.15 m/s. Then some basic parameters are computed:

Friction slope:

$$I_f = \frac{U^2}{M^2 y^{\frac{4}{3}}} = \frac{2.5^2}{50^2 x 1.5^{\frac{4}{3}}} = 0.001456$$

Bed shear:

$$\tau = \rho g y I_f = 1000x9.81x1.5x0.001456 = 21.42745673 \text{ N/m}^2$$

Shear velocity:

$$u_* = \sqrt{\frac{\tau}{\rho}} = \sqrt{\frac{21.42}{1000}} = 0.146381203 \text{ m/s}$$

Particle Reynolds number:

$$R_* = \frac{u_* d}{\nu} = \frac{0.14638x0.001}{10^6} = 146$$

Shields curve gives the Shields parameter: $C = 0.05$

Critical shear stress:

$$\tau_c = Cg(\rho_s - \rho_w)d = 0.05x9.81x(2650 - 1000)x0.001$$

$= 0.809 \text{ N/m}^2$

The suspension parameter:

$$Z = \frac{w}{\kappa u_*} = \frac{0.15}{0.4x0.1464} = 2.5618$$

Engelund-Hansens formula:

$$q_s = 0.05\rho_s U^2 \sqrt{\frac{d_{50}}{g\left(\frac{\rho_s}{\rho_w} - 1\right)}} \left[\frac{\tau}{g(\rho_s - \rho_w)d_{50}}\right]^{\frac{3}{2}}$$

$$q_s = 0.05x2650x2.5^2 \sqrt{\frac{0.001}{9.81\left(\frac{2650}{1000} - 1\right)}} \left[\frac{21.43}{9.81(2650 - 1000)0.001}\right]^{\frac{3}{2}}$$

$= \underline{9.9 \text{ kg/m/s}}$

Then we use van Rijn's formula for bed material load:

$$\frac{q_b}{D_{50}^{1.5}\sqrt{\frac{(\rho_s-\rho_w)g}{\rho_w}}} = 0.053\frac{\left[\frac{\tau-\tau_c}{\tau_c}\right]^{2.1}}{D_{50}^{0.3}\left[\left(\frac{(\rho_s-\rho_w)g}{\rho_w\nu^2}\right)\right]^{0.1}}$$

$$q_b = 0.053\frac{\left[\frac{21.43-0.809}{0.809}\right]^{2.1}}{0.001^{0.3}\left[\frac{(2650-1000)9.81}{1000x(10^{-6})^2}\right]^{0.1}}\left(0.001^{1.5}\sqrt{\frac{(2650-1000)9.81}{1000}}\right)$$

q_b = 0.002295 m^2/s

Van Rjin gives q_b in m^2/s. This is transformed to kg/s by multiplying it with the sediment density: 2650 kg/m^3, giving:

q_b = 6.082 kg/s/m

Then we use Van Rijn's formula for suspended load. We assume the reference level at the bed is equal to 5 % of the water depth, or 1.5x0.05 = 0.075 m. The reference concentration is:

$$c_{bed} = 0.015\frac{D_{50}}{a}\frac{\left[\frac{\tau-\tau_c}{\tau_c}\right]^{1.5}}{\left\{D_{50}\left[\frac{(\rho_s-\rho_w)g}{\rho_w\nu^2}\right]^{\frac{1}{3}}\right\}^{0.3}} = 0.015\frac{0.001}{0.075}\frac{\left[\frac{21.43-0.809}{0.809}\right]^{1.5}}{\left\{0.001\left[\frac{(2650-1000)9.81}{1000x(10^{-6})^2}\right]^{\frac{1}{3}}\right\}^{0.3}}$$

c_{bed} = 0.009756758 (volume fraction)

The sediment transport caused by this reference concentration only takes place above the reference level. To compute the suspended sediment transport, we can divide the water column in layers. For convenience, let us assume the first layer is twice as high as the reference level. This is then 10 % of the water depth, or 0.15 m. And that there are three more layers of equal size:

(1.5 - 0.15)/10 = 0.45 m

We then use the Hunter Rouse formula to compute the concentration in the center of each cell, and the logarithmic velocity profile to compute the velocities. This can then be multiplied with the height of each cell to give an estimate of the suspended load.

Table 2:

Cell no.	Distance from bed	Velocity	Hunter Rouse concentration	Cell height	Cell flux
4	1.275	2.77	6.22E-06	0.45	7.7E-06
3	0.825	2.61	0.0003168	0.45	0.00037
2	0.375	2.32	0.00883	0.45	0.00923
1	0.075	1.73	1	0.075	0.130

The sum of the cell fluxes is: 0.14. This can be multiplied with the bed concentration to give the sediment transport in m^2/s. Then multiplied with the density, we get the sediment transport in kg/s/m:

q_s = 0.14* 0.009756758*2650 = 3.6 kg/s/m.

Note that the height of the cell closest to the be has only been set to 0.075 m, although it is 0.15 meters. This is because the sediment transport below the reference level is considered bed load, and computed by the bed load formula.

Total load according to van Rijn is then:

q_t = 3.6 + 6.08 = 9.7 kg/s/m.

Also note that there are only four layers in the vertical direction. If 11 layers had been used, we would have gotten 2 % higher result for the suspended load.

In our case, the results by van Rijn's method and Engelund-Hansens formula are very similar. This is normally not the case. Often, results from different sediment discharge formulas may deviate with a factor 2-3 or more.

Appendix IV: An introduction to programming in C

This chapter is written as a brief introduction to C programming for students who has not had previous courses on programming.

A computer program is written as text file using an editor. In the text file, different commands tells the computer what to do. This text file is often called a source code. The text file needs to be transformed into a computer program. The file containing the computer program is often called the executable file. The transformation of the text file to the executable file is done using a compiler. Depending on the language of the text file, different compilers are used. For the C language, we need a C compiler. In the present course we will use the LCC compiler, which is freeware.

The C program consists of the following structure:

main () {

Variable declarations

Commands on what to do

}

Note the brackets, which are necessary. Omitting one leads to the compiler giving an error message, and the executable is not produced.

Variable declarations

To make the program compute something, we need to declare variables. In a spreadsheet, a variable is named after its address, for example **b12**. In C, we can give any name to a variable. For example:

int **counter**;
double **flux**;

The variable named **counter** is declared as an integer, and the variable **flux** is declared as *double*, a floating point number with 12 digits precision. Note the ; after each declaration.

It is also possible to declare arrays of integers or floats:

double **velocity**[100], **depth**[100];

If we have 100 cross-sections in a river, the velocity in section *14* is given as **velocity**[*14*].

We can also use multi-dimensional arrays:

double **discharge**[2][100];

In C, the first number in the array is zero, and the last array in the arrays above is 99, if decreased with 100 elements.

We can also declare files with different names, used to read input-data from and write output-data to:

FILE * **input**:
FILE * **result**;

Note the * that needs to be included for the files.

A file needs to be opened before we can read from it. The syntax for this is:

input = *fopen*("inflow","r");

Similar for a file we want to write to:

result = *fopen*("outflow","w");

The file names are here given as inflow and outflow. These are text files.

After writing to a file, it needs to be closed for other programs to read from it:

fclose(**result**);

To read information from a file to a variable, the following syntax is used :

fscanf(**input**,"%lf",&**depth**[1]);

Note the syntax. If this is not correct, the compiler will produce an error message, or the program will not work.

Similarly, the following syntax is used to write to files:

fprintf(**result**,"%lf ",**velocity**[0]);

Note the *&* is used when reading data and not when writing data to files.

Commands

The program is made up of a series of commands. They will be carried out in the same order as given in the file. There are several types of commands.

Variables can be initialized using the = operator. For example:

velocity[0] = 2.0;

Variables can be incremented. For example, in the following, the variable **counter** will increase its value by one:

counter = **counter** + 1;

If count was 3 before this line, it will be 4 afterwards. Incrementing an integer with one can also be written

counter++;

This does the same as the line before.

A typical command is to write a formula:

velocity[1] = **discharge** / **depth**[1];

A formula can be long and complex, and one can use * for multiplication, and + and - for addition and subtraction. Also, one can use brackets in complex formulas, to several levels:

velocity[1] = **discharge** / (**depth**[1] + 1.0e-20);

The above formula is a trick to avoid errors if **depth**[1] is zero.

Repetition of formulas over many cross-sections is done in a loop. There are different types of loops, but the *for* loop is often used. The following loop repeats the above formula for all the 100 cross-sections in the river, starting from cross-section no. 0 to cross-section no. 99:

for(**counter** = 0; **counter** <100; **counter**++) {

    velocity[**counter**] = **discharge** / (**depth**[**counter**] + 1.0e-20);

}

Several formulas can be used inside a loop, and it is also possible to nest several loops inside each other.

An *if* sentence can be used to give a special logic. For example:

if (**froude** > 1.0) {

  depth = 2.0;

}

An *if* sentence can also be used to break out of a loop:

for(**counter** = 0; **counter** <100; **counter**++) {

    if (**depth**[**counter**] < 1.0e-20) break;

    velocity[**counter**] = **discharge** / **depth**[**counter**];

}

This loop will be stopped if **depth** is below 10^{-20}, even if **counter** has not reached 99. The program will then jump out of the loop and do the next thing in the file.

Remember that the syntax is very important. One wrong type of brackets, for example, will give a compiler error.

The introduction given above is only a very small fraction of all the commands, declarations etc. available in C. For more details, a textbook on C programming should be consulted.

Appendix V: Diffusion equation

We want to find a physical explanation of the equation for the diffusive flux:

$$F = \Gamma A \frac{dc}{dx} \qquad \text{(V.1)}$$

We are looking at a channel with turbulent flow, as shown in the figure below. The average water velocity is zero, but there is turbulence in the channel, illustrated in the figure by an eddy. The particle concentrations in points 1 and 2 are constant, and the turbulence transports particles between 1 and 2 with a certain rate. This is the flux: number of particles pr. time unit.

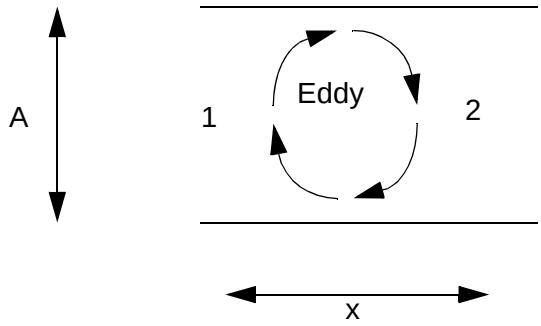

Figure V 1. Sketch for explenation of flux from turbulent diffusion.

The cross-sectional area of the channel is called A, and the distance between point 1 and 2 is x.

From a physical point of view, the area A, in Eq. V.1 must be correct. If we have two channels beside each other, there will be twice as many particles transported in the x direction. The flux must therefore be proportional to A.

If we have an equal amount of particles in points 1 and 2, then there will be no net flux between the points. The flux must therefore be a function of the difference between the particle concentrations in point 1 and 2.

If we double the number of particles in 1 and 2, the flux will also double. Therefore, the flux must be proportional to the concentration gradient: c1-c2.

Why is the flux inversely proportional to the distance, x, between point 1 and 2? To see this, we consider the situation with three points in the flow, as given in figure V.1

For a steady situation with constant concentrations in points 1, 2 and 3, we have also the same flux between point 1 and point 2 as between point 2 and 3. This means the concentration difference between point 1 and 2 is the same as between point 2 and 3. The concentration difference between point 1 and 3 is therefore twice as high as the concentra-

tion difference between point 1 and 2. Or between point 2 and 3.

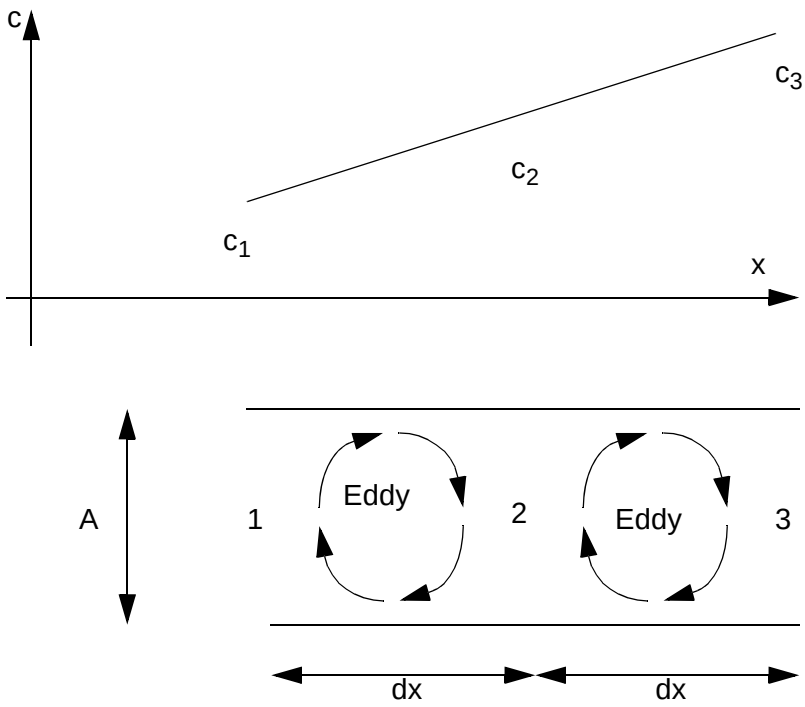

Figure V 2. Sketch for explenation of flux from turbulent diffusion.

Therefore, the flux can not be proportional to the concentration difference directly. If we divide the concentration difference with the distance, we get a concentration gradient. The flux must be proportional to the concentration gradient. Which is what is given in Eq. V 1.